

170  
19-76  
18

OR-452

ORNL/TM-5497

## **A Review of Concrete Properties for Prestressed Concrete Pressure Vessels**

**R. K. Nanstad**

**MASTER**

**OAK RIDGE NATIONAL LABORATORY**  
OPERATED BY UNION CARBIDE CORPORATION FOR THE ENERGY RESEARCH AND DEVELOPMENT ADMINISTRATION

DISTRIBUTION OF THIS DOCUMENT IS UNLIMITED

## **DISCLAIMER**

**This report was prepared as an account of work sponsored by an agency of the United States Government. Neither the United States Government nor any agency Thereof, nor any of their employees, makes any warranty, express or implied, or assumes any legal liability or responsibility for the accuracy, completeness, or usefulness of any information, apparatus, product, or process disclosed, or represents that its use would not infringe privately owned rights. Reference herein to any specific commercial product, process, or service by trade name, trademark, manufacturer, or otherwise does not necessarily constitute or imply its endorsement, recommendation, or favoring by the United States Government or any agency thereof. The views and opinions of authors expressed herein do not necessarily state or reflect those of the United States Government or any agency thereof.**

## **DISCLAIMER**

**Portions of this document may be illegible in electronic image products. Images are produced from the best available original document.**

Printed in the United States of America. Available from  
National Technical Information Service  
U.S. Department of Commerce  
5285 Port Royal Road, Springfield, Virginia 22161  
Price: Printed Copy \$6.00; Microfiche \$2.25

This report was prepared as an account of work sponsored by the United States Government. Neither the United States nor the Energy Research and Development Administration/United States Nuclear Regulatory Commission, nor any of their employees, nor any of their contractors, subcontractors, or their employees, makes any warranty, express or implied, or assumes any legal liability or responsibility for the accuracy, completeness or usefulness of any information, apparatus, product or process disclosed, or represents that its use would not infringe privately owned rights.

ORNL/TM-5497  
Distribution  
Category UC-77

Contract No. W-7405-eng-26

METALS AND CERAMICS DIVISION

**NOTICE**  
This report was prepared as an account of work sponsored by the United States Government. Neither the United States nor the United States Energy Research and Development Administration, nor any of their employees, nor any of their contractors, subcontractors, or their employees, makes any warranty, express or implied, or assumes any legal liability or responsibility for the accuracy, completeness or usefulness of any information, apparatus, product or process disclosed, or represents that its use would not infringe privately owned rights.

A REVIEW OF CONCRETE PROPERTIES FOR PRESTRESSED  
CONCRETE PRESSURE VESSELS

R. K. Nanstad

Date Published: October 1976

OAK RIDGE NATIONAL LABORATORY  
Oak Ridge, Tennessee 37830  
operated by  
UNION CARBIDE CORPORATION  
for the  
ENERGY RESEARCH AND DEVELOPMENT ADMINISTRATION

DISTRIBUTION OF THIS DOCUMENT IS UNLIMITED

*[Signature]*

THIS PAGE  
WAS INTENTIONALLY  
LEFT BLANK

## CONTENTS

ABSTRACT . . . . .	1
1. INTRODUCTION . . . . .	1
2. PCPV CONCEPT . . . . .	2
2.1 PCPV Description . . . . .	2
2.2 Design Philosophy . . . . .	6
3. CONCRETE PROPERTIES . . . . .	8
3.1 General . . . . .	8
3.2 PCRV Concretes . . . . .	8
3.3 Effects of Temperature . . . . .	12
3.3.1 Compressive Strength . . . . .	12
3.3.2 Elastic Properties . . . . .	37
3.3.3 Tensile Strength . . . . .	47
3.3.4 Shrinkage and Creep . . . . .	49
3.3.5 Thermal Properties . . . . .	64
3.3.6 Properties Under Multiaxial Stress States . . . . .	71
3.3.7 Mechanisms Causing Observed Temperature Effects . .	84
3.4 Effects of Radiation . . . . .	87
3.5 Moisture Migration . . . . .	94
3.6 Hot Spots and Models . . . . .	98
4. SUMMARY, CONCLUSIONS, AND RECOMMENDATIONS . . . . .	101
4.1 Summary . . . . .	101
4.2 Conclusions . . . . .	107
4.3 Recommendations for Further Study . . . . .	108
ACKNOWLEDGMENTS . . . . .	110
REFERENCES . . . . .	110

A REVIEW OF CONCRETE PROPERTIES FOR PRESTRESSED  
CONCRETE PRESSURE VESSELS

R. K. Nanstad

ABSTRACT

For years, many research programs have been conducted on the properties of concrete for prestressed concrete reactor vessels (PCRVs). The desire for increasing power output along with safety requirements has resulted in consideration of the prestressed concrete pressure vessel (PCPV) for most current nuclear reactor systems, as well as for the very-high-temperature reactor for process heat and as primary pressure vessels for coal conversion systems.

Results are presented of a literature review to ascertain current knowledge regarding plain concrete properties under conditions imposed by a mass concrete structure such as a PCRV. The effects of high temperature on such properties as strength, elasticity, and creep are discussed, as well as changes in thermal properties, multiaxial behavior, and the mechanisms thought to be responsible for the observed behavior. In addition, the effects of radiation and moisture migration are discussed.

It is concluded that testing results found in the technical literature show much disagreement as to the effects of temperature on concrete properties. The variations in concrete mixtures, curing and testing procedures, age at loading, and moisture conditions during exposure and testing are some of the reasons for such disagreement. Test results must be limited, in most cases, to the materials and conditions of a given test rather than applied to such a general class of materials such as concrete. It is also concluded that sustained exposure of normal concretes to current PCRV operating conditions will not result in any significant loss of properties. However, lack of knowledge regarding effects of temperatures exceeding 100°C (212°F), moisture migration, and multiaxial behavior precludes a statement advocating operation beyond current design limits.

The report includes recommendations for future research on concrete for PCPVs.

1. INTRODUCTION

The use of prestressed concrete as the primary pressure-retaining structure for nuclear power reactors was first introduced in 1954 at Saclay, France.<sup>1</sup> Since that time, prestressed concrete reactor vessels (PCRVs) have become a basic component of gas-cooled reactors constructed

in France, England, Germany, and the United States, and more are being designed and planned. The desire for reactors having increased power output along with additional safety requirements has resulted in the development of PCRVs for pressurized-water reactors and boiling-water reactors. PCRVs are also being planned for the very-high-temperature reactors for process heat and as the primary pressure vessel for coal conversion systems. Expanding interest in the concept of prestressed concrete pressure vessels (PCPVs) operating under such conditions as high pressures, high temperatures, and hostile environments has necessitated detailed investigations of concrete behavior under specific operating conditions.

Many research programs have been conducted, and much valuable knowledge has been gained about PCPV structural behavior in general and concrete properties in particular. Much of the accumulated data for a particular property, however, precludes reasonable correlations and conclusions with regard to behavior of concrete. The reason for this is the widespread use of a variety of concrete mixtures and materials. In addition, accurate structural representation in mechanical testing is a problem, since laboratory simulation of mass concrete curing conditions and moisture migration is not a simple proposition when using reasonably small test specimens. Allied with these problems are difficulties with experimental techniques such as testing of small sealed concrete specimens at temperatures of 100°C (212°F) or greater, multiaxial testing, and measurement of long-term behavior.

Oak Ridge National Laboratory is conducting a program of PCRV research and development. As part of the program, this investigation is to provide an assessment of the state of the art as regards relevant concrete properties and test procedures and identify those areas requiring further investigation. Thus, this report will first briefly discuss the general concept of the PCPV and the PCRV environment and then provide a detailed discussion of the relevant material properties of plain concrete within that context.

A general description of the PCRV is given in Sect. 2. It is suggested that those familiar with the use of the PCRV in the high-temperature gas-cooled reactor (HTGR) and/or in the gas-cooled fast reactor systems<sup>2</sup> proceed directly to Sect. 3.

## 2. PCPV CONCEPT

### 2.1 PCPV Description

The PCPV is designed to serve as the primary pressure containment structure. Although the concept of a PCPV is not limited to nuclear applications, this report will emphasize consideration for nuclear power systems and, in particular, the HTGR. However, most of the discussion is equally relevant to many other concrete structural applications.

PCRVs used for HTGRs can be either the relatively simple single-cavity type, used for the Fort St. Vrain Nuclear Generating Station, or

the newer and more complex multicavity type, used for the British Hartlepool and Heisham reactors and proposed for the larger Delmarva Power and Light Company Summit Station.<sup>3</sup>

A cutaway view of the HTGR designed by General Atomic (GA) Company is shown in Fig. 1. This design is based on the so-called "integral concept," whereby the entire primary circuit, consisting of reactor core, primary coolant system, and portions of the secondary coolant system, is contained within a single concrete vessel. The reactor core is located within a large central cavity surrounded by smaller cylindrical cavities which contain the primary cooling system, auxiliary cooling loops, and pressure relief wells. The steam generators and helium circulators are located in the primary cooling system cavities. These cavities are connected, at the top and bottom, to the central core cavity by radial ducts and are sealed at the upper end by concrete plugs that support the helium circulators.<sup>3</sup>

ORNL-DWG 70-2920R

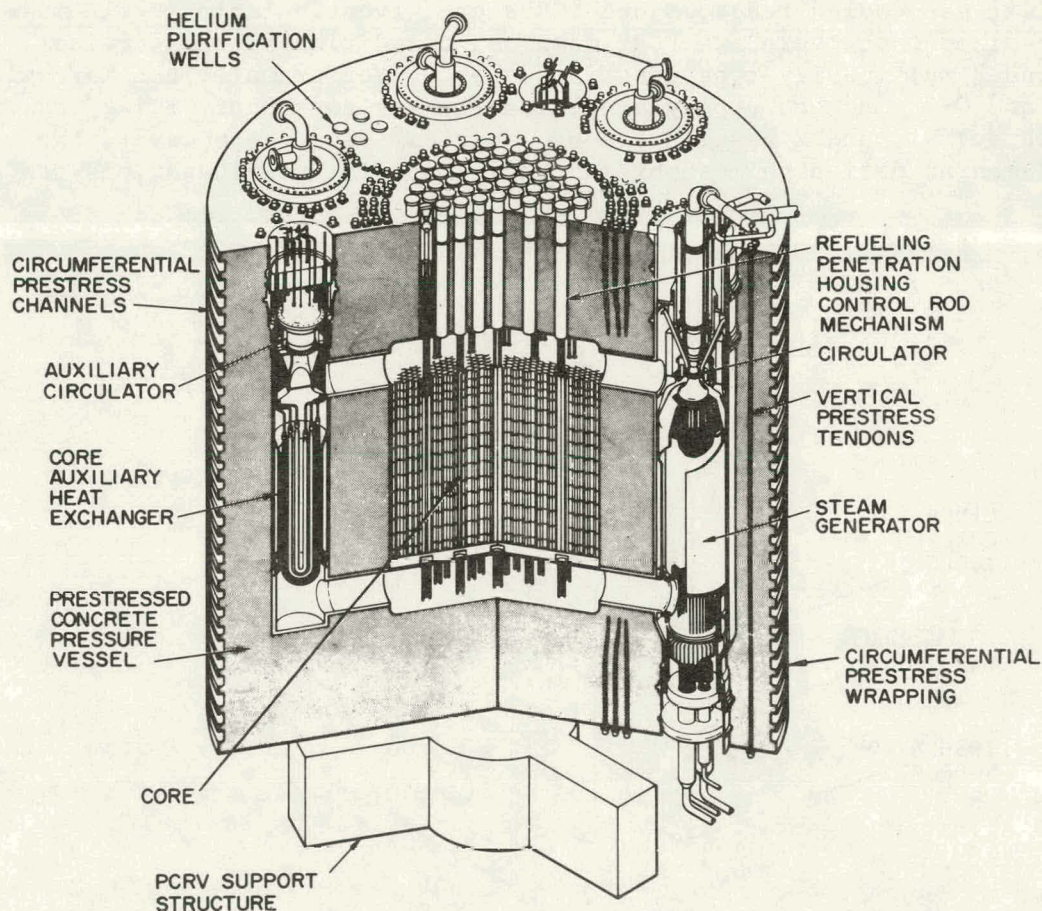


Fig. 1. HTGR with Multicavity PCRV. Source: *Planning Guide for HTGR Safety and Safety-Related Research and Development*, ORNL-4968 (May 1974).

A continuous welded steel liner, attached to the walls of each cavity, acts as the barrier against leakage of the primary coolant. In turn, the concrete vessel supports the liner and serves as the structural resistance to internal coolant pressure. Figure 2 shows a typical design for the thermal barrier and liner cooling tube system. These tubes are welded to the liner and, in conjunction with the insulation, serve to maintain a specified temperature [about 65°C (150°F)] at the liner-concrete interface during normal operation.<sup>3</sup>

As shown in Fig. 1, there are many penetrations through the vessel head for nozzles, control rods, fuel elements, piping, refueling stand-pipes, etc. These penetrations are sealed to prevent loss of coolant.

The PCRV is constructed of relatively-high-strength concrete and is actually a spaced steel structure, since its strength is derived from a multitude of linear steel elements made up of reinforcing bars and prestressing tendons. PCRVs for the large HTGR systems are massive, thick-walled, right circular cylinders having flat heads. The vessel is prestressed with interior longitudinal unbonded tendons and external circumferential strand windings, both of which are capable of being monitored and adjusted if necessary. Some of the design parameters for typical gas-cooled reactors and PCRVs are given in Table 1. It must be emphasized that there are PCRV designs in addition to the vertical cylinder multicavity type described above. For example, the Marcoule G-2 and G-3 reactors employ single-cavity horizontal or "lying" cylinders, while Wylfa 1 and 2 vessels are of spherical design. However, the fundamental design philosophy and basic material considerations are similar.

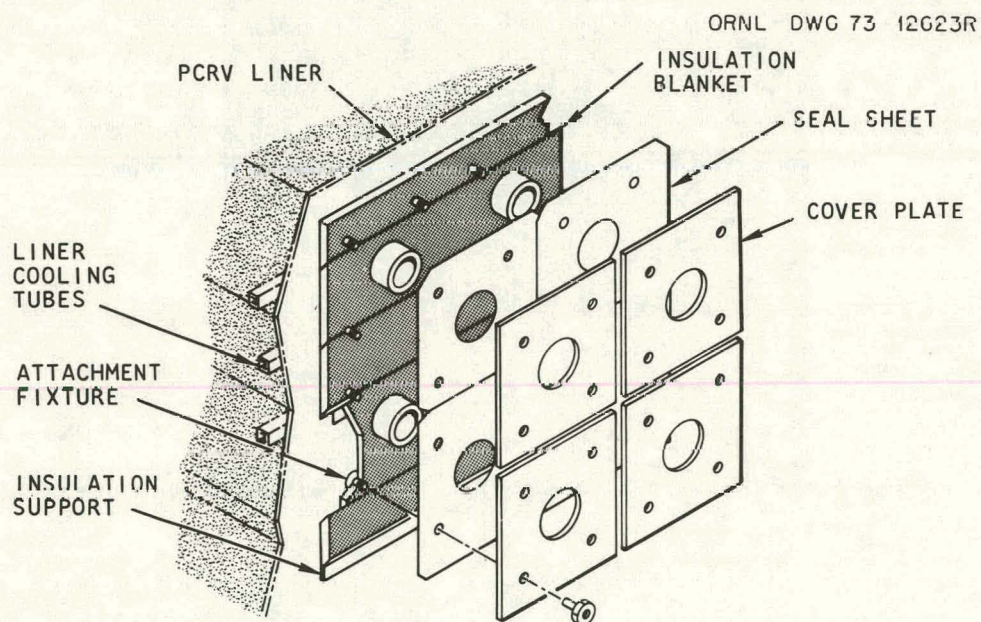


Fig. 2. PCRV Liner and Class A Thermal Barrier. Source: *Planning Guide for HTGR Safety and Safety-Related Research and Development*, ORNL-4968 (May 1974).

Table 1. Data for Gas-Cooled Nuclear Power Stations

Reactor Type		Marcoule G-2, G-3		EDF 3		St. Laurent 1, 2		Bugey 1		Oldbury 1, 2		Wyfia 1, 2		Dungeness B 1, 2		Hartlepool		Fort. St. Vrain		300 MW(e) THTR		1160 MW(e) Gulf HTR	
Country		France				MAGNOX				AGR				USA		FRG		USA					
Unit Power	MW(e)	40	480	487	547	300	590	600	1250	330	300	1160	300 MW(e)	THTR	300 MW(e)	THTR	1160 MW(e)	Gulf HTR					
Geometry of Vessel		LC		VC		SP		VC															
Working Pressure	lb/in. <sup>2</sup> kp/cm <sup>2</sup>	214 15.0	428 30.0	406 28.5	616 43.3	350 24.6	384 27.0	435 30.5	645 45.3	698 49.0	570 40.0	670 47.0											
Outlet Temperature	°F °C	626 330	770 410	770 410	770 410	770 410	777 414	1247 675	1198 648	1440 770	1382 750	1400 760											
Permissible Concrete Temperature	°F °C	122 50	167 75	176 80	158 70	140 60	113 45	131 55	140 60	130 55													
Diameter of Vessel																							
Inside	ft m	45.9 14.0	62.3 19.0	62.3 19.0	56.1 17.1	77.0 23.5	96.0 29.26	65.5 19.95	43.0 13.1	31.0 9.4	52.2 15.9	37 <sup>a</sup> 11.3											
Outside	ft m	65.6 20.0		93.5 28.5		107.2 32.7		90.3 27.6	85.0 25.9	61.0 21.0	81.1 24.8	106 <sup>a</sup> 32.3											
Height (Length) of Vessel																							
Inside	ft m	67.0 20.5	68.7 21.0	119.0 36.3	125.5 38.25	50.9 18.3		58.0 17.7	60.0 10.3	75.0 23.0	50.0 15.3												
Outside	ft m	110.5 33.65	105.0 32.0	161.0 49.1		104.0 31.7		98.4 30.0	96.0 29.3	106.0 32.0	83.5 25.5	91 <sup>a</sup> 27.7											
Breaking Load/Working Load		4.00	3.00	2.50	2.50	3.00	2.65	2.50	2.50														
Concrete Mass	ft <sup>3</sup> .10 <sup>3</sup> m <sup>3</sup> .10 <sup>3</sup>	742 21	884 23	855 24.2		654 18.5	750 21.2	443 12.52	410 11.6	175 4.95													
Reinforcement	tons t	2955 3000	985 1000	787 800		280 284	2400 2440																
Cables	tons t	738 750		2225 2260		2540 2580	2256 2292			1000 1016													

Note: LC = lying cylinder, VC = vertical cylinder, and SP = spherical.

<sup>a</sup>Data from *Planning Guide for HTR Safety and Safety-Related Research and Development*, ORNL-4968 (May 1974), added by author.

Source: W. Fürste, G. Hohnerlein, and H. G. Schafstall, "Prestressed Concrete Reactor Vessels for Nuclear Power Plants Compared to Thick-Walled and Multilayer Steel Vessels," Second Int. Conf. on Pressure Vessel Technology, Part 1, San Antonio, October 1973.

## 2.2 Design Philosophy

In a traditional steel pressure vessel the material is a continuous medium, and, depending on operational requirements, a thick wall must be used to resist the internal pressure and temperature. To design larger systems, one must increase the vessel thickness (undesirable because of temperature gradients and fabrication) or increase the material strength to cope with the larger stresses (usually at the expense of toughness and increased sensitivity of higher-strength steels to defects). In addition, safety considerations have led vessel designers to the redundancy of the PCRV. Fürste et al.<sup>4</sup> cite the following examples of factors involved in the choice of a PCRV for primary containment:

1. Radiation is absorbed by the concrete; the vessel serves as a biological shield.
2. Leak-tightness is secured by the steel liner.
3. Heat is restrained by the internal insulation and the cooling system.

Although not mentioned by Fürste et al., the PCRV is field erected and is usually constructed with materials from the local area; they continue with other PCRV characteristics:

4. reaction to a burst is such that, after decrease of pressure, fissures vanish and a catastrophe by release of radioactivity is prevented;
5. redundancy of the tendons makes burst by brittle fracture impossible;
6. control of the tendons allows for the possibility of restressing or replacing them as needed.

The concept of loading is that, under normal operation, the tensile stresses created by the internal pressure do not overcome the compressive stress created by the vertical and circumferential prestressing, except locally, where stress concentrations exist. The prestressed concrete carries the normal pressure loads. Because of its viscoelastic-plastic behavior, the concrete is able to transfer load from highly stressed regions to regions of low stress. Thus, local defects in the concrete are insignificant. Under operating conditions the PCRV responds, because of the prestress, like an isotropic material.<sup>5</sup>

The general load-strain behavior of a PCRV is shown in Fig. 3. In the first regime the vessel behaves elastically and the concrete is being unloaded as the internal pressure increases. In the second regime the vessel behavior is still elastic, but the stress in the concrete becomes tensile and cracks begin to appear. In the third regime the concrete is fully cracked and the steel begins to deform plastically up to the ultimate load. It is on the behavioral basis described that catastrophic failure of a PCRV is considered incredible,<sup>6</sup> providing the head is sufficiently overdesigned.

Costes et al.<sup>7</sup> emphasize the desirable safety characteristics of PCRVs that can permit ample warning before rupture. These characteristics are provided by the strength and plasticity of the bonded and unbonded steel in the structure, along with the rigidity of the concrete and the leak-tightness of the liner. A large density of reinforcing steel in the concrete will help to control size and distribution of cracks. The large "crack opening displacement" of prestressed concrete means that a crack will be well extended and, thus, visible or detectable before vessel rupture can occur.

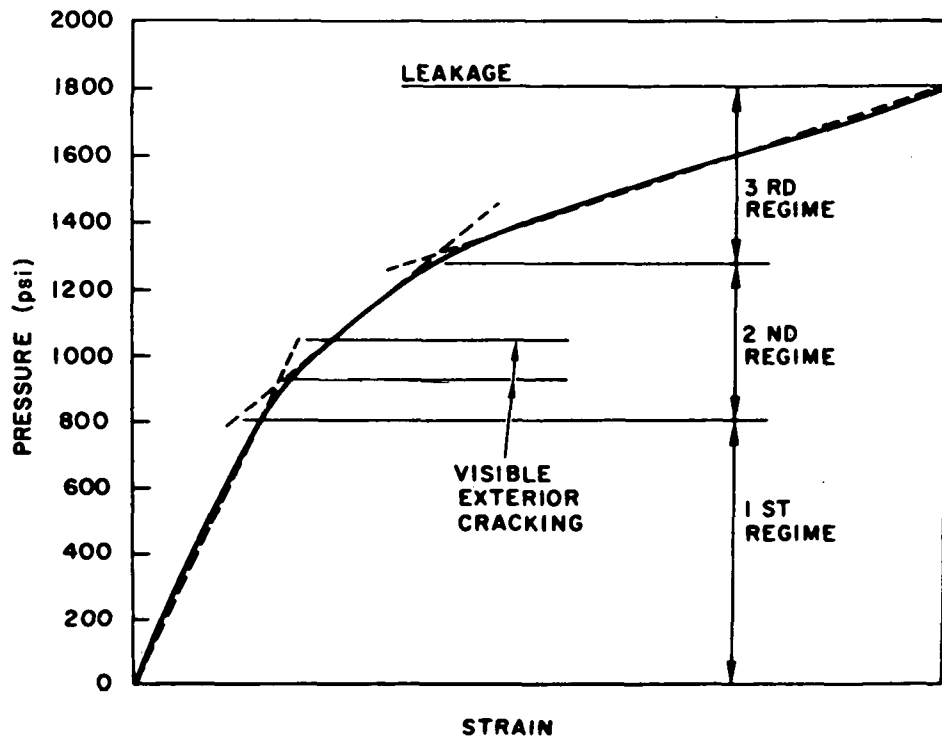


Fig. 3. Predicted Strain Behavior of a PCRV. Source: C. P. Tan, *Prestressed Concrete in Nuclear Pressure Vessels. A Critical Review of Current Literature*, ORNL-4227 (May 1968).

It is very difficult to develop a clear understanding of diagonal-tension and shear failures in a redundant structure such as a PCRV, since the concrete is frequently in a complex state of multiaxial stress. However, it is possible to formulate a conservative design based on current knowledge of shear in beams and slabs.<sup>6</sup> Since a PCRV cannot be rationally designed because of lack of knowledge of concrete failure under multiaxial states of stress and shear mechanisms, further study is needed. Other properties of concrete, both short term and long term, are also important in design. Figure 3 represents time-independent behavior. During the design life of a PCRV (30 to 40 years), irreversible deformation (primarily from creep and shrinkage) occurs. Although thermal loads do in themselves produce significant deformations of the highly redundant PCRV, creep and shrinkage rates are altered by temperature, and long-term behavior is affected.<sup>8</sup> An understanding of the compressive strength of concrete with aging, long-time curing, and various thermal conditions is important, because the concrete must remain prestressed in compression for the effective life of the vessel. Physical properties such as thermal expansion, thermal conductivity, and diffusivity, as well as the mechanical properties, need to be evaluated with respect to their separate or combined effects on the structural integrity of the vessel. Specific conditions such as temperature, radiation, moisture, state of stress, and age can affect various properties and must

be evaluated for their impact on short- and long-term behavior. The increased understanding of concrete properties and vessel behavior can lead directly to increased vessel efficiency, safety, and reliability.

### 3. CONCRETE PROPERTIES

#### 3.1 General

Concrete is a general term for a class of ceramic materials which vary widely in their properties and their applications. The American Concrete Institute defines concrete as "a composite material that consists essentially of a binding medium within which are embedded particles or fragments of aggregate; in portland cement concrete, the binder is a mixture of portland cement and water."<sup>9</sup> By varying the constituents and their relative proportions in the mixture, one can obtain concretes of widely differing properties. There are five types of portland cement and other kinds of cement as well. Aggregates such as natural sand, manufactured sand, crushed stone, gravel, crushed gravel, slag materials, etc., will vary considerably in their properties. In addition, of course, the size and distribution of aggregates may be varied as desired for certain effects. The water content has a great effect on concrete properties, and, even from a chemical standpoint, variations of water chemistry between different geographical locations can result in different properties.

In the face of this wide range of specific concrete variables, we will attempt to direct discussion toward the relatively-high-strength structural-grade concretes. For the purposes of this report, that means concrete made by recognized standard practice and with the types of materials used in PCRV construction to date.

It is well known, and often stated,<sup>6, 10, 11</sup> that the great variability in properties of concretes used in laboratory investigations and field construction precludes precise comparisons of experimental data. Thus, Browne<sup>10</sup> indicated that precise data of many properties are required for a specific vessel design and that, because of considerable variation in materials and mixture proportions, tests must be performed on the concrete mixture designed for each vessel. The following section will describe the concrete used thus far in PCRV design and construction.

#### 3.2 PCRV Concretes

Reference 6 provides data concerning the concrete mixtures used for construction of the Oldbury, G2, G3, and EDF3 vessels. The following represent typical characteristics of PCRV concrete:<sup>6</sup>

1. cement, air entraining type 2;
2. sand, graded to meet ASTM specifications;
3. aggregate, gravel, or limestone crushed and graded to meet ASTM specifications with size about 2.54 cm (1 in.) or less;

4. amount of cement, about 6 to 6 1/2 sacks per cubic yard;
5. water-to-cement ratio, 0.4 to 0.5;
6. compressive strength, 34.47 to 41.37 MPa (5000 to 6000 psi) at 28 days; and
7. slump, 5.08 to 10.16 cm (2 to 4 in.).

The design data for the concretes used in General Atomic model 2 are given in Table 2 as specific examples.

Section III, Division 2, of the ASME Boiler and Pressure Vessel Code (Standard Code for Concrete Reactor Vessels and Containments)<sup>12</sup> provides some requirements for the materials and mixture design of concrete for PCRVs. For example, type II portland cement and aggregates must conform to ASTM C-33. In addition, the maximum size of coarse aggregate shall not be larger than 1/5 of the narrowest dimension of the finished wall or slab nor larger than 3/4 of the minimum clear spacing between reinforcing steel and/or embedments. The water used for mixing shall have less than 2000 ppm total solids content and shall not contain more than 250 ppm of chlorides as Cl<sup>-</sup>. Admixtures are allowed in accordance with the construction specification of a particular PCRV. Measurement of certain properties is required prior to construction. These are: slump, compressive strength, flexural strength, splitting tensile strength, static modulus of elasticity, Poisson's ratio, coefficient of thermal conductivity, coefficient of thermal expansion, creep of concrete in compression, shrinkage coefficient (length change or cement-mortar and concrete), density, and aggregates for radiation shielding concrete.

With regard to applicable environmental or design conditions, or specifics of the age and temperature at which the properties shall be obtained, the construction specification must specify them as well as any other properties to be measured. In addition, if a particular property listed above is not of interest, the construction specification will so state. Applicable testing specifications are given for each listed property. More details are given in the ASME Code concerning bases for selection of concrete mix proportions. The construction specification is a design document which specifies the actual vessel design parameters, and the concrete mix proportions are selected on the basis of meeting the property requirements.

With regard to desirable concrete properties, Browne<sup>10</sup> lists the property and justification for each in Table 3. Tan<sup>6</sup> lists essentially the same properties with the additions of: high specific heat, low heat of hydration, and satisfactory hydrogen content materially unaffected by the operating temperature. The main concerns, according to Tan, are the effects of irradiation and, particularly, temperature above the normal ambient on those properties. Many investigators have reached similar conclusions.

As stated in the Introduction, this report is concerned with the properties of plain concrete. Reference to reinforced or prestressed concrete will only occur when required to tie the discussion to the primary application of interest. The PCRV is designed to withstand the high reactor operating pressure, contain the reactor coolant, and serve as a biological shield against radiation. Thus, it is a mass concrete structure. As such, it is desirable to relate the properties of the

Table 2. Mix Design Data for Conventional Concrete  
Used for General Atomic Model 2

	Mix Designation <sup>a</sup>								
	3/4 A	3/4 B	3/4 C	3/4 D	3/4 E	3/4 F (JS) <sup>b</sup>	1 1/2 A	1 1/2 B	1 1/2 C
Aggregate, <sup>c</sup> lb/yd <sup>3</sup>	3077	3025	2906	2975	5948	5448	3189	3145	3089
Cement, <sup>d</sup> sacks/yd <sup>3</sup>	6.38	6.94	8.21	7.35	7.69	7.69	5.44	6.12	6.69
Water, lb/yd <sup>3</sup>	334	338	339	344	333	333	319	319	318
Water-to-Cement Ratio	0.555	0.517	0.440	0.498	0.459	0.459	0.623	0.550	0.505
Aggregate-to-Cement Ratio	5.12	4.64	3.78	4.30	4.08	4.08	6.22	5.47	4.92
Unit Weight, lb/ft <sup>3</sup>	146.1	146.3	148.4	147.0	147.9		149.3	150.0	150.1
Slump, in.	1 1/2	1 5/8	1 1/2	1 3/8	1 1/2	1 1/4	1 3/4	1 5/8	1 3/4
Compressive Strength, <sup>e</sup> psi									
At 28 days	4963	5528	7067	5998	6106	6413	4298	5207	6260
At 60 days	6006	6780	8360	6751			5670		7215
At 90 days									6380
Modulus of Elasticity at 28 days, psi				4.11 × 10 <sup>6</sup>					

<sup>a</sup>Prefix 3/4 is 3/4 in. maximum-size aggregate; prefix 1 1/2 is 1 1/2 in. maximum-size aggregate.

<sup>b</sup>Mixed at job site with job mixer.

<sup>c</sup>Andesite from Lyons, Colorado.

<sup>d</sup>Type 2 portland cement from Denver, Colorado.

<sup>e</sup>Average of three specimens.

Source: E. G. Endebrock, *Prestressed Concrete Reactor Vessels: Review of Design and Failure Criteria*, LA-5902-MS, Los Alamos Scientific Laboratory (May 1975). Work done by Testing Engineers, Inc., San Diego, Calif. SIKA Plastiment water-reducing agent used in all mixes (2 oz. per sack of cement).

Table 3. Preferred Concrete Properties

Preferred property	Reasons
High compressive strength at normal and elevated temperature	To reduce vessel thickness and increase allowable stresses. Other strength properties are to some extent related to compressive strength.
Good mix workability	To ensure good compaction in placing, particularly in areas where high concentrations of reinforcement and prestress ducting exist.
High density	To provide good neutron and gamma ray absorption properties.
Low elastic and creep deformation under load	To reduce movements and the redistribution of stresses under varying load and temperature cycles. To reduce prestress losses.
Low drying shrinkage	To reduce movements and temperature stresses.
Low thermal expansion	To reduce movements and temperature stresses.
Resistant to thermal shock	To prevent damage to structure under rapid heat application, i.e. adjacent to steam openings.
High thermal conductivity	To minimize the cooling system required to keep the vessel concrete at a permissible temperature.
Immunity to radiation damage	To minimize the possible deterioration of concrete in high irradiated areas.

Source: R. D. Browne, "Properties of Concrete in Reactor Vessels," group C, paper 13, Conference on Prestressed Concrete Pressure Vessels, Westminster, S.W.I., March 1967.

plain concrete to those in mass concrete. The term "mass concrete" refers to concrete as used in massive structures and is defined as:<sup>13</sup> "Any large volume of cast-in-place concrete with dimensions large enough to require that measures be taken to cope with the generation of heat and attendant volume change to minimize cracking." For PCRVs, thicknesses of a few feet to more than 30 ft are of concern. In addition, the migration of free moisture in a massive section will not necessarily be represented by a small laboratory specimen. Thus, a primary concern in PCRV concrete investigations is the modeling of mass concrete in the laboratory. This has generally been accomplished by sealing the specimens against loss of free moisture. The moisture migration problem and its effects on mechanical properties will be discussed later.

### 3.3 Effects of Temperature

As previously mentioned, temperature is an important environmental parameter in a PCRV. PCRV designs to date have provided for elaborate cooling systems and insulation barriers to maintain the concrete at a relatively low temperature. An example of this system is shown in Fig. 1 for the GA-designed HTGR.<sup>3</sup> Technical discussion of this cooling system is not intended; rather, the point to be emphasized is that the procedures required for cooling the concrete are elaborate and therefore, from fabrication and operational viewpoints, expensive. Designs of PCRVs relative to allowable concrete temperatures are necessarily conservative because of a lack of knowledge of concrete behavior at elevated temperatures. An understanding of high-temperature behavior is also required to assure safety in the event of accidental over-temperature and/or over-pressure conditions.

Table 4 gives the ASME code temperature limits for various locations in the PCRV for the appropriate conditions (normal operation, etc.).<sup>12</sup> As seen, the temperature should not exceed 65°C (150°F) at the liner-concrete interface and in the bulk concrete. Between cooling tubes (near the liner), 93°C (200°F) is given as the maximum allowable. For comparison, Table 1 provides the design temperature limits for some existing PCRVs. Thus, PCRV designs to date show a wide range of allowable concrete temperature from 45°C (113°F) for Wylfa to 80°C (176°F) for St. Laurent. The allowable temperature drops across the wall range from 15°C (59°F) in Wylfa to 50°C (122°F) for the French vessel.<sup>6</sup> In any case, the maximum allowable temperatures are very low compared with the reactor coolant temperatures, and effective thermal barriers are required, especially for the HTGR.

#### 3.3.1 Compressive Strength

Although the concrete of a PCRV is in its least stressed condition during normal operation, concern for compressive strength is valid, because the concrete is under a compressive stress during nonoperating conditions owing to the axial and circumferential prestressing forces.

Table 4. Condition Categories and Temperature Limits  
for Concrete and Prestressing System

Load Category	Area	Temperature Limits, F
Construction	Bulk concrete	130
Normal	Liner Effective at liner-concrete interface	150
	Between cooling tubes	200
	Bulk concrete	150
	Bulk concrete with nuclear heating	160
	Local hot spots	250
	Distribution asymmetry	50
	At prestressing tendons	150 <sup>1</sup>
	Liner interface transients (twice daily) range	100—150
Abnormal and Severe Environmental	Liner Effective at liner-concrete interface	200
	Between cooling tubes	270
	Bulk concrete	200
	Local hot spots	375
	Distribution asymmetry	100
	At prestressing tendons	175
	Liner interface transients range	100—200
Extreme Environmental	Liner Effective at liner-concrete interface	300
	Between cooling tubes	400
	Bulk concrete	310
	Local hot spots	500
	Distribution asymmetry	100
	At prestressing tendons	300
	Liner interface transients range	100—200
Failure	Bulk concrete Unpressurized condition	400
	Pressurized condition	600

NOTE:

(1) Higher temperatures may be permitted as long as effects on material behavior for example relaxation, are accounted for in design.

Source: "Concrete Reactor Vessels and Containments," ASME Boiler and Pressure Vessel Code, Section III, Division 2 (1975).

Also, the concern for elevated-temperature behavior stems from the fact that the concrete will be hot after reactor shutdown and, because of no internal pressure, will be subjected to the maximum compressive stresses at the elevated temperature or possible tensile stresses in the event of postoperational cool-down of the PCRV.

In discussing strength testing of concrete, Dougill<sup>14</sup> points out that only sufficiently stiff machines can provide true representation of concrete behavior and that care must be taken in using the peak stress as a value of strength. Figure 4 shows typical stress-strain curves for concrete in uniaxial compression tested at various strain rates. There is a danger in assuming that the peak stress is the stress at failure, and that behavior, under decreasing strain rates with consequential redistribution of stress, is neglected. Figure 4 shows that the peak stress did not change appreciably but that behavior changed dramatically.

In examining concrete test results, one must always keep in mind that differences in concrete can be quite substantial and that experimental techniques for evaluating elevated-temperature properties are not standardized and are difficult to perform. Thus, wide variation in data should be expected, and conflicting results can be found in the literature.

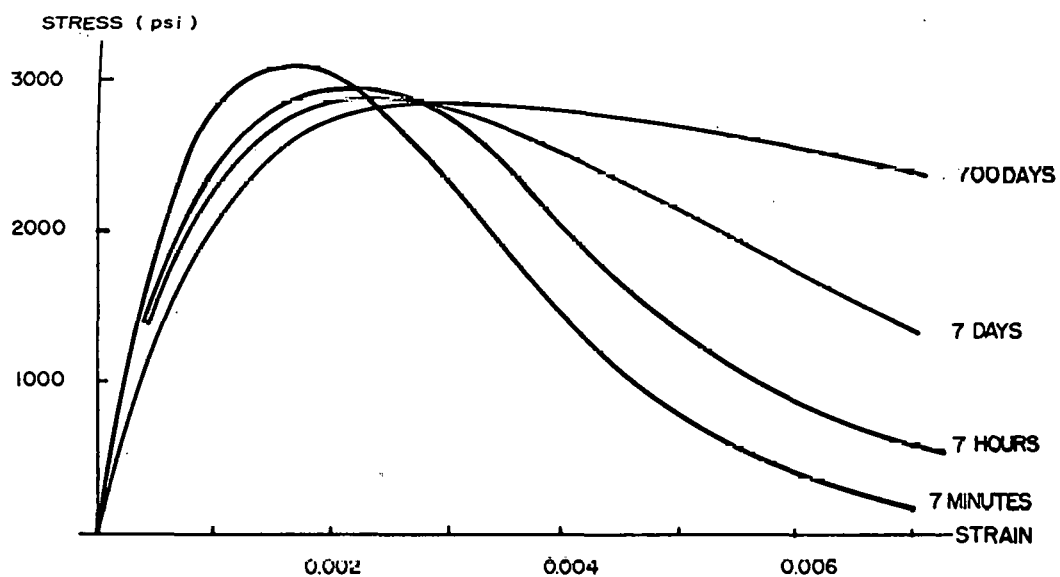


Fig. 4. Stress-Strain Curves for Concrete in Compression. Source: J. W. Dougill, "Structural Properties of Concrete: A Review," lecture X of lecture notes from the program; *Prestressed Concrete Nuclear Reactor Structures*, March 1968.

Tan<sup>6</sup> states that the strength of concrete, like its modulus of elasticity, is believed to be very little affected over the temperature range used in the current PCRV designs. However, he presents the data of Hannant,<sup>15</sup> which show that, at 100°C (212°F), unsealed and sealed concrete (limestone aggregate) suffered a 30% loss of compressive strength (compared with the reference 28-day strength). Further tests at 150°C (302°F) revealed a strength gain for the dry (unsealed) concrete, but the sealed concrete strength decreased further for a total loss of 40%. Results from Saemann and Washa's<sup>16</sup> tests on an unsealed gravel concrete showed a relative strength of 88% at 75°C (167°F) and 80% at 100°C (212°F). Further increases in temperature resulted in a relative strength of about 105% at 200°C (392°F). The authors offered no explanation for the results.

Davis,<sup>17</sup> in a review paper, discussed the high-temperature strength of concrete and emphasized the importance of age at testing. As he stated, the properties after 28 days of moist storage at room temperature are considered standard; however, it is known that concrete will continue to gain strength with age if moisture is available for continued hydration. In this regard, he references tests by Withey<sup>18</sup> in which 50-year-old specimens had strengths of 35.8 and 44.8 MPa (5200 and 6500 psi) compared with their 28-day reference strength of 13.8 MPa (2000 psi), strengths of 260 and 325% of reference. Davis also presents previously unpublished data in which specimens were moist-cured for 28 days, air-dried until 90 days old, heated for 2 weeks at temperature, and tested at room temperature. Based on a 90-day reference strength, 28-day moist concrete had only 78% of reference strength at 20°C (68°F). Davis states that specimens which are more or less saturated with water at the time of test have lower compressive strength than dry specimens. This is an interesting point which was made without the benefit of much data on concrete specimens sealed against moisture loss. Davis attributes that effect to the presence of pore water during testing and says that is why some researchers (such as Hannant, Saemann and Washa) noted a 10 to 40% strength loss from 66 to 149°C (150 to 300°F) and less compressive loss at higher temperatures. With regard to testing at the exposure temperature (hot testing) or elevated-temperature exposure followed by testing at room temperature (cold testing), Davis concluded that, generally, greater strength losses are incurred with cold-tested specimens. The effect of thermal cycling was considered by Davis, and he states that the loss in strength for concrete subjected to wide fluctuations in temperature has been observed to be two or three times as great as for constant exposure to high temperature, depending on the severity of thermal cycling. He did not reference any specific investigations. He presented some previously unpublished Hanford data, however, which shows strength drops to 73% for 20 thermal cycles of 38 to 200°C (100 to 392°F). For a cyclic pattern of 38 to 350°C (100 to 662°F), the strength was 60% after 1 cycle and 65% after 20 cycles (90-day reference). Thus, his data do not substantiate the conclusion regarding cycling. Davis concludes by stating that, for constant exposure to 66 to 93°C (150 to 200°F), the loss in strength, if any, is quite small; and for temperatures as high as 260 or 316°C (500 or 600°F), the deterioration in structural properties is ordinarily tolerable.

Campbell-Allen, Low, and Roper<sup>19</sup> presented data on unsealed concrete exposed to high temperatures and cold-tested. They also performed thermal cycling tests (one to ten cycles). They found that up to 250°C (482°F) the loss of compressive strength after one cycle is small (<10% loss). However, for ten cycles exposure to 200°C (392°F), the strength went to 74% of reference, while five and ten cycles at 300°C (572°F) resulted in 64 and 60% respectively. One test was performed on 90-day-cured concrete, and one exposure to 300°C (572°F) resulted in a strength of 86% of reference. The authors state that lengthy curing periods above 28 days do not improve the heat resistance of concrete tested in compression. Their conclusion was based on one temperature, one cyclic rate, and only two relatively short curing times (especially compared with the mass concrete in a PCRV). In addition, the 90-day concrete was 20% stronger than at 28 days. They made an interesting observation of failure behavior during testing. The reference specimens failed with a loud explosion, indicating high dissipation of energy, whereas the heated cylinders failed gently. They attribute that to the differences in elastic moduli and strengths.

Campbell-Allen and Desai<sup>20</sup> performed tests on many different concretes with variations in aggregate and cement. Some specimens were subjected to thermal cycling, and all tests were performed at room temperature on unsealed specimens. The specimens with limestone aggregate showed significant deterioration with increasing temperature, as shown in Fig. 5. The most marked effect at 65°C (149°F) is the reduction in compressive strength of the all-limestone concrete (with cement 2) to less than 75% of reference. Sustained exposure at 65°C (149°F) for the same concrete did not substantially affect the strength. As seen in Fig. 5, the first cycle at 200 or 300°C (392 or 572°F) causes most of the resultant damage to strength, and continued cycling causes further deterioration. Cement 2 differed from cement 3 (both portland cements) primarily in its lower content of tricalcium aluminate. In addition, the concrete incorporating the fireclay brick showed the best mechanical properties, while the limestone concrete deteriorated the most. The same observation was made in this report as in a previous one<sup>19</sup> with regard to observed failure behavior. That is, the unheated specimens failed suddenly with a loud report, while after heating, failures were gradual and with little noise. In addition, tests of aggregate compressive strength after 20 cycles to 300°C (572°F) resulted in no reduction for the fireclay brick and a 10% reduction for limestone.

Kawahara and Haraguchi<sup>21</sup> performed tests on gravel concrete in which they investigated the effect of unsealed and sealed curing at 20°C (68°F) and 80°C (176°F). Basically, they found that the compressive strength of concrete is substantially reduced if young concrete is subjected to 80°C (176°F) heating. Three months of moist curing at 20°C (68°F) followed by 80°C (176°F) heating resulted in only a 7% strength loss. However, for specimens subjected to 80°C (176°F) heating one day after casting for 13 weeks, the strength at 80°C (176°F) was only 38% of reference strength [based on 20°C (68°F) curing]. Thus the authors emphasize the importance of a lengthy time for hydration to take place at lower temperatures.

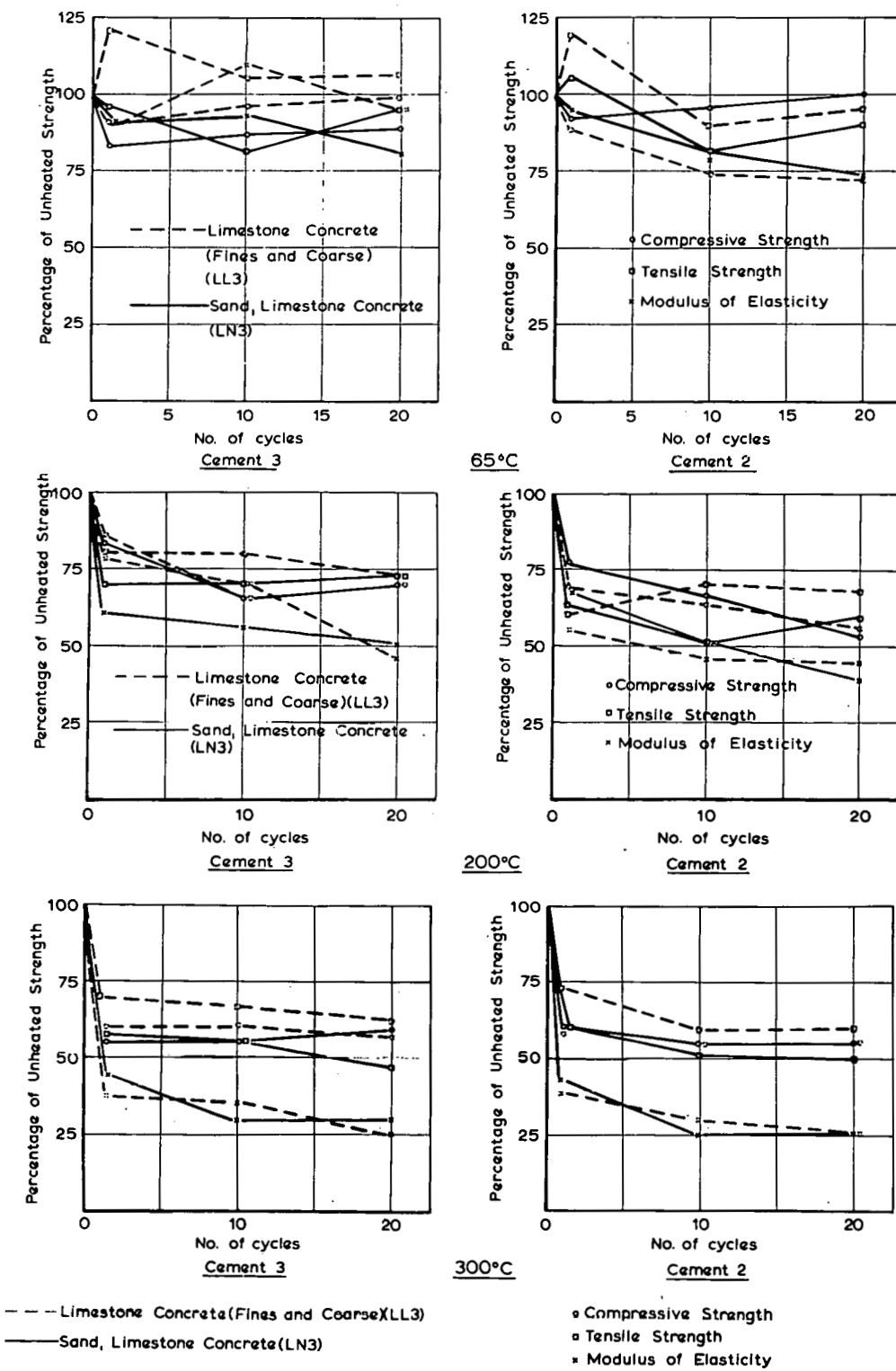


Fig. 5. Effects of Temperature Cycles on Limestone Concretes. Source: D. Campbell-Allen and P. M. Desai, "The Influence of Aggregate on the Behavior of Concrete at Elevated Temperatures," *Nucl. Eng. Des.* 6(1): 20 (August 1967).

The effect of sustained stress during heating of concrete was investigated by Abrams<sup>22</sup> on gravel and expanded shale concretes. Hot tests were performed on stressed and unstressed specimens, while some unstressed specimens were heated and then cold-tested for residual compressive strength. Results for the siliceous aggregate concrete are shown in Fig. 6. Reference strengths for their tests were determined on companion specimens tested at 21°C (70°F) within two days of the heated specimen tests in the same group. Testing was begun when the center of the cylinder recorded a 75% relative humidity (performed with control specimens for each group). As shown in Fig. 6, the specimens heated in the unstressed condition and cold-tested showed the greatest reduction in compressive strength. For exposure to 200°C (392°F), the strength decreased to 85%, while exposures to 370°C (698°F) and 700°C (1292°F) resulted in residual strengths of 65 and 10% respectively. In comparison, the unstressed specimen which was hot-tested did not substantially decrease in strength until 400°C (752°F) had been reached. The stressed specimens showed a strength increase of a few percent up to 400°C (752°F) and at 650°C (1202°F) still retained 50% strength.

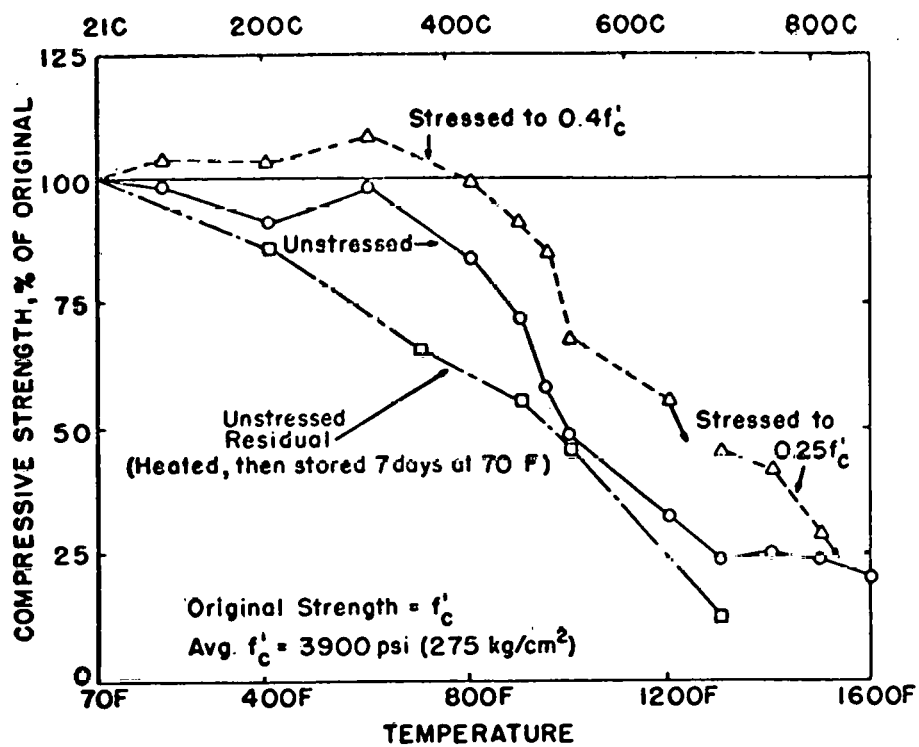


Fig. 6. Siliceous Aggregate Concrete Compressive Strength vs Temperature and Stress. Source: M. S. Abrams, "Compressive Strength of Concrete at Temperatures to 1600°F," ACI SP-25, *Temperature and Concrete* (1970).

Thus, stressing the concrete even to  $0.25 f_c'$  ( $f_c'$  = original strength) had a beneficial effect over the entire temperature range. Abrams states that Malhotra<sup>23</sup> attributed the smaller strength loss under the stressed condition to a retardation of crack formation. Figures 7, 8, and 9 depict the effect of aggregate type on the strength under the various conditions shown. There is not a great difference between the various concretes until a temperature of about  $500^\circ\text{C}$  ( $932^\circ\text{F}$ ) is reached, at which point the siliceous gravel concrete loses strength most rapidly with increasing temperature. Concerning the effect of stressing during heating, the stress level (whether 0.25, 0.40, or  $0.55 f_c'$ ) had little effect on the compressive strength of concrete at any given test temperature. These results were also independent of (1) original strength of the concrete, (2) aggregate type, and (3) test temperature. Also, original strength had little to do with subsequent strength behavior for all types of tests. Thus, Abrams results showed that specimens stressed during heating retained higher strengths than the unstressed and that unstressed specimens showed greater strength loss in cold testing than in hot testing. The latter point agrees with the observations of Davis.<sup>17</sup>

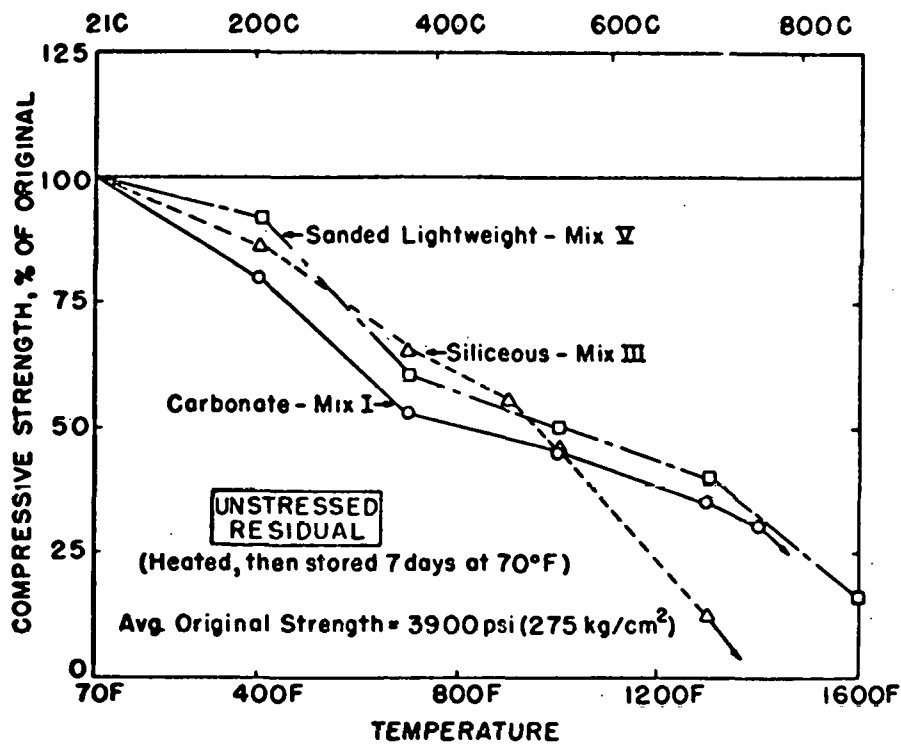
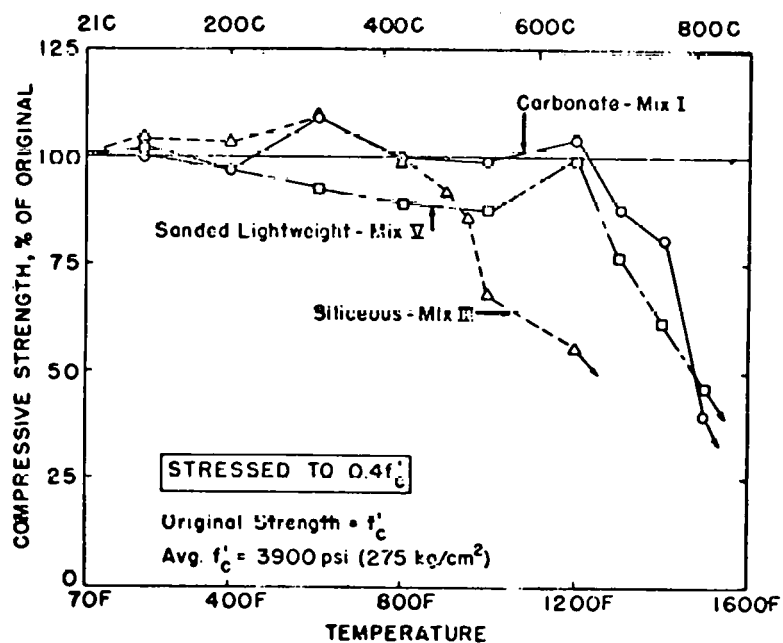
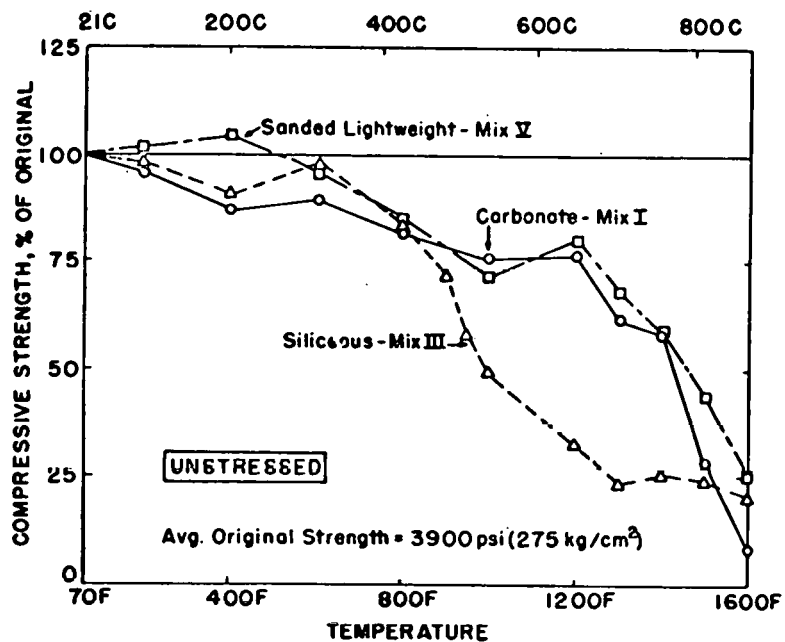


Fig. 7. Residual Compressive Strength vs Temperature for Various Concrete Mixtures. Source: M. S. Abrams, "Compressive Strength of Concrete at Temperatures to  $1600^\circ\text{F}$ ," ACI SP-25, *Temperature and Concrete* (1970).



Nasser<sup>24</sup> concluded that up to 100°C (212°F) the compressive strength of mass concrete is not influenced after early age. Ravina and Shalon<sup>25</sup> concluded that the effect of temperature at casting and early curing, within the range of 15 to 45°C (59 to 113°F), on compressive strength of concrete made with portland cement (types I and V) varies considerably and appears to depend on the specific cement composition and, possibly, also on its fineness. They feel that systematic studies of portland cement concrete with varying composition will help to explain the mechanism of temperature effect on strength.

Browne and Blundell,<sup>26</sup> in their review paper on concrete property research, stated that results of Hannant,<sup>27</sup> Parkinson,<sup>28</sup> and Campbell-Allen and Desai<sup>29</sup> indicate that when limestone crushed rock materials are used with ordinary portland cement, the resultant strength of concrete heated to 90°C (194°F) can be reduced to 60%. They conclude that limestone should be avoided as a PCRV concrete aggregate because of the thermal incompatibility between the coarse aggregate and the cement paste. Thus, they would limit aggregate selection for pressure vessels to medium-silica-content crushed rock (basalts, dolerites, hornfels, etc.) or to flint gravels. The early temperature cycle is mentioned by Browne and Blundell as an important factor that will influence the compressive strength of mass concrete. That is, the rapid rate of heat evolution produced during the initial stages of cement hydration affects the compressive strength of concrete. Figure 10 shows results of early age heat cycling (to simulate heat evolution of *in situ* mass concrete) on limestone concretes<sup>29</sup> and a siliceous concrete.<sup>26</sup> Both types were subjected to early heat cycles of about 35°C (95°F), and the limestone concrete with type I cement was subjected to a 53°C (127°F) cycle. The authors state that the limestone concrete is most adversely affected by the early age heat cycle and that the siliceous concretes are affected to a far lesser extent. This is true as regards the absolute magnitude of the effect. However, it appears from the data shown that, for the 35°C heating, the limestone concrete (type IV) did not experience a strength reduction at 28 days compared with the standard cured specimen. Also, at 220 days, the heated limestone concrete, although 15% less strong than the standard cured, increased in strength to 140% of reference. The siliceous concrete, on the other hand, only increased to 120% of reference after 300 days. It is true that the limestone concrete subjected to a 53°C (127°F) early heat cycle experienced a strength reduction to only 70% of reference. That is significant, but no comparable data are shown for the siliceous concrete with which to base a comparison for that higher-temperature heat cycle. It is presumed that Browne's and Lapinas' studies were conducted on unsealed specimens.

The results of Kawahara and Haraguchi,<sup>21</sup> discussed previously, on early age hardening at 80°C (176°F) showed that a gravel concrete had only 38% of the compressive strength of a standard cured specimen. Yet the strength ratio of concrete cured in sealed condition at 80°C (176°F) to concrete cured in sealed condition at 20°C (68°F) was 185% at 1 week, 120% at 4 weeks, and 105% at 13 weeks.

The previously discussed observation by Davis<sup>17</sup> that concrete saturated by moisture exhibits less strength at elevated temperature than dry specimens is of fundamental concern to discussion of concrete strength in a mass concrete situation. Lankard et al.<sup>30</sup> investigated

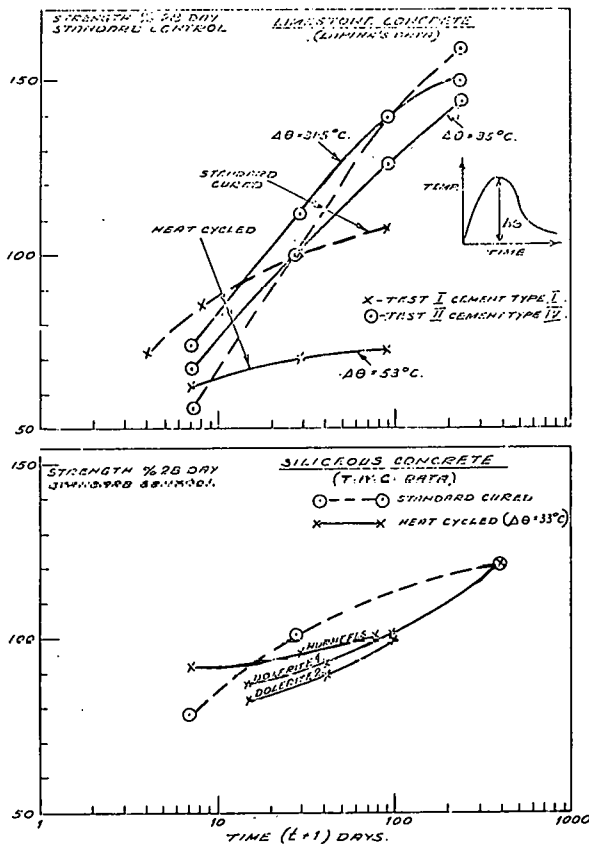


Fig. 10. Effect of Hydration on Concrete Strength. Source: R. D. Browne and R. Blundell, "Relevance of Concrete Property Research to Pressure Vessel Design," ACI SP-34, *Concrete for Nuclear Reactors*, pp. 69-102 (1972).

concrete properties with that situation in mind. Their study was directed at determining the effects of moisture content on structural properties of concrete at temperatures up to 260°C (500°F). Concretes with gravel or limestone aggregates and type II cement were studied with water/cement ratios of 0.40 and 0.42 respectively. Cylindrical specimens 10.2 cm (4 in.) in diameter and 20.3 cm (8 in.) long were cured in 100% humidity for 28 to 200 days. The authors performed hot and cold testing on unsealed concrete heated at atmospheric pressure as well as hot and cold testing on concrete heated at saturated steam pressure (referred to as sealed concrete, although no actual sealing of the specimens with an impermeable covering was used) in an autoclave device. In all cases, heating to the desired temperature was carried out slowly to minimize temperature gradients.

The sealed specimens that were tested hot were heated under water in the pressure device shown in Fig. 11. The device used pressure seals and a bellows assembly which allowed application of a compressive load to the specimens while maintaining an equilibrium pressure around them. In addition, the entire assembly was placed in a furnace for heating.

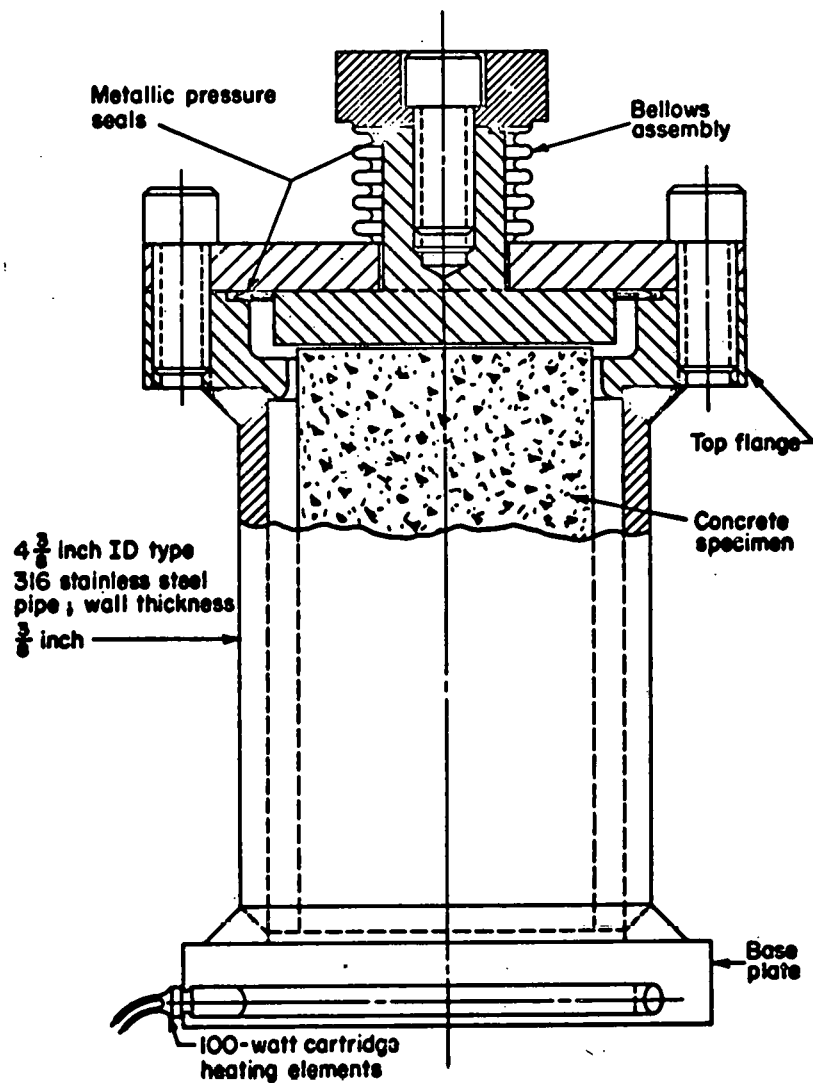


Fig. 11. Pressure Can Test Assembly. Source: D. R. Lankard et al., "Effects of Moisture Content on the Structural Properties of Portland Cement Concrete Exposed to Temperatures up to 500°F," ACI SP-25, Temperature and Concrete (1970).

The temperatures and corresponding times at temperature for the unsealed specimens were 260°C (500°F) (75 days), 190°C (374°F) (82 days), 121°C (249°F) (91 days), and 80°C (176°F) (98–109 days). Figures 12 and 13 show their data for unsealed hot- and cold-tested concrete specimens, using limestone and gravel aggregates respectively. Both limestone and gravel concretes first showed increases in compressive strength compared with the reference strength (as cured 28-day strength on saturated surface-dry specimens), whether they were tested hot or cold. At 190°C (374°F) the cold-tested limestone concrete decreased to about 90% of reference, with the hot-tested limestone specimens not decreasing to that level until 260°C (500°F). Only the cold-tested series of the gravel concretes resulted in a strength decrease, and that did not occur until 260°C (500°F), with the strength being 90% of reference. The primary observation made by the authors was that the effect of test temperature on the compressive strength of both unsealed concretes heated for long times up to 260°C (500°F) was minimal. One problem with representing the results as the effect of elevated-temperature exposure on strength is that the reference strength was based only on the as-cured, saturated, surface-dry, 28-day strength. It would be of interest to use a reference strength based on specimens that had been air-dried at room temperature for the various lengths of time corresponding to the heat-treated specimens. That is not to say that using the 28-day strength was inappropriate, since most concrete mixture specifications for PCRVs and other structures require the attainment of a certain specified strength at 28 days. However, beyond 28 days, further cement hydration would result in a continual strength gain, and the actual effect of elevated temperature as a single parameter could be evaluated more directly.

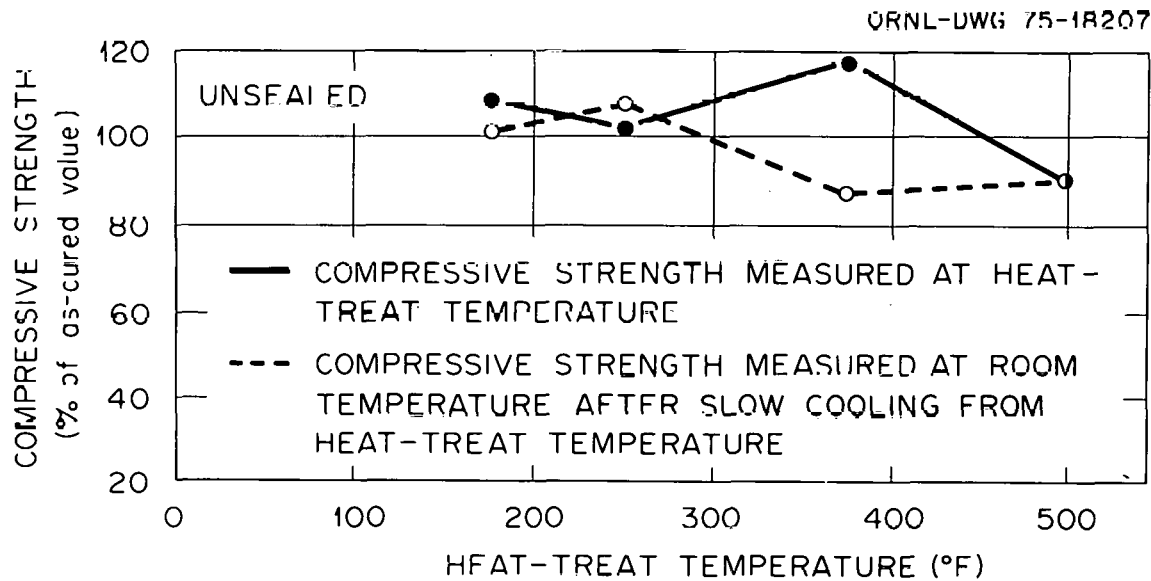


Fig. 12. Compressive Strength vs Temperature for Limestone Concrete, Unsealed. Source: D. R. Lankard et al., "Effects of Moisture Content on the Structural Properties of Portland Cement Concrete Exposed to Temperatures up to 500°F," ACI SP-25, *Temperature and Concrete* (1970).

ORNL-DWG 75-18208

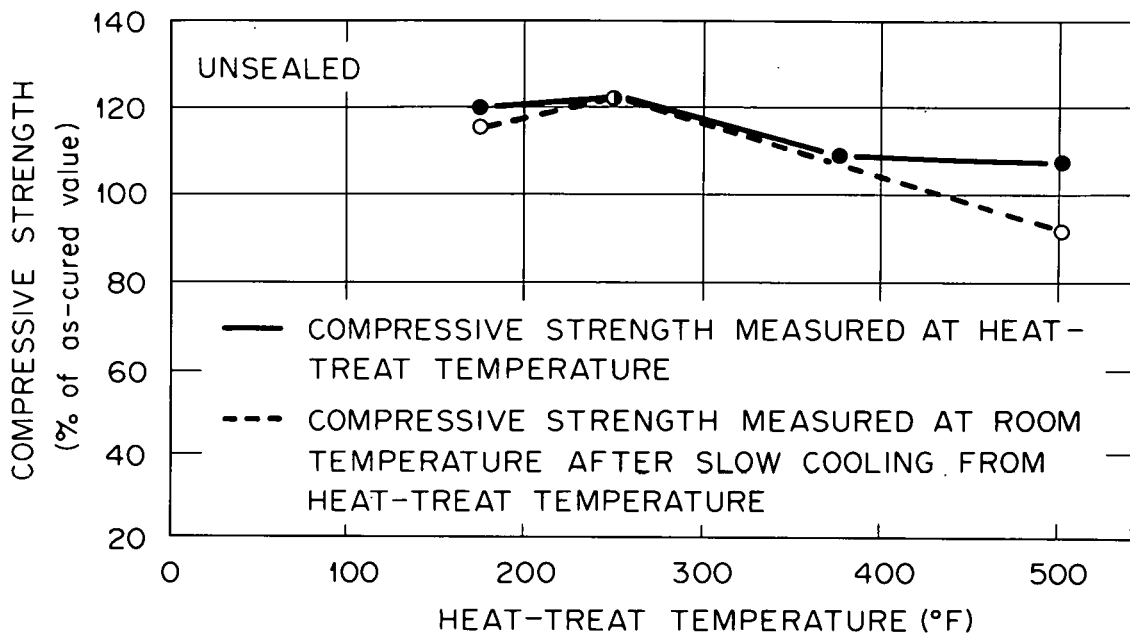


Fig. 13. Compressive Strength vs Temperature for Gravel Concrete, Unsealed. Source: D. R. Lankard et al., "Effects of Moisture Content on the Structural Properties of Portland Cement Concrete Exposed to Temperatures up to 500°F," ACI SP-25, *Temperature and Concrete* (1970).

In the case of sealed concrete, the test temperatures and corresponding fog-room curing times were 80°C (176°F) (150 days), 121°C (249°F) (157 days), 190°C (374°F) (180 days), and 260°C (500°F) (260 days). In this case the reference strength was taken on concrete fog-room-cured for 115 days at room temperature. The holding time at testing temperature was 20 to 28 hr. The results of hot testing under saturated steam pressure conditions are shown in Fig. 14 for the gravel concrete. The compressive strength at 121°C (249°F) was reduced to about 77% of reference, while further reductions to 70 and 48% took place at 190 and 260°C (374 and 500°F), respectively. The results of cold testing of specimens following heating under saturated steam pressure in a conventional autoclave are depicted in Fig. 15. Tests were conducted only at 121 and 260°C (249 and 500°F) for this series. All specimens were fog-room-cured from 95 to 121 days prior to testing. As indicated in the figure, some specimens received various cycles of air and autoclave exposures. For the gravel concrete, no strength reduction took place at 121°C (249°F), and, in fact, strength increases occurred for two of the conditions shown. At 260°C (500°F) the specimen heated for one cycle was reduced to 60% of reference strength, while the specimen that was autoclave-heat-cycled three times was reduced to only 80% of reference. The limestone concrete showed reductions to 87 and 93% at 121°C (249°F) for one and three autoclave cycles respectively. At 260°C (500°F) the specimens were independent of cycles, and both one- and three-cycled specimens were reduced to 45% of reference.

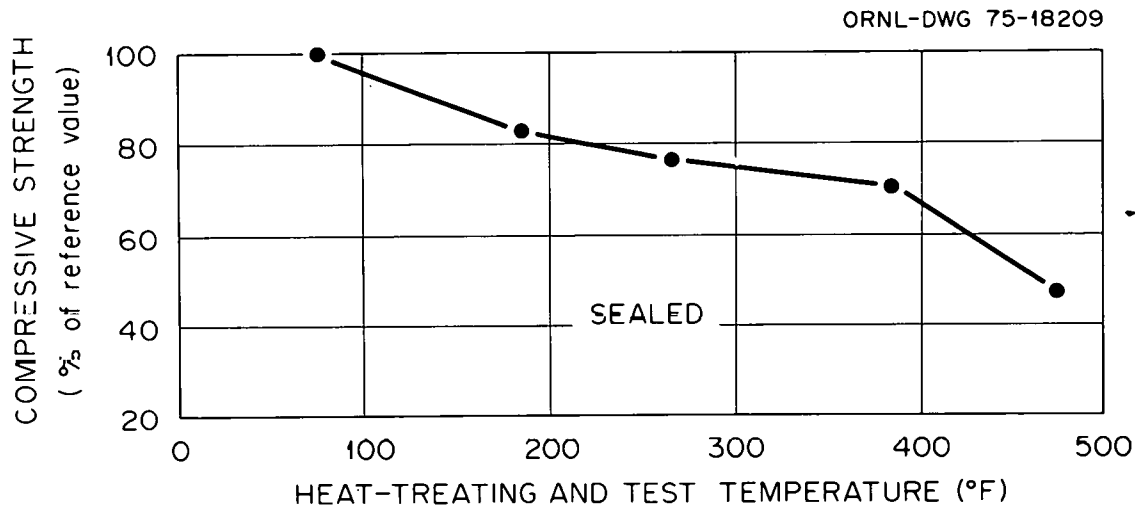


Fig. 14. Compressive Strength vs Temperature for Gravel Concrete, Sealed. Source: D. R. Lankard et al., "Effects of Moisture Content on the Structural Properties of Portland Cement Concrete Exposed to Temperatures up to 500°F," ACI SP-25, *Temperature and Concrete* (1970).

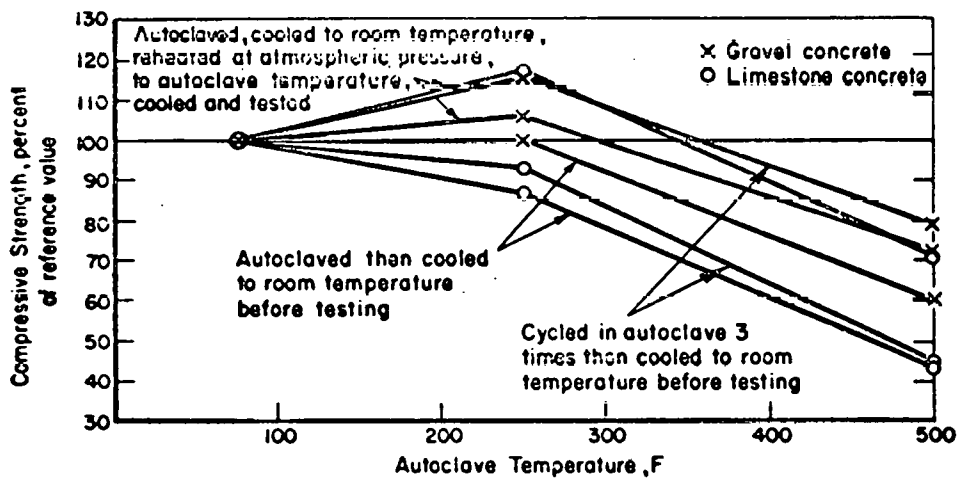


Fig. 15. Compressive Strength vs Temperature for Gravel and Limestone Concrete, Autoclaved. Source: D. R. Lankard et al., "Effects of Moisture Content on the Structural Properties of Portland Cement Concrete Exposed to Temperatures up to 500°F," ACI SP-25, *Temperature and Concrete* (1970).

For the limestone concrete reheated in air after one autoclave cycle, the strength went to 120% at 121°C (249°F) and 70% at 260°C (500°F). Thus the limestone aggregate concrete showed the greatest reduction in residual strength following exposure to elevated temperatures in the autoclave environment.

The authors concluded that concrete which retains its free water exhibits greatly reduced compressive strength at elevated temperatures compared with concrete which is allowed to dry. They state that laboratory studies using unsealed specimens cannot be used to predict the behavior of sealed specimens. In addition, they recommend that siliceous aggregates be utilized for structural concrete applications in which the free moisture will be retained on heating. It is difficult to make a comparison between the hot strength and residual (cold) strength in this study, because the specimens that were autoclaved to high temperature and then cooled and tested contained less free water than the specimens hot-tested in the pressure can (Fig. 11).

Another major study of interest is that performed by Bertero and Polivka<sup>31</sup> at the University of California. They performed experiments similar to those of Lankard et al., in that they tested sealed and unsealed specimens at elevated temperatures and conducted cold tests for residual strength. They used 15.2- by 45.7-cm (6- by 18-in.) concrete cylinders cured for 90 days at room temperature in the sealed condition. The concrete mixture consisted of type II portland cement and limestone sand aggregate (fine and coarse) with a w/c ratio of 0.425 and a 28-day compressive strength of about 44.8 MPa (6500 psi). Embedment gages were cast into the specimens for measurements of strains and temperatures. Details of their techniques and instrumentation are provided in a separate paper.<sup>32</sup> The basic factors which they considered were: sustained temperature of 149°C (300°F), cycling to 149°C, influence of free-moisture content, and differences between hot and cold testing. Figure 16 shows the design of their sealing system, consisting of a 0.038-cm-thick (0.015-in.) copper jacket silver-soldered to copper end plates and provided with moisture seals at the lead wire penetrations. Figure 17 shows a schematic of the instrumentation system used for both sealed and unsealed specimens. The compressive strengths are compared with reference specimens, which were sealed and cured for 90 days at 21°C (70°F), having an average compressive strength of 44.2 MPa (6420 psi). Only one specimen was used for each type of test. Specimens tested dry had their containers punctured prior to testing to allow for moisture escape.

The results of all the testing are shown in Table 5 for compressive strength (and other properties to be discussed later). Figure 18 shows the results for sealed and unsealed (dry) specimens held at 149°C (300°F) for various lengths of time and tested hot. As shown, the dry specimens lost about 10% of their strength initially but, after seven days, had regained strength back to that of the control specimen. The sealed specimens, on the other hand, continuously lost strength with increasing time at temperatures until, at 25 days, only 29% of reference strength remained. With regard to the effect of thermal cycling on the compressive strength [21-150-21°C (70-300-70°F)], the dry specimens were not affected significantly. In fact, five thermal cycles resulted in slight increases in strength for the dry specimens. Figure 19 depicts the effect of the number

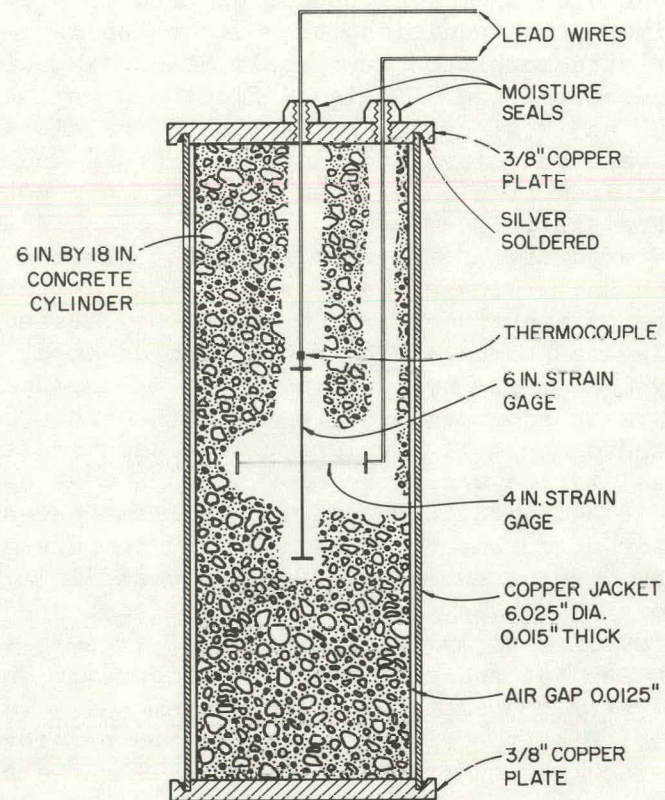


Fig. 16. Test Specimen and Sealing Assembly. Source: V. V. Bertero and M. Polivka, "Influence of Thermal Exposure on Mechanical Characteristics of Concrete," ACI SP-34, *Concrete for Nuclear Reactors*, pp. 505-31 (1972).

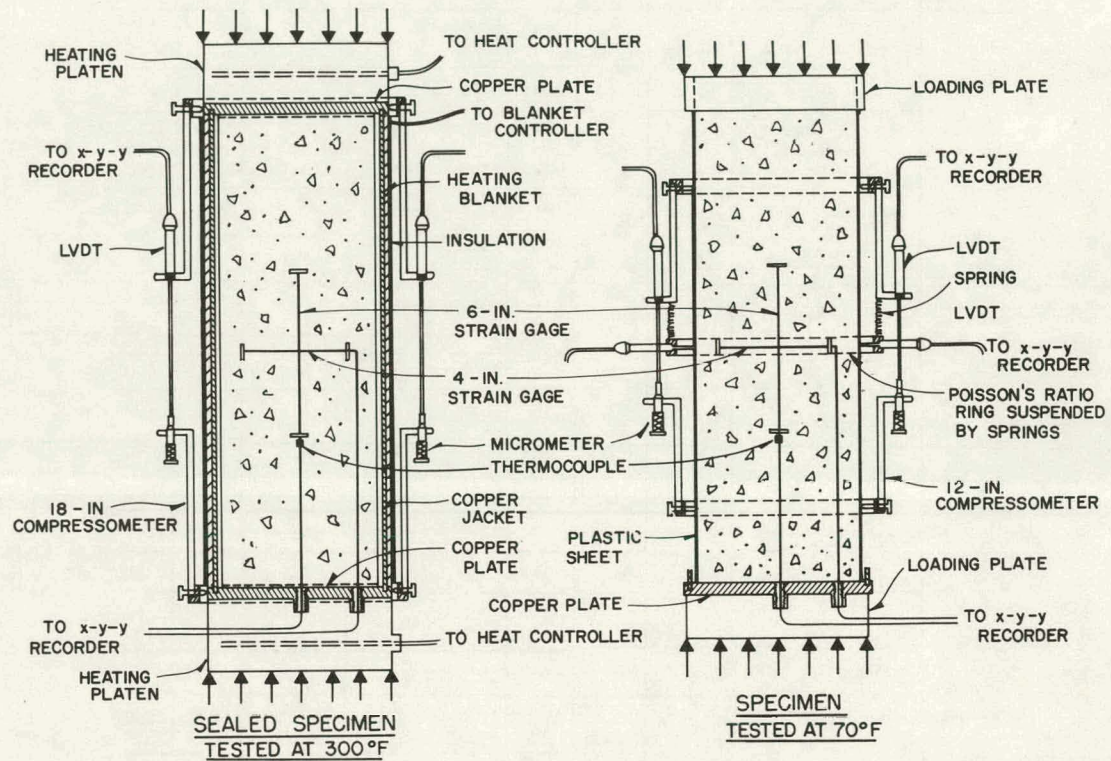


Fig. 17. Instrumentation used During Compression Tests. Source: V. V. Bertero and M. Polivka, "Influence of Thermal Exposure on Mechanical Characteristics of Concrete," ACI SP-34, *Concrete for Nuclear Reactors*, pp. 505-31 (1972).

Table 5. Effect of Type of Thermal Treatment on Mechanical Characteristics of Concrete

Test Series	Thermal Exposure, Applied at Age 90 days	Moisture Condition	Compr. Test Temp., °F	Spec. No.	Compressive <sup>(a)</sup> Strength $f_c'$ , psi	Modulus <sup>(3)</sup> of Elasticity, $E$ , psi $\times 10^6$	Poisson's Ratio	Strain at Max. Stress, $\mu-\epsilon$
"A" Short-Term Thermal Treatment	Constant 70°F (Control)	Sealed	70	1	6390	5.2	0.23	1680
				2	6450	4.5	0.22	1650
				Avg.	6420 (100%)	4.9	0.22	1670
	Heated to 300°F and tested	Sealed Dry	300	3	4470 (70%)	5.0	0.18	1410
				4	5750 (90%)	4.9	0.15	1500
	Sustained 300°F for 7 days	Sealed Dry	300	5	4250 (66%)	4.2	0.15	1900
				6	6350 (99%)	4.9	0.19	1320
	Number of Cycles of 70-300-70 °F	Sealed	300	7	4950 (77%)	4.3	0.19	1750
				8	5210 (81%)	4.7	0.25	1580
		Dry	70	9	6100 (95%)	4.2	0.13	1640
		Sealed	300	10	4420 (69%)	4.0	0.15	1680
		Dry	300	11	6600 (103%)	4.6	0.16	1650
		Dry	70	12	6550 (102%)	4.5	0.24	1850
"B" Long-Term Thermal Treatment	Sustained 300°F for: 25da.	Sealed	300	13	2240 (35%)	2.5	0.21	1280
				14	1850 (29%)	2.4	0.18	1240
	Number of Cycles of 70-300-70 °F	Sealed	300	15	3380	2.9	0.19	1500
				16	3280	3.2	0.18	1580
		Sealed	70	Avg.	3330 (52%)	3.1		
				17	3770	4.3	0.21	1330
				18	3780	3.5	0.21	1350
				Avg.	3780 (59%)	3.9	0.22	1670

(1) "Sealed" - Specimen remained sealed during thermal exposure and testing in compression.

"Dry" - Specimen remained sealed up to age 90 days, then permitted to lose moisture during thermal exposure and testing.

(2) The percentage compressive strength values shown refer to the compressive strength of the control which is taken as 100 percent.

(3) At 0.45 $f_c'$ .

Source: V. V. Bertero and M. Polivka, "Influence of Thermal Exposure on Mechanical Characteristics of Concrete," ACI SP-34, *Concrete for Nuclear Reactors*, pp. 505-31 (1972).

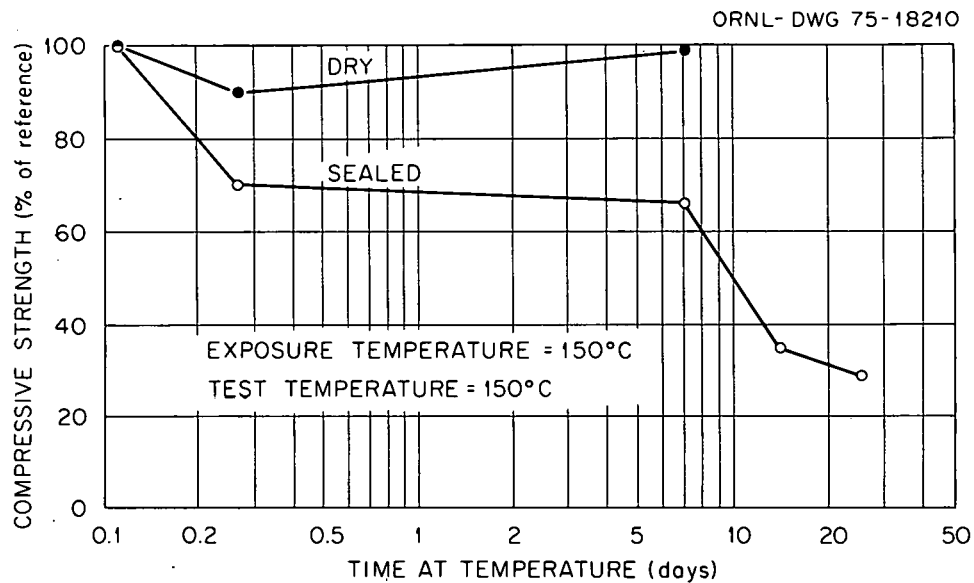


Fig. 18. Compressive Strength vs Time at Temperature, Sealed and Unsealed. Source: V. V. Bertero and M. Polivka, "Influence of Thermal Exposure on Mechanical Characteristics of Concrete." ACI SP-34, *Concrete for Nuclear Reactors*, pp. 505-31 (1972).

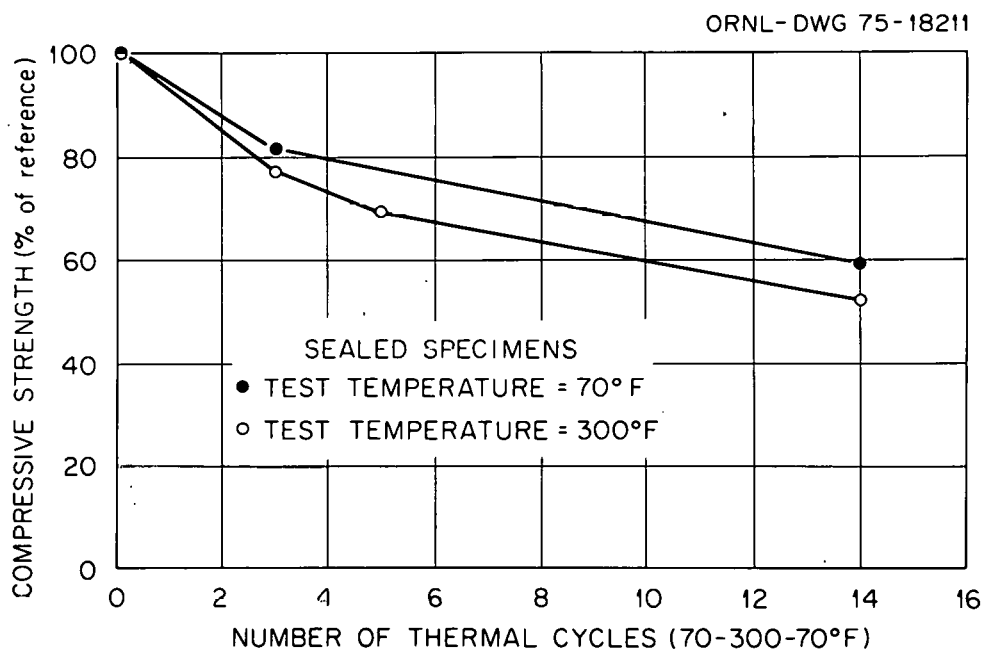


Fig. 19. Compressive Strength vs Number of Thermal Cycles, Sealed. Source: V. V. Bertero and M. Polivka, "Influence of Thermal Exposure on Mechanical Characteristics of Concrete, ACI SP-34, *Concrete for Nuclear Reactors*, pp. 505-31 (1972).

of thermal cycles on the compressive strength for sealed specimens tested at 21°C (70°F) and 149°C (300°F). The specimens tested at 149°C (300°F) gave slightly lower strength than the ones cold-tested for residual strength, but both hot and cold testing showed continual decreases in strength as the number of heating cycles increased.

It is difficult in this study to separate the effect of thermal cycling from that of simple exposure to elevated temperature. The specimens containing free moisture were significantly affected by heating time at 149°C (300°F), whereas specimens allowed to dry did not experience a loss of compressive strength either during continuous exposure at 149°C (300°F) for seven days or during five thermal cycles to 149°C (300°F).

Bertero and Polivka also reported a difference in the type of failure between sealed and unsealed specimens. The mode of failure for the dry specimens was sudden and brittle, while the sealed specimens failed in a more ductile manner. The studies of both refs. 19 and 20 reported loud, sudden failures for unheated specimens and gentle failures for specimens exposed to elevated temperatures. It is not understood why Bertero and Polivka's dry specimens exposed to elevated temperature failed in a brittle, loud manner, while the other investigators reported slow, gentle failures for dry, heated concrete. The primary conclusion of this work is, as was the case for Lankard et al., that the main parameter for observed deterioration of concrete strength at elevated temperature appears to be the continuing presence of moisture.

Nasser and Lohtia<sup>33</sup> performed tests on sealed concrete specimens also. Their tests were designed to investigate the effects of elevated temperature on mass concrete for relatively long periods of time. They tested 7.62 × 23.5 cm (3 × 9 1/4 in.) cylinders made with type III high-early-strength cement. The aggregates were composed of dolomite and hornblend. A high water/cement ratio of 0.6 was used, and specimens were sealed against loss of moisture immediately after casting. Specimens not subjected to temperatures above 21°C (70°F) were sealed in polypropylene jackets.<sup>34</sup> For higher temperatures 0.16-cm thick (1/16-in.), 8.25-cm-diam (3.25-in.) welded steel pipes were used for sealing containers. Specimens were heated either at 1 day after casting (concrete A) or 14 days after casting (concrete B). Times of exposure were either 1, 3, 7, 14, 28, 56, 91, or 180 days.

Following heat exposure, specimens were cooled to room temperature and removed from the container. Testing was then performed at room temperature. The authors do not state the amount of time that passed from removal of the specimen to testing, except that removal and testing occurred in the same day. Presumably, the specimens were not allowed to air-dry except for the short time it took to weigh and test them in compression. The reference strength in each case was based on the strength of sealed concrete cured at 21°C (70°F) for the same length of time as was the particular heat-exposed specimen. Table 6 provides the results of Nasser and Lohtia's cold testing for the relative compressive strength at various ages and temperatures. Figure 20 is a graphical representation of the data in terms of absolute strength.

Plotting the data for concrete B according to the ratio of percentage of the particular reference strength results in the graph shown in Fig. 21. The data shows, generally, that exposure at high temperatures caused

Table 6. Ratio of Compressive Strength at Various Temperatures and Ages to the One at 21.4°C (70°F) for Both Concretes A and B<sup>a</sup>

Type of Concrete	Age (days)	Compressive Strength, psi (kgf/cm <sup>2</sup> ) at 21.4°C (70°F)	Ratio of Compressive Strength at Indicated Temperature to that at 21.4°C (70°F)						
			1.7°C (35°F)	71°C (160°F)	121°C (250°F)	149°C (300°F)	177°C (350°F)	205°C (400°F)	232°C (450°F)
A (1-day)	4	4200 (290)	0.68	1.17	1.00	1.15	1.20	1.10	1.07
	14	5300 (372)	0.83	0.97	1.01	0.93	0.95	0.79	0.75
	91	5810 (408)	1.06	0.97	0.85	0.77	0.69	0.62	0.58
	180	6080 (427)	1.12	0.97	0.78	0.68	0.59	0.56	0.50
B (14-day)	4	5400 (380)		0.95	0.95	1.07	0.95	0.38	0.80
	14	5500 (386)		1.01	1.05	1.02	0.97	0.79	0.75
	91	5850 (412)		1.05	1.07	0.87	0.73	0.63	0.59
	180	6100 (428)		1.05	1.05	0.80	0.64	0.56	0.53

<sup>a</sup> Sealed specimens.

Source: K. W. Nasser and R. P. Lohtia, "Mass Concrete Properties at High Temperatures," *J. Am. Concr. Inst.* 68: 180-86 (March 1971).

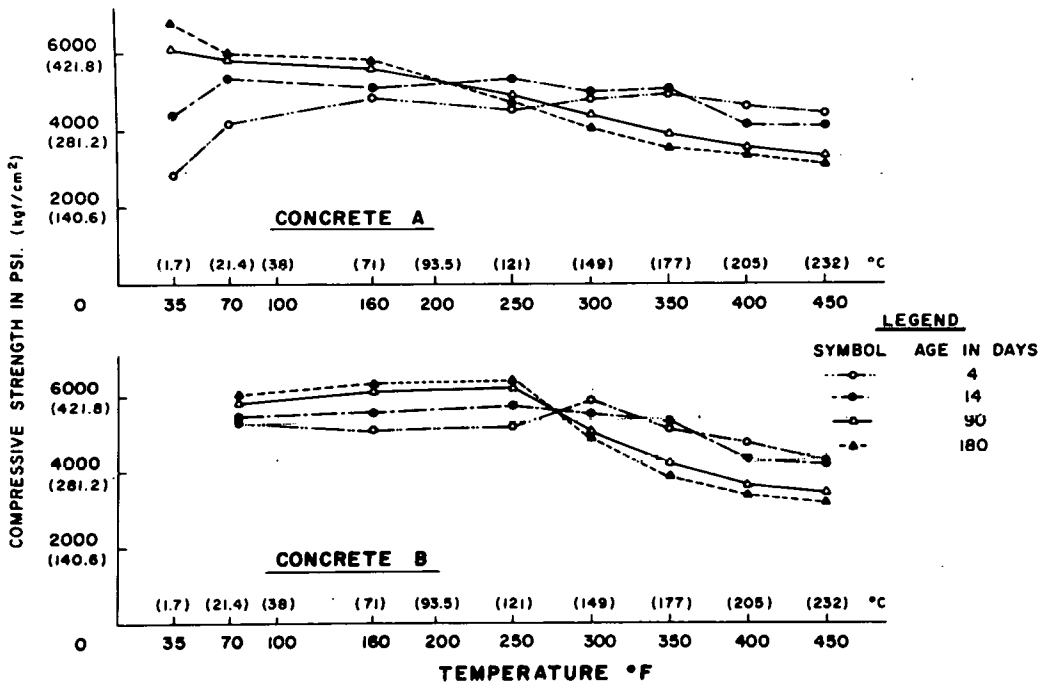


Fig. 20. Residual Compressive Strength vs Temperature and Age, Sealed. Source: K. W. Nasser and R. P. Lohtia, "Mass Concrete Properties at High Temperatures," *J. Am. Concr. Inst.* 68: 180-86 (March 1971).

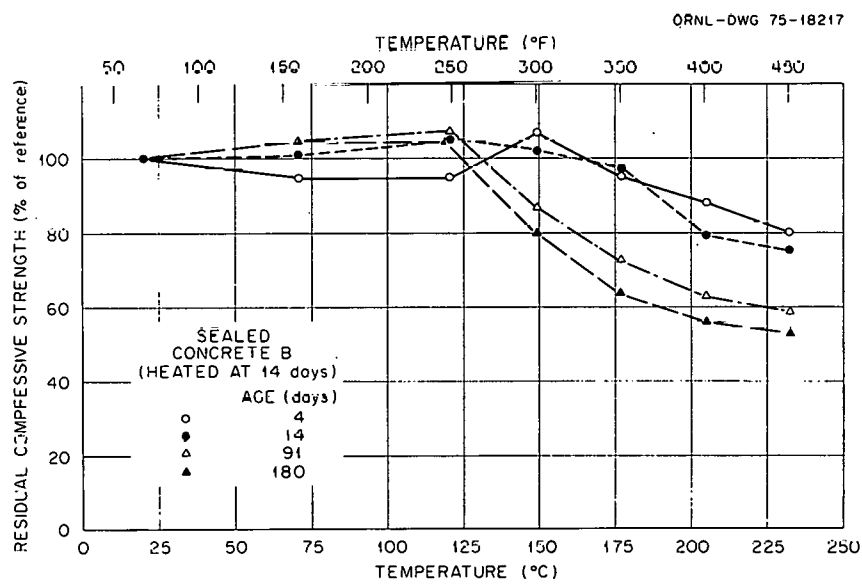


Fig. 21. Residual Compressive Strength vs Temperature and Age, Sealed. Source: K. W. Nasser and R. P. Lohtia, "Mass Concrete Properties at High Temperatures," *J. Am. Concr. Inst.* 68: 180-86 (March 1971).

deterioration of the concrete residual strength. For concrete B (exposed to heat 14 days after casting) the residual compressive strength was generally higher at 120°C (248°F) and began to show decreased strength at 150°C (302°F) (0.80 reference strength for 180 days). With higher temperatures the effect became more pronounced, and the greatest loss was for 180-day concrete at 230°C (446°F), the residual strength being only 53% of that cured for 180 days at 20°C (68°F). Figures 20 and 21 show that temperature exposure up to 125°C (257°F) on 14-day-old concrete did not have much effect regardless of the time of exposure. Beyond 125°C (257°F), however, the residual strength was reduced [except for the four-day exposures for which significant reduction did not occur until after 175°C (347°F)].

In this report, contrary to most of the others examined, the reference strength for a particular specimen is based on concrete of equal age cured at 20°C (68°F). It is felt that this approach is more valid from the standpoint of evaluating the actual effect of temperature exposure. However, a significant drawback is that all of the concrete B specimens exposed to various temperatures were exposed at the age of 14 days after casting. No exposure tests were performed on specimens cured at room temperature (or a simulated curing temperature for mass concrete) for long periods of time (90 or 180 days). Although the authors used a high-early-strength cement and at 14 days the strength was 87% of that at 180 days, it is felt that the continuing hydration and strength gain during that time may be significant as regards temperature effects for PCRV applications. As stated previously, the concrete in a PCRV would not be exposed to elevated temperatures (except from heat of hydration) as a result of reactor operation for at least a year and probably longer. Because some of the specimens were subjected to high temperatures at a relatively early age, moisture required for hydration may have been driven off. The authors state that moisture was free to expel out of the concrete into the void region within the steel pipe during heating. The loss of moisture was found to increase with temperature but did not vary much with duration of curing. However, they also state that concrete A (cured one day) lost only a little more moisture than did concrete B (14-day-cured), and therefore the effect of relatively early age heat exposure to their concrete may not be significant. With regard to failure, the authors observed that specimens cured at 20 and 70°C (68 and 158°F) were brittle and sudden, whereas at 121°C (249°F) and beyond, a tendency of gradual yielding started to appear, and a smell of wet condensed steam became conspicuous. From 150 to 232°C (302 to 450°F), the mode of failure changed to one which was dull and slow, with greater strain to failure and a whitish appearance of the fracture surface. Nasser and Lohtia concluded that strength (residual) of mass concrete deteriorates at sustained temperatures above 100°C (212°F) and that residual strength continues to decrease with increasing temperature and time of exposure.

The results presented as to effects of elevated temperatures on compressive strength of concrete are what is considered a reasonable sampling of representative studies using various concrete mixtures and testing methods. Reference strengths were, in some cases, based on 28-day, room-temperature, as-cured strength, while other reports used the strength of specimens cured from the same length of time as for the heat-exposed

specimens (as long as 180 days). In addition, specimens were tested in sealed and unsealed conditions, tested at temperature or cooled, and tested at room temperature. Other specimens were exposed to thermal cycling for varying numbers of cycles and rates.

It is therefore not surprising that a plot of the referenced data would appear as shown in Fig. 22. It can be seen that the data points representing unsealed specimens (open symbols) fall toward the top of range, while those for sealed concrete (closed symbols) fall toward the lower portion. This is expected from previously discussed results and

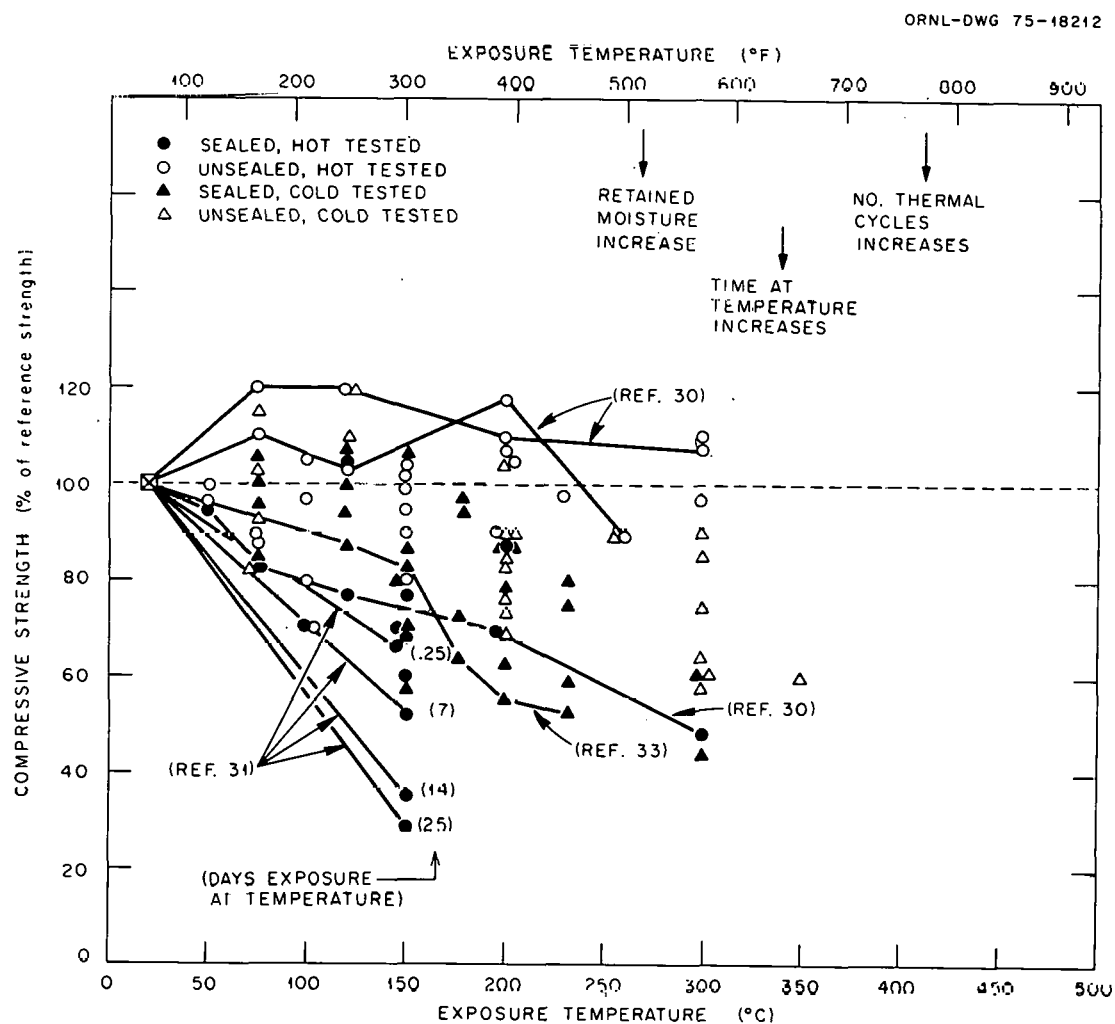


Fig. 22. Compilation of Data on Compressive Strength vs Temperature.  
Source given for each curve.

amplifies the concern expressed for reduced compressive strengths of mass concrete having substantial amounts of retained moisture. Bertero and Polivka<sup>31</sup> reported losses up to 71% at 149°C (300°F), while Lankard et al.<sup>30</sup> reported only a 30% loss of strength at 200°C (392°F). One major difference in their results of sealed specimen tests is the time of exposure to the elevated temperature. Lankard's specimens were held at temperature for only 20 to 28 hr prior to testing, while Bertero and Polivka varied exposure time from 4 hr to 25 days. The loss of 71% for the latter tests were obtained for the 25-day exposure, while the 4-hr exposure resulted in only a 30% loss, comparable to Lankard's 28-hr results. Additionally, Lankard used a siliceous gravel for that test, while Bertero's was accomplished with an all-limestone aggregate. For the unsealed specimens, which were allowed to lose free moisture, the greatest strength loss at 200°C (392°F) was 30% as reported by Campbell-Allen and Desai.<sup>20</sup> That data was also for a concrete with an all-limestone aggregate. Even at 300°C (572°F) the greatest reported loss for unsealed concrete was 40%.<sup>20</sup>

Thus, up to 300°C (572°F), deleterious effects of elevated-temperature exposure on the compressive strength of concrete are considered to be significant only for the sealed condition, that is, for the condition of substantial amounts of retained free moisture. Discussion of the mechanisms responsible for significant loss of compressive strength will be presented after the sections summarizing experimental data for other concrete properties. Thus far, only uniaxial compressive strength has been considered. Since the PCRV concrete is generally under a multiaxial state of stress, concrete multiaxial strength will be discussed in a later section.

### 3.3.2 Elastic Properties

Figure 23 shows a typical diagram for the stress-strain relationship of concrete. As shown in the figure, there are various accepted methods of measuring the elastic modulus for concrete when there is no straight portion to the curve. The initial tangent modulus is of little practical importance, and the tangent modulus at any point applies only to very small load changes about the point of tangency. Because of the creep characteristics of concrete, even at room temperature, the dependence of instantaneous strain on the speed of loading makes the demarcation between elastic and creep strains difficult. Thus, the secant modulus satisfies the arbitrary distinction that deformation during loading is considered elastic, and any subsequent strain increase is regarded as creep.<sup>35</sup> In addition, the chord modulus is used by some investigators presumably to eliminate the small concave-up portion of the curve, sometimes encountered at the beginning of compressive loading, resulting from shrinkage cracks. Some researchers use the secant modulus (at various stress levels; i.e., 20, 30, and 50% of ultimate load), while others have used the chord modulus or tangent moduli. In addition to the static moduli discussed thus far, one can measure the dynamic modulus of elasticity by measurement of natural frequencies or by measurements of ultrasonic pulse velocity (ref. 35, p. 318).

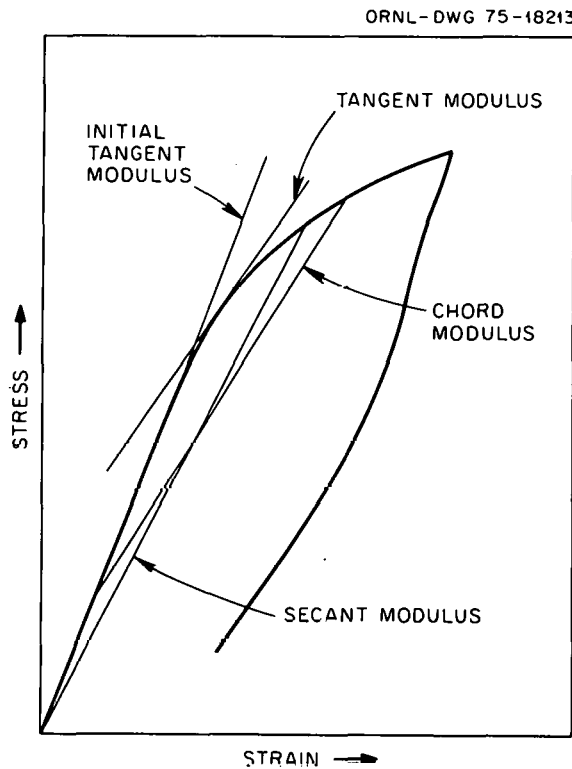


Fig. 23. Methods for Determination of Concrete Modulus of Elasticity.

Poisson's ratio,  $\mu$ , is the ratio between the lateral strain and an applied axial strain. For ordinary and lightweight concrete, Poisson's ratio varies in the range 0.11 to 0.21 (generally 0.15 to 0.20) when determined from strain measurements, whereas dynamic measurements yield higher values, around 0.24.<sup>35</sup> Poisson's ratio can also be calculated from measurements of the modulus of elasticity,  $E$ , and the modulus of rigidity,  $G$  (determined from torsional measurements). Values of  $\mu$  obtained by this method are intermediate between the direct method and the dynamic method.<sup>35</sup>

Thus, precise correlations of various investigations are prohibited by the lack of standard techniques of measurement. In the face of this adversity, however, it is believed that most of the methods of measurement will respond similarly when subjected to a given condition such as elevated temperature. Many of the investigators referred to in the previous section on compressive strength will be referenced again for results of modulus testing. Therefore, a detailed discussion of techniques and procedures will not be reported.

Saemann and Washa's<sup>16</sup> results with a calcareous gravel concrete showed almost negligible effects of temperature on the modulus of elasticity for hot-tested, unsealed specimens, similar to their results for compressive strength. The greatest effect was at 250°C (482°F), where the concrete achieved 80% of its reference modulus; at 150°C (302°F), 96% of the reference was attained. Saemann and Washa used the secant modulus at one-third ultimate load as their technique.

Philleo<sup>36</sup> performed tests for the elastic modulus at temperatures up to 816°C (1500°F). Specimens were small,  $3.81 \times 5.08 \times 15.24$  cm (1 1/2 × 2 × 6 in.), unsealed, and hot-tested for the dynamic modulus of elasticity by determining the resonant frequencies in flexural vibration inside the furnace. Water-to-cement ratios of 0.4, 0.6, and 0.8 were investigated. As temperatures increased, the modulus of elasticity underwent drastic reductions in all test specimens. Data obtained on specimens moist-cured for 90 days are shown in Fig. 24. The modulus decreased in every case, but the decrease was slightly greater with increased water/cement ratios. At even higher temperatures than shown on the graph, the modulus was reduced to as low as 31% of reference at 760°C (1400°F) for the 0.4 w/c concrete and 21% for the 0.8 w/c concrete. For each water/cement ratio considered, the moist-cured specimens (90 days) underwent greater reductions in modulus at a given temperature than did the air-dried specimens. The 90-day modulus values for moist-cured specimens of 0.4 and 0.6 w/c ratios were about 20% higher than the values for 28 days. Philleo also reported that there was a general tendency for Poisson's ratio to decrease as the temperature rose, although the results were erratic. He stated that a 1% error in resonant frequency determination may produce as much as a 20% error in Poisson's ratio.

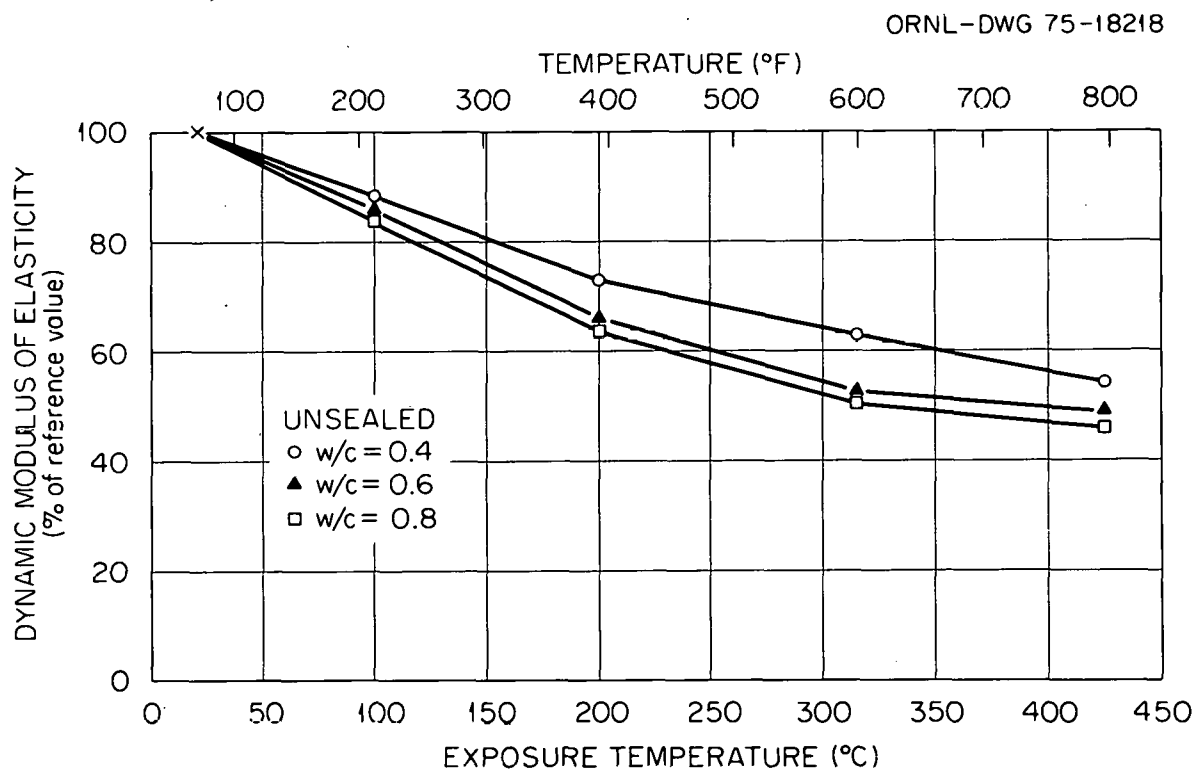


Fig. 24. Dynamic Modulus vs Temperature and Water/Cement Ratio, Unsealed. Source: R. Philleo, "Some Physical Properties of Concrete at High Temperatures," *J. Am. Concr. Inst.* 29(10): 857-64 (April 1958).

Davis<sup>17</sup> stated in his review that heating has a pronounced effect upon the modulus of elasticity of concrete. For the unsealed specimens of 0.53 w/c ratio, Davis showed that the static modulus decreased to 64% of the 90-day value at 140°C (284°F) and 33% at 350°C (662°F). Interestingly, the dynamic modulus decreased only to 92% at 140°C (284°F), then dropped sharply to 50% at 200°C (392°F) and 28% at 350°C (662°F). Davis also reported that the effect of 20 thermal cycles from 20 to 200°C (68 to 392°F) was no more damaging than one cycle for the static modulus, but the dynamic modulus decreased from 50% of reference for one cycle to 32% for 20 cycles. Similar results took place for 20 to 350°C (68 to 662°F) cycling.

Cruz<sup>37</sup> did a comprehensive study of temperature effects on elastic properties. However, all specimens were unsealed, moist-cured for three days, then stored in air at 50% humidity for 25 days. Results are presented for the modulus of elasticity and shear modulus determined by using an optical method. Poisson's ratios were calculated from the moduli. Cylindrical specimens 3.49 cm (1 3/8 in.) in diameter and 61 cm (24 in.) long were loaded as cantilevered beams after being slightly preloaded to minimize creep effects on deformation measurements. The elastic constants were determined in the range of about one-third ultimate load at normal temperature. Normal-weight concretes with type I portland cement and three different aggregate types as well as a lightweight concrete were tested. Figure 25 shows the results obtained from 20 to 650°C (68 to 1202°F) for the modulus of elasticity and shear modulus. Clearly, both moduli decrease substantially with increases in temperature. The elastic modulus of limestone concrete decreased only to 93% at 150°C (302°F), whereas the other two moduli decreased to about 75% at that temperature. At 315°C (599°F) the values for all three types were similar, ranging from 64 to 68% of the reference value at room temperature. The siliceous concrete underwent severe reduction through 650°C (1202°F), where the moduli were only about 20% of reference. The other concretes were reduced to 35-40% at 650°C (1202°F). Up to about 300°C (572°F) the results of Cruz<sup>37</sup> and Philleo<sup>36</sup> for Elgin sand and gravel concrete were very similar. This indicates that the reduction of the modulus of elasticity may be considered to be independent of the method of determination (optical method for Cruz and dynamic method for Philleo), at least for the concrete mixture and temperature range considered. However, generalization would certainly not be justified on the basis of that one comparison. With regard to Poisson's ratio, the high-strength concrete gave lower values at room temperature than did the lower-strength concrete. As reported by Philleo, elevated-temperature results were erratic, and no clear trends could be observed.

Kawahara and Haraguchi<sup>21</sup> reported that, up to 80°C (176°F), the effect of elevated temperature on the static elastic modulus of concrete is greatly affected by the presence of moisture in the concrete. However, the reported difference was only 12%. They also reported that the Poisson ratio of concrete cured at 80°C (176°F) tends to be somewhat smaller (0.14 vs 0.17) than that of concrete cured at 20°C (68°F). However, they also reported substantial scatter in results, even at these relatively low temperatures, by using a wire resistance strain gage.

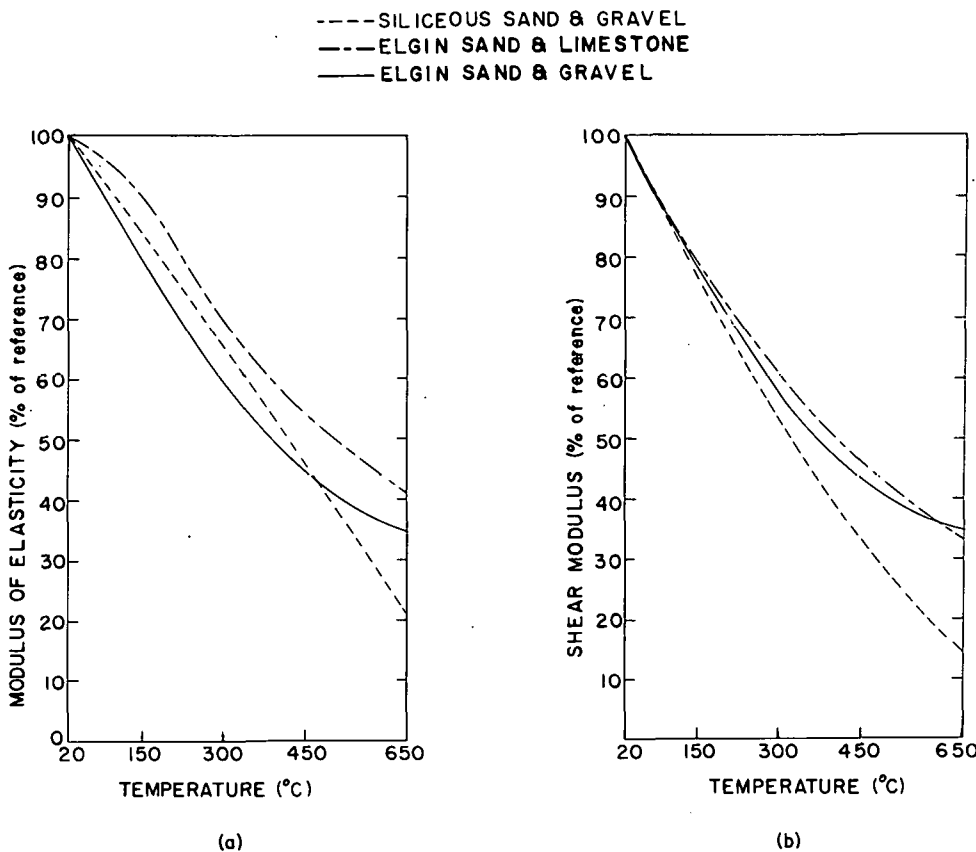


Fig. 25. Elastic and Shear Moduli vs Temperature for Various Concretes, Unsealed. Source: C. R. Cruz, "Elastic Properties of Concrete at High Temperatures," *Portland Cem. Assoc., Res. Dev. Lab. Dev. Dep. Bull. D 8: 37-47* (January 1966).

Investigations by Campbell-Allen, Low, and Roper<sup>19</sup> and by Campbell-Allen and Desai<sup>20</sup> also showed marked deterioration of the elastic modulus at temperatures up to 300°C (572°F) and emphasized the detrimental effects of thermal cycling. Ten cycles to 200°C (392°F) reduced the modulus to 41% of reference for a dolomite concrete,<sup>19</sup> while limestone concrete was reduced to 45% after 10 cycles and 38% after 20 cycles. For 20 cycles at 300°C (572°F), both types of concrete were reduced to only 25% of the reference modulus. Both reports considered unsealed specimens exposed to temperatures and cold-tested. Figure 25 shows the results of Campbell-Allen and Desai for limestone concretes. The latter authors also stated that Poisson's ratio tended to increase at higher temperatures, as reported by Cruz,<sup>37</sup> but they said nothing about erratic variation as observed by Cruz.

Sullivan and Poucher's<sup>38</sup> tests on beams, using the initial tangent modulus, showed similar deterioration in the elastic modulus. Also, they concluded that permanent damage took place on heating, because the hot testing and cold testing resulted in similar reductions of the modulus.

The study by Lankard et al.,<sup>30</sup> described earlier for compressive strength, showed that the modulus of elasticity of gravel and limestone concretes decreased under all conditions of heating and testing (unsealed or sealed, hot- or cold-tested). They measured the chord elastic modulus between 20 and 80% of ultimate stress. In the unsealed condition, both gravel and limestone concretes decreased only to about 80% of reference moduli up to 260°C (500°F). Under saturated steam pressure (sealed condition, Fig. 11), however, Figs. 26 and 27 show the decrease in modulus and the load deflection behavior with temperature respectively. Figure 28 shows the results of autoclave testing. In the sealed condition, and when hot tested, the modulus experienced a drastic decrease to 40% of reference at 80°C (176°F), a slight increase at 121°C (249°F), then a decrease to about 30% at 260°C (500°F). This effect is apparent also from Fig. 27. The results of autoclaving contrast sharply with the pressure-can results. At 121°C (249°F) for one cycle, the gravel concrete showed no modulus reduction as compared with the loss to less than 50% reference when tested hot under saturated-steam pressure (Fig. 26). In fact, three cycles in the autoclave at 121°C (249°F) resulted in a modulus increase to about 120% for the gravel concrete, much the same as for the compressive strength (Fig. 15). Lankard et al. attribute this effect to a time-temperature interaction because of the presence of available silica. Their discussion of causes for property deterioration under various conditions will be presented in more detail later.

Bertero and Polivka<sup>31</sup> used the tangent method at 45% of the ultimate load to compute the tangent modulus of elasticity as well as Poisson's ratio. The effects of elevated temperature on those properties are given in Table 5. The effect of time at temperature is given in Fig. 29, which shows that the modulus of elasticity for sealed specimens decreased

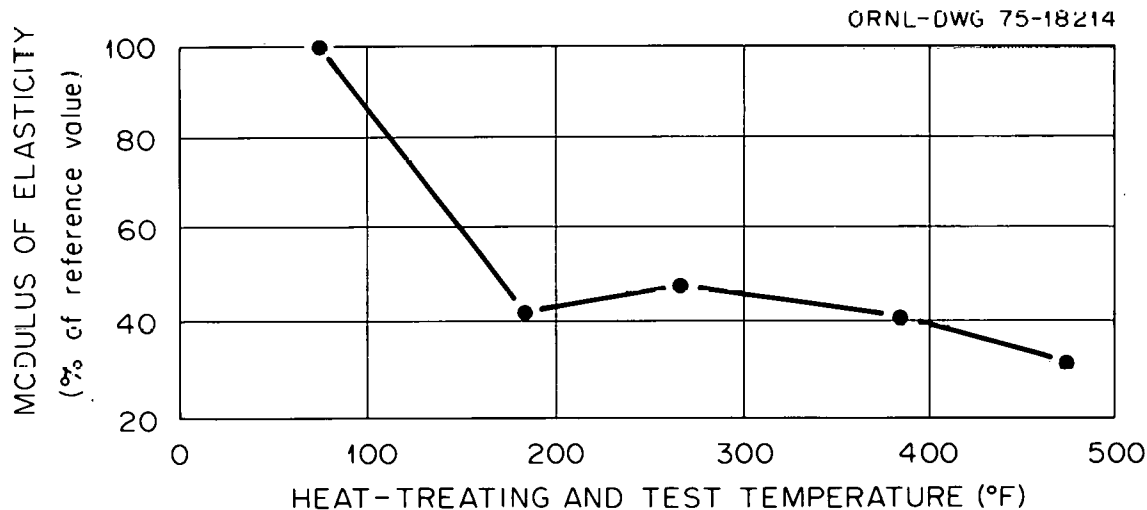


Fig. 26. Modulus of Elasticity vs Temperature for Gravel Concrete, Sealed. Source: D. R. Lankard et al., "Effects of Moisture Content on the Structural Properties of Portland Cement Concrete Exposed to Temperatures up to 500°F," ACI SP-25, *Temperature and Concrete* (1970).

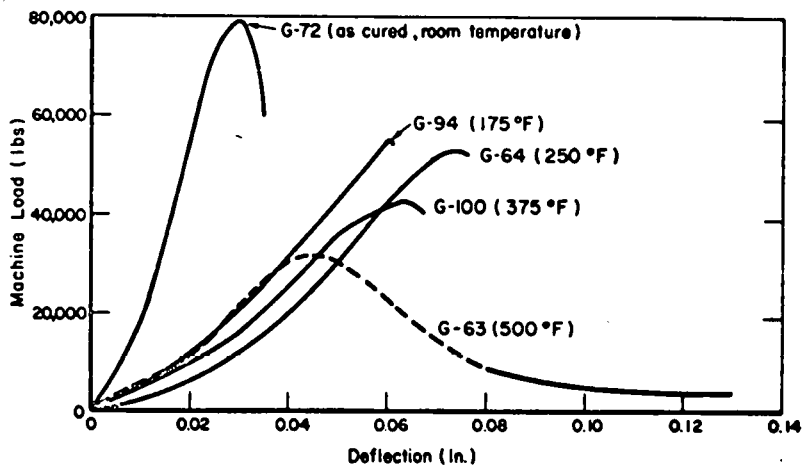


Fig. 27. Load Deflection Behavior vs Temperature for Gravel Concrete, Sealed. Source: D. R. Lankard et al., "Effects of Moisture Content on the Structural Properties of Portland Cement Concrete Exposed to Temperatures up to 500°C," ACI SP-25, *Temperature and Concrete* (1970).

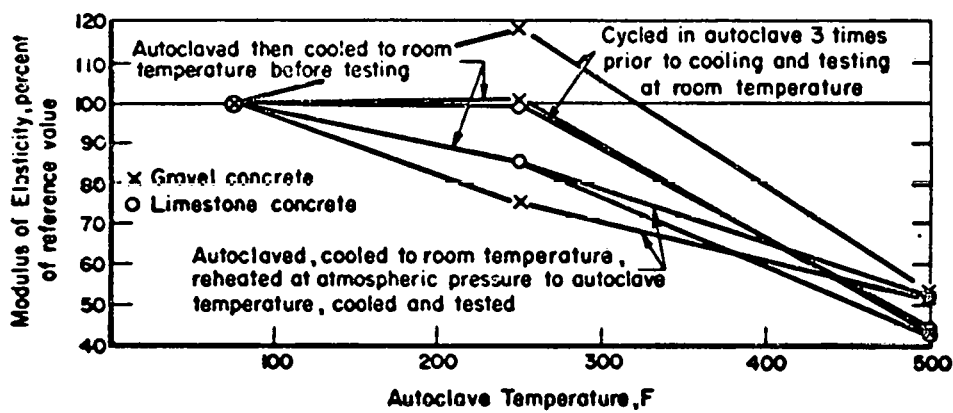


Fig. 28. Effect of Test Conditions on the Modulus of Elasticity of Autoclaved Gravel and Limestone Concrete. Source: D. R. Lankard et al., "Effects of Moisture Content on the Structural Properties of Portland Cement Concrete Exposed to Temperatures up to 500°F," ACI SP-25, *Temperature and Concrete* (1970).

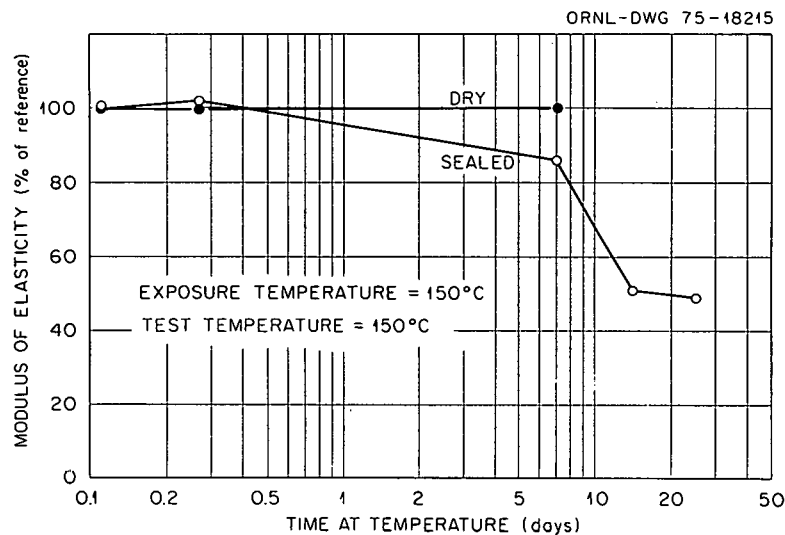


Fig. 29. Modulus of Elasticity vs Time at Temperature, Sealed and Unsealed. Source: V. V. Bertero and M. Polivka, "Influence of Thermal Exposure on Mechanical Characteristics of Concrete," ACI SP-34, *Concrete for Nuclear Reactors*, pp. 505-31 (1972).

substantially as exposure time increased, as did the compressive strength (Fig. 18). For sealed specimens which had been cycled to 149°C (300°F) for 3, 5, and 14 cycles,  $E$  was reduced to 88, 82, and 63% of reference, respectively, when hot-tested at 149°C (300°F). In addition, they reported that the initial tangent modulus was generally smaller than the tangent modulus corresponding to higher stresses when cycling was involved. They attribute this observation to an increase in the amount of microcracking with higher numbers of thermal cycles. From the values given in Table 5, Poisson's ratio appeared to decrease when testing at 149°C (300°F). Specimens which were cold-tested gave values of Poisson's ratio essentially unchanged from the reference test. Poisson's ratio varied in the range 0.13 to 0.25 for all tests.

Nasser and Lohtia<sup>33</sup> reported that the modulus of elasticity of sealed specimens decreased severely at exposure temperatures above 120°C (248°F) (specimens were cold-tested). The same effect was reported for compressive strength in that study (Fig. 21). Figure 30 shows the results of their work where the reference value of  $E$  is for a sealed specimen cured at 20°C (68°F) for the same length of time as for its corresponding group of heated specimens. As the figure shows, the decrease in the modulus becomes substantial at 150°C (302°F) and above, until, for 180 days exposure at 232°C (450°F), the modulus is only 32% of reference. The authors emphasize that the strength and elasticity results show consistent response of sealed concrete to the test variables.

Marechal<sup>39</sup> measured Poisson's ratio at elevated temperatures and reported a decrease to 83% of reference at 150°C (302°F) and a decrease to 40% at 300°C (572°F). He observed that cooling to room temperature resulted in little difference whether the evaporable water is retained or removed. Reported values ranged from 0.10 to 0.28. He measured only

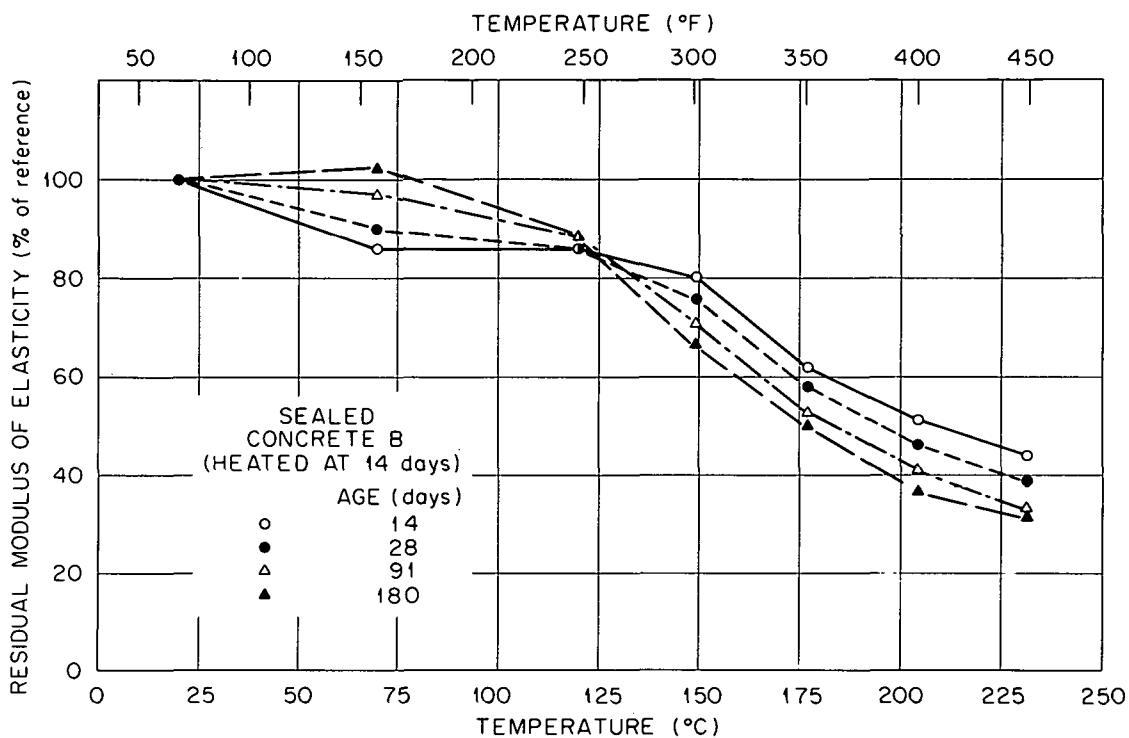


Fig. 30. Residual Modulus of Elasticity vs Temperature, Sealed.  
Source: K. W. Nasser and R. P. Lohtia, "Mass Concrete Properties at High Temperatures," *J. Am. Concr. Inst.* 68: 180-86 (March 1971).

the transverse strains and concluded that the decrease was brought about by the increase in temperature and resulting water desorption.

The effect of temperature on Poisson's ratio is not clear from the small amount of data available. The range of values reported extended from 0.11 to 0.25. Some studies reported general increases in Poisson's ratio with increasing temperature for unsealed specimens<sup>19, 20, 37</sup> and general decreases for sealed specimens.<sup>21, 31</sup> However, erratic behavior in the measurement of Poisson's ratio was common, and no definite conclusions can be made.

With regard to the modulus of elasticity, the effects of temperature appear to be similar to those for compressive strength. As stated previously, representative data for unsealed and sealed concrete include measurements on a wide range of concrete mixtures with a multitude of experimental techniques and methods of calculation. Figure 31 provides a plot of all the elastic modulus data discussed previously. Generally, the modulus decreases with increasing temperature for all types of testing. In addition, further decreases are observed to occur with an increase in the number of thermal cycles and in the holding time at the exposure temperature. The specimens sealed for moisture retention were more sensitive to those factors. The decrease in modulus for sealed specimens appears to become acute at 150°C (302°F) and above. The open triangles at 200 and 350°C (392 and 662°F) showing the lowest values of  $E$  (32 and 15% respectively) are from Davis<sup>17</sup> and represent dynamic measurements on

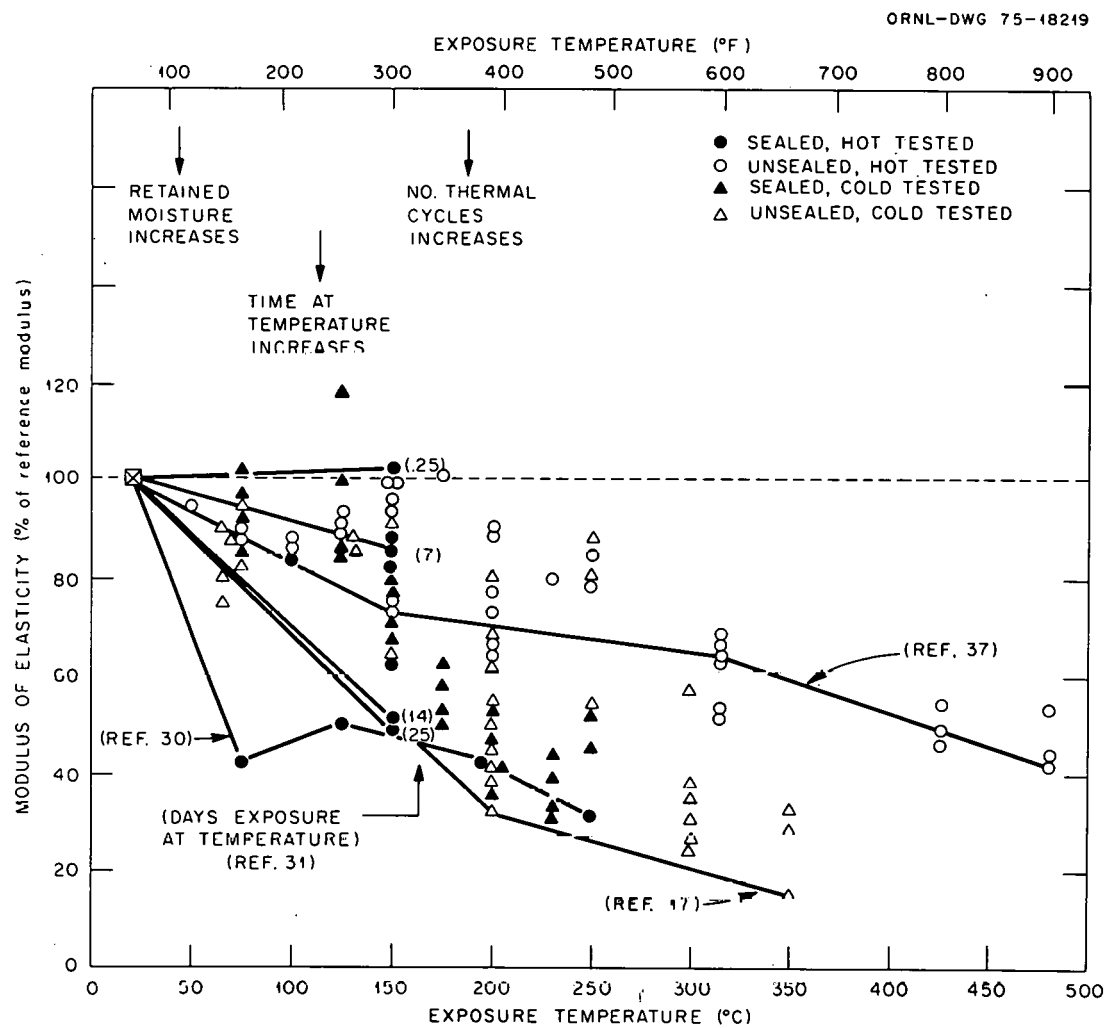


Fig. 31. Compilation of Data on Modulus of Elasticity vs Temperature. Source given for each curve.

specimens subjected to 20 thermal cycles. There appears to be a conflict of results shown by the sealed, hot tests (closed circles). At 75 and 125°C (167 and 257°F), for a one-day exposure, Lankard et al.<sup>30</sup> reported values of 42 and 50% respectively. At 149°C (300°F), Bertero and Polivka<sup>31</sup> obtained values of 102, 86, 51, and 49% for exposure times of 4 hr, 7 days, 14 days, and 25 days respectively. From the descriptions of sealing chambers provided in each reference, it would seem that the pressure-can device of Lankard et al., which allows for heating of the specimen under water, would result in greater retention of free moisture, especially below 100°C (212°F). The copper jacket of Bertero and Polivka allowed for an air gap around the specimen, and free moisture could migrate out of the concrete to fill the gap between the jacket and specimen on heating. Thus, for the two data points mentioned, the one at 149°C (300°F)

for 4 hr, tested by Bertero and Polivka, may have begun to dry out near the surface and provide the initial stiffness necessary to show no change in modulus measured at  $0.45 f_c'$ . The modulus, for that specimen, did decrease beyond about  $0.5 f_c'$ , and the resultant strength was only 70% of reference. Also, Bertero and Polivka utilized embedment strain gages, whereas Lankard et al. measured strain according to testing machine platen travel. All of these observations could account for much of the difference in results.

### 3.3.3 Tensile Strength

Although structures are generally not designed to withstand direct tensile stresses, one must be aware of the ability of the concrete in the structure to resist cracking. This is especially true in a reinforced structure. The tensile strength of concrete is generally very low [6.89 MPa (<1000 psi)], and if behavior of reinforced concrete is to be understood, the tensile strength under various conditions should be known. If a concrete of 4.13 MPa (600 psi) tensile strength is subjected to high temperature, and strength is reduced by 50% to 2.07 MPa (300 psi), the designer should be made aware of that fact.

The tensile strength of concrete is closely related to the compressive strength. As the compressive strength increases, the tensile strength also increases, but at a decreasing rate.<sup>35</sup> There are many empirical relationships suggested for the concrete strengths, but none have been found to be applicable in the general sense. A common rule of thumb, which is used for concretes with compressive strengths of the range generally considered applicable for PCRV applications, 27.6 to 55.2 MPa (4000 to 8000 psi), is that the tensile strength is about 10% of the compressive strength. The standard test for measurement of tensile strength is the beam flexure test, in which the modulus of rupture is measured with a two-point loading.<sup>35</sup> The modulus of rupture overestimates the tensile strength, reasons for which are discussed by Neville.<sup>35</sup> Another commonly used test is the splitting test, in which a concrete cylinder is compressed in the radial direction rather than in the longitudinal (as in compression testing). It is believed that splitting strength is generally about 5 to 12% higher than direct tensile strength.<sup>35</sup> However, as mentioned previously, the effects of temperature on the tensile strength probably do not vary much with the method used.

Saemann and Washa<sup>16</sup> used  $5.08 \times 5.08 \times 40.6$  cm ( $2 \times 2 \times 16$  in.) beams in three-point loading to determine the modulus of rupture, while standard mortar briquets were used to determine the tensile strength of mortar specimens at various temperatures. The tensile strength at  $65^\circ\text{C}$  ( $149^\circ\text{F}$ ) decreased to about 57% of the room-temperature value, increased back to the reference value at  $121^\circ\text{C}$  ( $249^\circ\text{F}$ ), and showed little change up to  $232^\circ\text{C}$  ( $450^\circ\text{F}$ ). The modulus of rupture changed in a similar manner.

Davis's<sup>17</sup> results on unsealed, cold-tested  $15.24 \times 15.24 \times 61$  cm ( $6 \times 6 \times 24$  in.) beams showed that the modulus of rupture did not change substantially to temperatures of  $200^\circ\text{C}$  ( $392^\circ\text{F}$ ). At  $350^\circ\text{C}$  ( $662^\circ\text{F}$ ), however, the value was only 33% of reference, although 20 thermal cycles to  $200^\circ\text{C}$  ( $392^\circ\text{F}$ ) decreased the modulus of rupture to 56% of reference.

Campbell-Allen, Low, and Roper<sup>19</sup> used the splitting test to determine tensile strength on unsealed, cold-tested specimens. In all cases the tensile strength of heat cylinders decreased from the reference value in much the same manner and to the same degree as did the compressive strength. The same effect resulted from cycling. Ten thermal cycles to 200°C (392°F) reduced the tensile strength to 86%, while ten cycles to 300°C (572°F) reduced it to 47% of the reference strength. The authors observed a number of microcracks on the surfaces of the cylinders after four cycles of exposure at 300°C (572°F) and concluded that they must materially affect the tensile strength. In most cases the tensile strength was about 8% of the compressive strength for both unheated and heated specimens.

Campbell-Allen and Desai<sup>20</sup> also used the split-cylinder test and reported losses up to 50% for limestone concrete exposed to ten thermal cycles at 200°C (392°F). They reported that failures in tension behaved much like failures in compression, in that unheated specimens failed suddenly and loudly, while heating produced gradual failures with little noise. Low-temperature heating around 65°C (149°F) produced only a 25% reduction in tensile strength after ten thermal cycles.

Sullivan and Poucher's<sup>38</sup> tests for flexural strength of beams revealed that, up to 200°C (392°F), the deterioration was gradual and small. Beyond 300°C (572°F) the strength drop was sharp, and at 400°C (752°F) the residual strength varied from 25 to 0% of the original. Hot and cold testing gave similar results. Also, contrary to results of others,<sup>17,19,20</sup> the number of thermal cycles did not significantly affect the strength drop.

All of the investigations discussed thus far used only unsealed specimens. Lankard et al.<sup>30</sup> conducted the only study reviewed which considered the tensile strength of sealed specimens to simulate mass concrete properties. They performed flexural strength tests on 7.62 × 6.35 × 25.4 cm (3 × 2 1/2 × 10 in.) beams which were prepared, cured, and heat-treated as discussed previously for compressive strength studies. All sealed tests were performed at room temperature after exposure in an autoclave device. Figures 32 and 33 show the results obtained for gravel and limestone concretes in the unsealed, hot, and cold test conditions and in the sealed, cold test condition. The greatest decrease for the unsealed specimens was for the cold-tested gravel concrete exposed to 260°C (500°F), for which the flexural strength was 75% of the reference value. In the case of sealed (autoclave), cold-tested specimens, 80 and 121°C (176 and 249°F) exposures resulted in decreases to 70–80% of reference, while exposure at 190°C (374°F) resulted in decreases to 40–50% of reference. It is not clear, and the authors do not offer an explanation, why the sealed specimens exposed at 260°C (500°F) showed less deterioration in flexural strength than they did at 190°C (374°F).

There is a limited amount of data available on tensile strength at elevated temperatures, especially for the case where free moisture was retained. However, it can be generally stated that the tensile strength (flexural strength or modulus of rupture) will be affected in approximately the same manner as the compressive strength. This applies in the case of unsealed or sealed specimens. Some studies resulted in greater loss of tensile strength,<sup>40,41</sup> while others found a greater loss in compressive strength. The primary point is that the tensile strength can be lowered substantially by exposure to elevated temperatures, especially when moisture is retained.

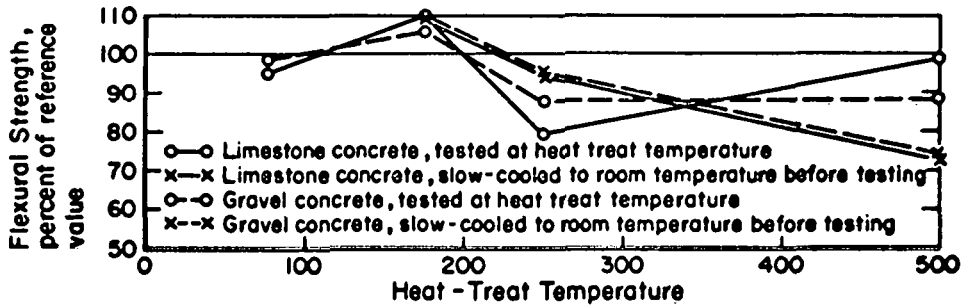


Fig. 32. Effect of Test Conditions on Flexural Strength of Gravel and Limestone Concrete, Unsealed. Source: D. R. Lankard et al., "Effects of Moisture Content on the Structural Properties of Portland Cement Concrete Exposed to Temperatures up to 500°F," ACI SP-25, *Temperature and Concrete* (1970).

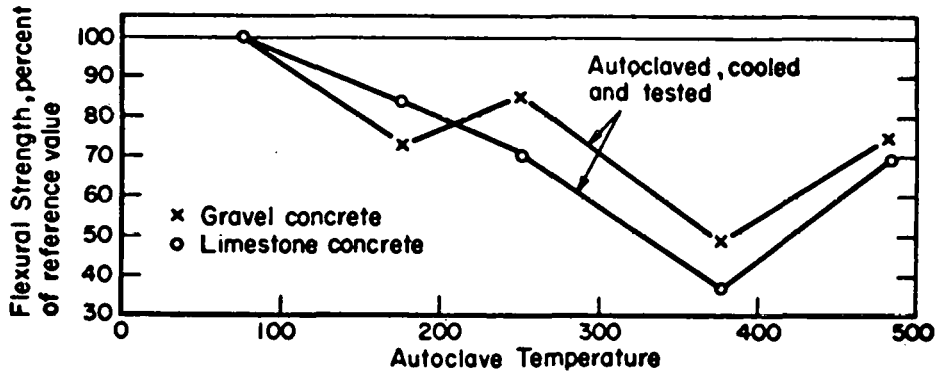


Fig. 33. Flexural Strength of Autoclaved Gravel and Limestone Concrete. Source: D. R. Lankard et al., "Effects of Moisture Content on the Structural Properties of Portland Cement Concrete Exposed to Temperatures up to 500°F," ACI SP-25, *Temperature and Concrete* (1970).

### 3.3.4 Shrinkage and Creep

The shrinkage of concrete is due primarily to loss of moisture and is called drying shrinkage. In the interior of a large concrete mass, where moisture movement is restricted, continued hydration results in autogenous shrinkage. The magnitude of this movement, measured as a linear strain, is between about  $40 \times 10^{-6}$  at one month and  $100 \times 10^{-6}$  after five years.<sup>35</sup> Drying shrinkage normally includes the small autogenous changes, except in some cases for very large mass concrete situations.<sup>35</sup> For concrete, the aggregate restrains shrinkage of the cement paste. Thus the degree of shrinkage in a particular concrete depends very much on the type and amount of aggregate used. The shrinkage rate decreases rapidly with time; according to Neville:<sup>35</sup> 14 to 34% of

the 20-year shrinkage occurs in two weeks, 40 to 80% of the 20-year shrinkage occurs in three months, and 66 to 85% of the 20-year shrinkage occurs in one year. Shrinkage is important because of its effect on movement of the structure and tendency to induce cracking.

The gradual increase in strain with time for a stressed structure is due to creep. Creep can be defined as the increase in strain under a sustained stress. Creep is of great importance in structural analyses, because the strain can increase significantly from that immediately after loading. It is usually assumed that creep and shrinkage are additive. However, as Neville<sup>35</sup> points out, shrinkage and creep are not independent phenomena to which superposition can be applied. In fact, shrinkage increases the magnitude of creep. Most available data on creep of concrete were recorded on the basis of additive properties. In the case of mass concrete structures, however, it may be necessary to make a distinction between basic creep (conditions of moisture movement) and drying creep (conditions of drying). Thus, as with other properties, investigations of sealed specimens are necessary to represent the mass concrete situation. Figure 34 provides a graphical explanation of the above effects.

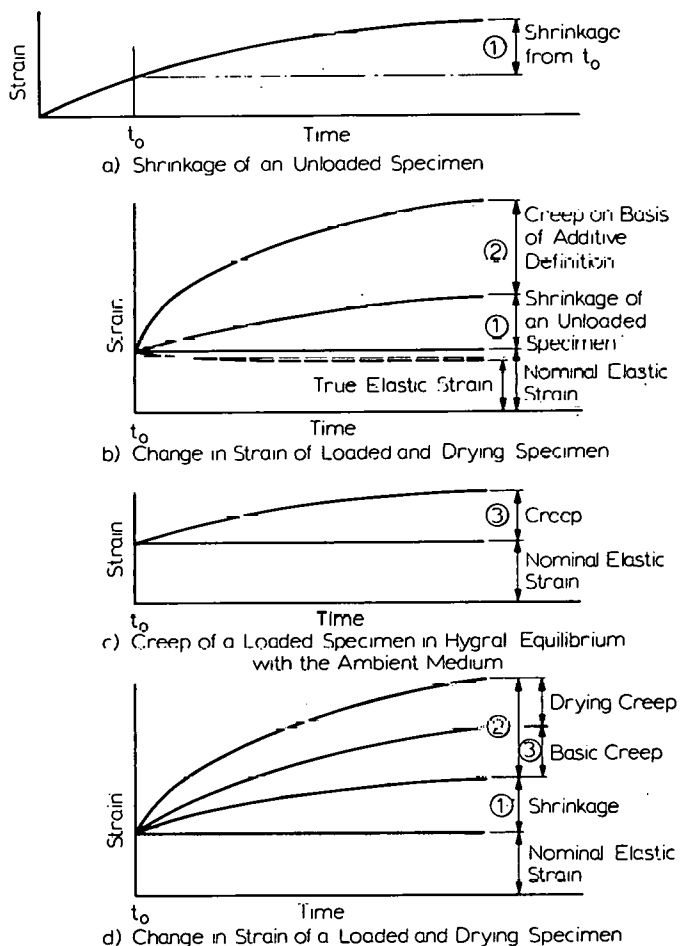


Fig. 34. Time-Dependent Deformations in Concrete Subjected to a Sustained Load. Source: A. M. Neville, *Properties of Concrete*, 2nd ed., Halsted, New York, 1973.

It is also necessary to understand the structural response on unloading, and Fig. 35 shows what is meant by instantaneous recovery and creep recovery of the deformation, showing that creep is not a fully reversible phenomenon. As one might expect, creep is influenced by many factors such as stress, age at loading, size of specimen, water/cement ratio, aggregate type, concrete strength, temperature, time, state of stress, etc. Creep influences the stability of a structure by increasing deformation. The ultimate strength may or may not be affected, but the structural performance under load is affected when deformation exceeds that for which it is designed. In addition, creep causes a loss of pre-stress for prestressed structures and thereby can affect the structural integrity. On the benefit side, creep in concrete relieves stress concentrations and, thus, contributes to structural integrity as well.

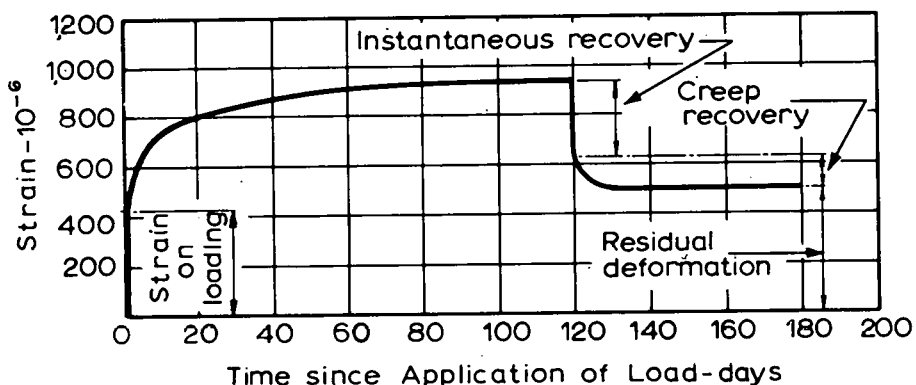


Fig. 35. Description of Creep and Creep Recovery Phenomena. Mortar specimen stored in air; RH, 95%; stress,  $14.8 \text{ MN/m}^2$ ; unloaded. Source: A. M. Neville, *Properties of Concrete*, 2nd ed., Halsted, New York, 1973.

Some of the effects of various parameters on creep are shown in Figs. 36-39. It can be seen that creep increases with increasing time and stress, but decreases with increasing relative humidity, age at loading, and maturity. In addition, Fig. 39 dramatizes the effect of aggregate on creep.

Creep of concrete is a complex subject and has been investigated and discussed for many years. Volumes of data are available on the effects of various conditions on creep. The problem of creep at higher than ambient temperatures has been studied only fairly recently [especially for temperatures above  $100^\circ\text{C}$  ( $212^\circ\text{F}$ )], yet a large number of investigations have been reported and many more are under way. As with most of the other concrete properties, because of the nature of a PCRV as a mass concrete structure, it is desirable to study the creep behavior of sealed specimens, which more nearly represent the moisture conditions in the bulk of PCRV concrete.

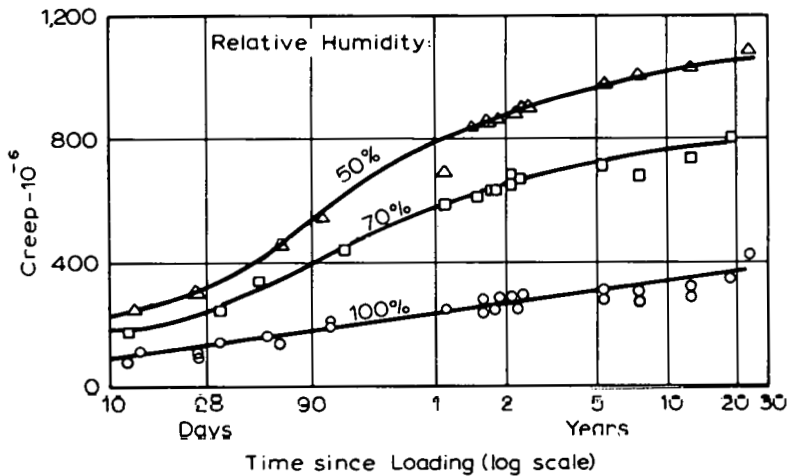


Fig. 36. Creep of Concrete Stored at Different Relative Humidities. Cured in fog for 28 days. Source: A. M. Neville, *Properties of Concrete*, 2nd ed., Halsted, New York, 1973.

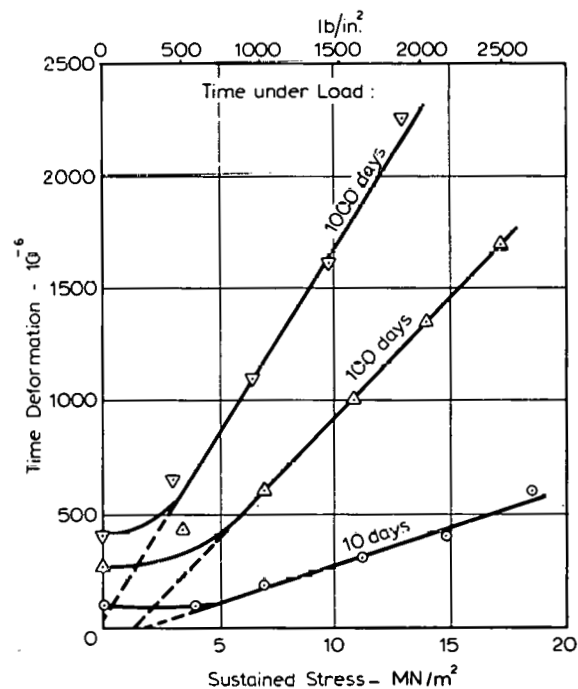


Fig. 37. Time Deformation (Creep Plus Shrinkage) of Concrete Stored in Air. Source: A. M. Neville, *Properties of Concrete*, 2nd ed., Halsted, New York, 1973.

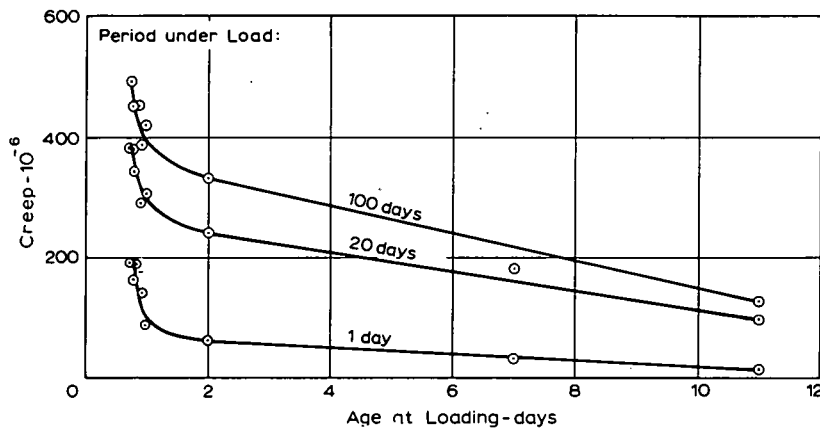


Fig. 38. Creep of Aluminous Concrete vs Age at Loading. Source: A. M. Neville, *Properties of Concrete*, 2nd ed., Halsted, New York, 1973.

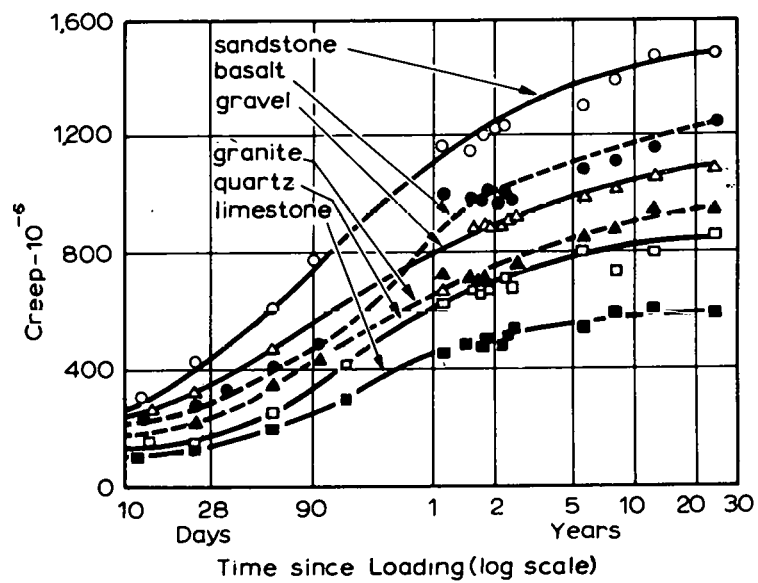


Fig. 39. Creep of Concretes with Different Aggregates. Loaded at age of 28 days; stored in air at 21°C; RH, 50%. Source: A. M. Neville, *Properties of Concrete*, 2nd ed., Halsted, New York, 1973.

A comprehensive review of the effects of temperature on creep of concrete was reported by Geymayer<sup>42</sup> in 1970. He briefly discussed the results of various investigations and normalized their data in terms of specific creep (creep strain per unit stress) and specific creep rate (the average slope of creep curve in a semilog presentation within the specified time period). Geymayer's review will be summarized along with an extended discussion of some of the investigations that he reported and that have been reviewed by this author. In addition, some results of other studies will be included as well as the results of more recent studies.

The graphs of data assembled by Geymayer are reproduced in Figs. 40-42. One of the major observations that has received much attention is the "creep maximum" effect observed by Nasser and Neville.<sup>34</sup> They observed that the specific creep and especially the specific creep rate reached a maximum at about 70°C (158°F) for specimens loaded under water. At higher temperatures, up to 96°C (205°F), the creep rate decreased. In plotting the specific creep rates, Geymayer shows, in Fig. 42, that studies by other investigators also resulted in similar observations. Marechal (see ref. 10 of ref. 42) observed a creep rate maximum (and corresponding maximum for total creep), but it occurred at about 50°C (122°F). Marechal's tests were conducted on unsealed specimens. In addition, the creep rate reached a minimum at just over 100°C (212°F) and increased greatly with temperatures to 400°C (752°F). The specific creep at 250°C (482°F) was about the same as at the 50°C (122°F) "maximum." Predrying of specimens for 30 days at 105°C (221°F) before load application reduced creep at temperatures below 105°C (221°F) drastically and eliminated the creep maximum (see Fig. 42).<sup>42</sup> The tests of Nasser and Neville

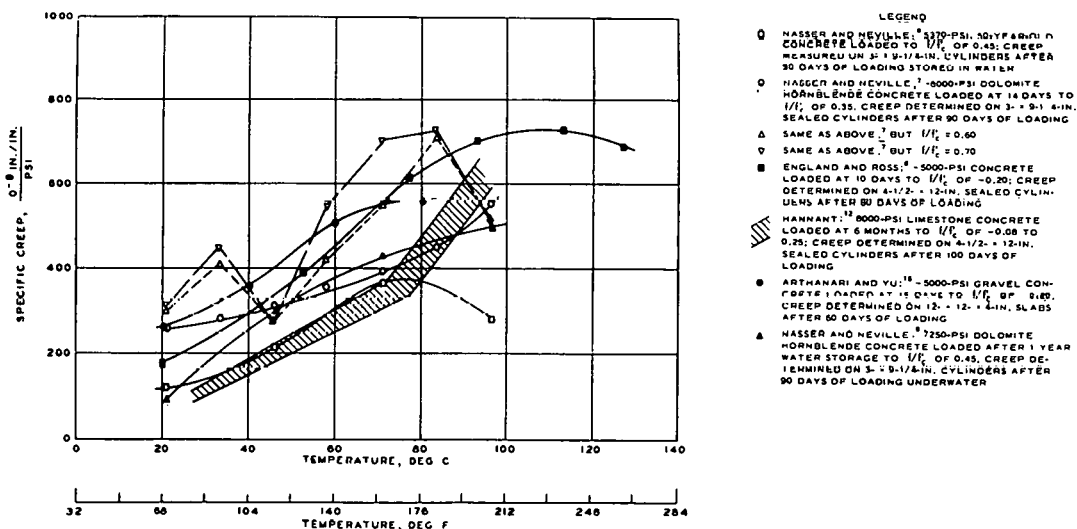


Fig. 40. Compilation of Temperature Effects on Concrete Creep, Sealed or Water Stored. Source: H. G. Geymayer, "Effect of Temperature on Creep of Concrete: A Literature Review," ACI SP-34, *Concrete for Nuclear Reactors*, pp. 565-90 (1972).

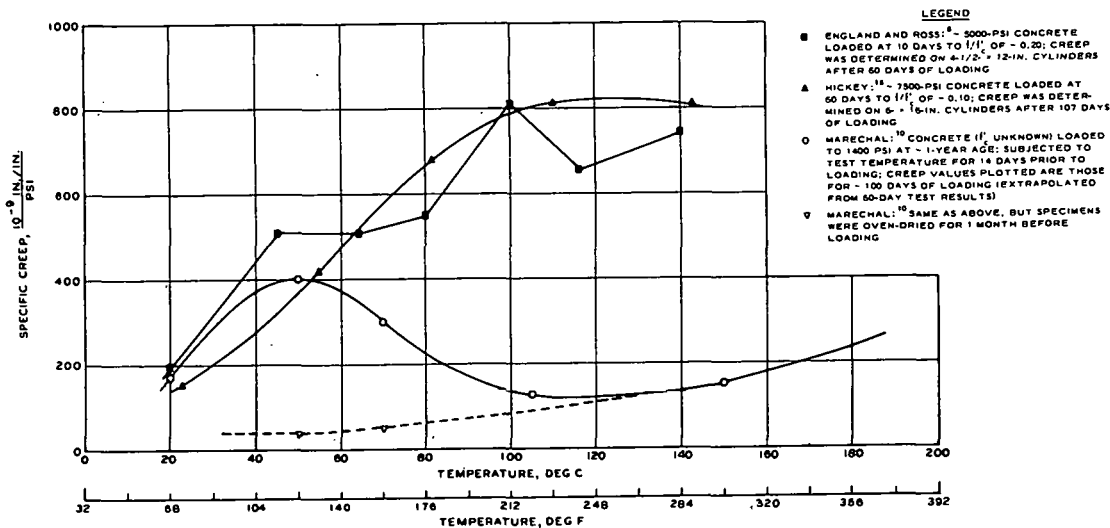


Fig. 41. Compilation of Temperature Effects on Concrete Creep, Unsealed. Source: H. G. Geymayer, "Effect of Temperature on Creep of Concrete: A Literature Review," ACI SP-34, *Concrete for Nuclear Reactors*, pp. 565-90 (1972).

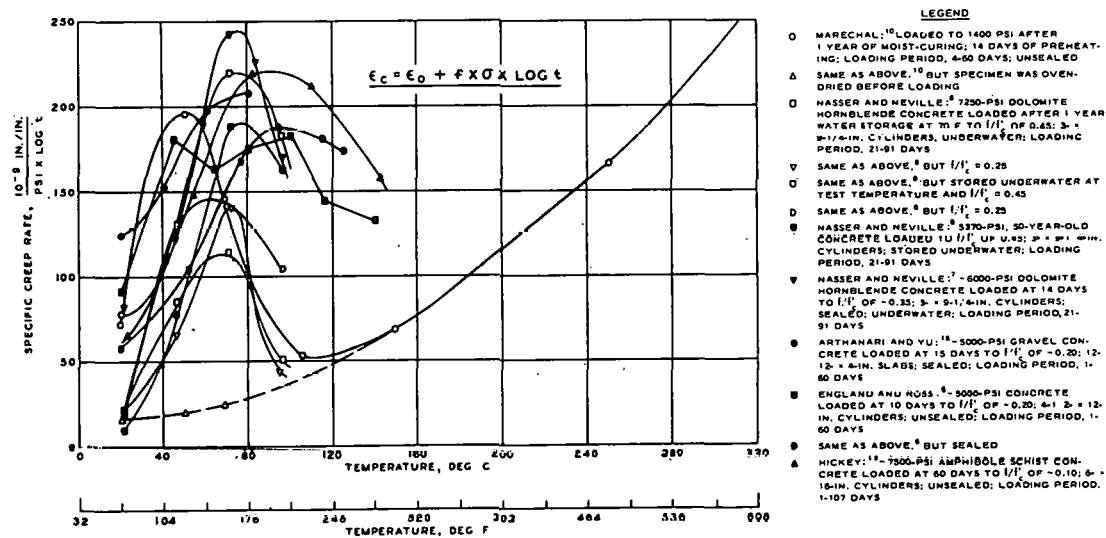


Fig. 42. Compilation of Temperature Effects on Concrete Creep Rate. Source: H. G. Geymayer, "Effect of Temperature on Creep of Concrete: A Literature Review," ACI SP-34, *Concrete for Nuclear Reactors*, pp. 565-90 (1972).

were conducted at stress/strength ratios of 35 and 70%. Further tests by Nasser<sup>24</sup> at stress/strength ratios of 10, 20, and 45% showed the same creep maximum at 70°C (158°F). Nasser<sup>24</sup> and Geymayer<sup>42</sup> both reference the work of Hickey (ref. 15 of ref. 42) on unsealed specimens, which showed a maximum creep rate around 50 to 80°C (122 to 176°F). Several other investigations of elevated-temperature creep did not reveal a maximum for total creep at comparably low temperatures, but most did indicate a maximum for the creep rate between 50 and 100°C (122 and 212°F) (if computed for some period between 1 and 100 days of loading). Nasser and Neville observed that there is a linear relation between creep and stress/strength ratio at elevated temperatures [up to 96°C (205°F)], just as at room temperature. They also observed that creep recovery is independent both of temperature and of the stress magnitude during creep. Third, the pattern of behavior, including the shape of the creep-time curve, does not change at elevated temperature. The mechanism postulated for their observations is based on Kesler's (ref. 2 of ref. 34) concept of basic creep and the effects of adsorbed water. They subscribed to the seepage theory of creep.

Geymayer<sup>42</sup> stated that results by DaSilviera and Florentino<sup>43</sup> challenge the hypothesis that creep recovery is independent of temperature. An examination of their report does show they concluded that the greater the temperature, the greater the creep recovery strains. However, in the text of their report (see pp. 175-76 of ref. 43) they state that the strain recovery was higher for the heated prisms. They also say that strain recovery rate was higher for heated prisms than for unheated prisms. It is not clear that DaSilviera and Florentino [sealed tests up to 45°C (113°F)] separated actual creep recovery from total strain recovery (as defined in Fig. 35). Nasser and Neville<sup>34</sup> did separate it and defined creep recovery as recovery in excess of the immediate strain change on unloading (see p. 1571 of ref. 34). DaSilviera and Florentino did, however, report that the creep Poisson ratio remains constant during a creep test and is equal to the elastic value. They also concluded that creep strains are the same in a water-soaked concrete and in a similar mass-cured concrete. They used 20 × 20 × 60 cm (7.9 × 7.9 × 23.6 in.) prisms with granite aggregate and water/cement ratios of 0.5 and 0.7. Also, they used very low stress/strength ratios of 0.08 (for w/c = 0.5) and 0.20 (for w/c = 0.7). McHenry's<sup>44</sup> expression was used to fit their data and gave a much better fit than the usual logarithmic representation. Specific creep strains in a concrete loaded at age  $\tau$  are given by

$$\bar{\epsilon} = Ae^{-\alpha\tau}(1 - e^{-\beta t}) + B(1 - e^{-\gamma t}) , \quad (1)$$

where  $t$  is the time after loading, and  $A$ ,  $B$ ,  $\alpha$ ,  $\beta$ , and  $\gamma$  are characteristic parameters that are determined experimentally.<sup>43</sup>

Browne and Blundell (ref. 19 of ref. 42) performed creep tests on sealed specimens up to 95°C (203°F) for ages up to 400 days. On a logarithmic plot of time from loading, initial data showed the creep vs log time plot to be linear, but the data deviated upward for the longer times under load. On a log/log basis, however, the creep curves remained linear

up to six years. They also used the log/log relationship with results from other investigations and obtained improved results. Their expression for creep curves was

$$\epsilon = \alpha(t)^n \text{ or } \log \epsilon = \log \alpha + n \log (t) , \quad (2)$$

where

- $\epsilon$  = specific creep strain,
- $\alpha$  = a factor decreasing with age at loading,  $k$ , and increasing with absolute temperature,  $\theta$ ,
- $t$  = time under load in days,
- $n$  = a factor, decreasing with age at loading,  $k$ , and varying with absolute temperature,  $\theta$ .

Browne and Blundell's results consistently showed an increase of total creep up to 95°C (203°F). Geymayer discussed the limited significance of a creep rate computed for a period of 1 to 100 days after loading and the possible reasons for observing maximum creep rates during a particular time period without observing a corresponding maximum total creep value at the end of the time period. Figure 43 represents a schematic creep curve typical of many of the creep curves in the literature review of Wagner (ref. 20 of ref. 42) and the report of Wallo and Kesler (ref. 21 of ref. 42). The double inflection observed between 3 and 10,000 days (~27 years) is obvious in the figure and shows how the creep rate calculated between  $t_0$  and  $t$  may not necessarily represent behavior at later times in the loading history. With reference again to Figs. 40-42, and the observations of creep maximums by some investigators, the most pronounced creep maxima and those found at the lower temperatures represented specimens which had been heated for about two weeks before load application. Geymayer suggests that the effect of elevated temperatures is to magnify and accelerate the creep phenomenon, resulting in a greater percentage of total creep to occur during the first days after loading. Results from unsealed specimens strongly support this simple concept. Also, results of some sealed or submerged specimens support it, while others do not.<sup>42</sup>

In a program to observe creep in mass concrete (sealed specimens) at high temperatures [above 100°C (212°F)], Nasser and Lohtia<sup>43</sup> subjected 7.62 × 22.9 cm (3 × 9 in.) cylinders to various stress/strength ratios (20, 30, and 50%) for room-temperature strength values (ratios change if strength at elevated temperature is considered) and high temperatures, 20 to 232°C (68 to 450°F), for up to six months. They also measured creep recovery. A type III cement with 1.91-cm (3/4-in.) maximum size aggregate (dolomite and hornblende) and a water/cement ratio of 0.60 was used in all tests. All tests were one day old when exposed to the test temperature and were cured for 13 days in the sealed condition. They were then loaded, and strains were measured periodically up to six months. After unloading, creep recovery was observed for 70 days. They corrected the applied axial stresses to account for saturated steam pressure due to moisture at temperatures of 121, 149, 177, and 232°C (250, 300, 350, and 500°F) [pressures were 0.14, 0.34, 0.83, and 2.89 MPa (20, 50, 120, and 420 psi) respectively]. The apparatus developed for measuring creep

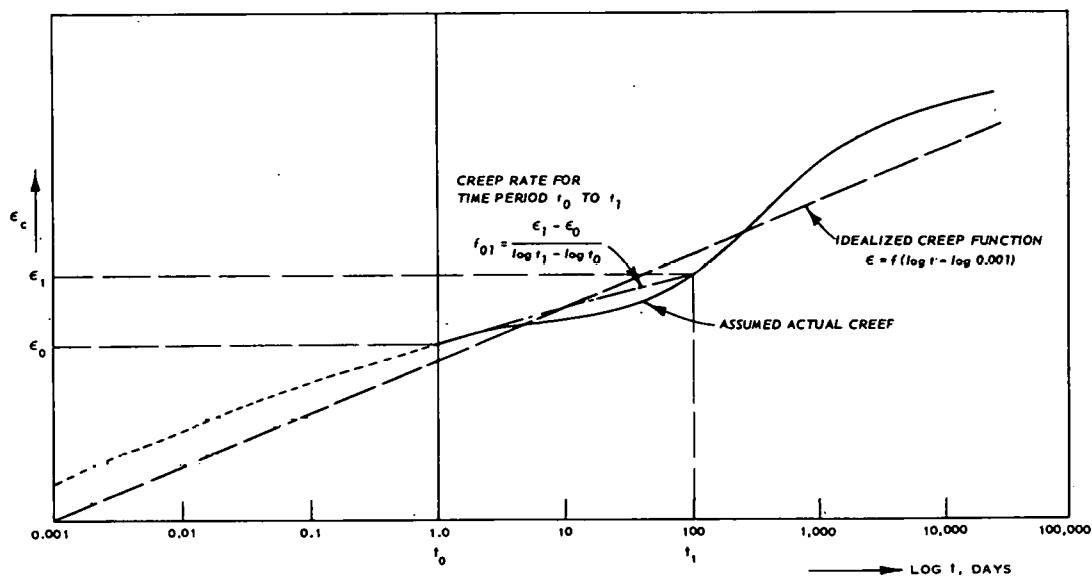


Fig. 43. Schematic Creep Curve. Source: H. G. Geymayer, "Effect of Temperature on Creep of Concrete: A Literature Review," ACI SP-34, *Concrete for Nuclear Reactors*, pp. 565-90 (1972).

in sealed specimens at temperatures to 232°C (500°F) deserves description here.<sup>46</sup> Figure 44 shows the details of the machine. Each unit is made of 7.94-cm-diam (3 1/8-in.), 0.79-cm-thick (5/16-in.) mild-steel pipe with 1.27-cm-thick (1/2-in.) mild-steel flanges and a mild-steel piston assembly. Brass diaphragms 0.025 cm (0.010 in.) thick seal the piston assembly and concrete against oil and moisture leakage. Load is applied through the piston assembly by oil pressure. The unit is designed for a pressure of 20.68 MPa (3000 psi). Displacements are measured by an extensometer attached to the cover plate and piston assembly. The pipe is wound with high-resistance wire for heating the enclosed concrete.

The results of some creep tests are presented in Figs. 45 and 46. Figure 45 represents tests at 177°C (350°F) for various stress levels. Two straight lines were fit to the data of each stress level, one from 1 to 21 days, and the other from 21 to 180 days. Figure 46 shows the creep curves obtained for a stress/strength ratio of 20% at various temperatures. The creep increased with temperatures up to 150°C (302°F) (after 40 days) and then decreased at 177 and 232°C (350 and 450°F). For stress/strength ratios of 35 and 50%, the maximum creep occurred at 177°C (350°F). At ratios of 35 and 50% they observed that the creep rate between 121 and 180 days increased up to 71°C (160°F) and thereafter decreased with temperature to 232°C (450°F). (This observation agrees with Nasser and Neville's<sup>34</sup> "creep maximum," as discussed previously.) The creep rate did not begin to decrease for the 20% test until after 150°C (302°F). Figure 47 shows the 180-day creep data up to 232°C (450°F) for the three stress levels used. The authors went through a procedure whereby values of actual stress/strength ratios corresponding to applied stresses at each temperature were calculated. They used the

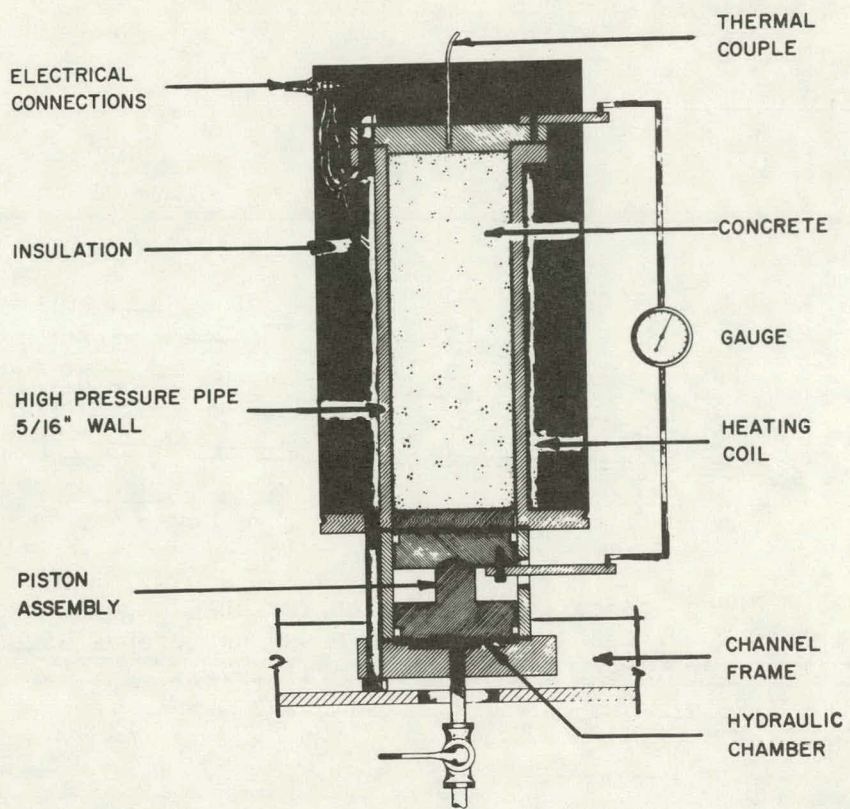


Fig. 44. Details of Apparatus for Sealed Creep Tests at High Temperatures. Source: R. P. Lohtia and K. W. Nasser, "Apparatus for High Temperature Creep Tests of Concrete," *J. Am. Concr. Inst.* 68(2): 114 (February 1971).

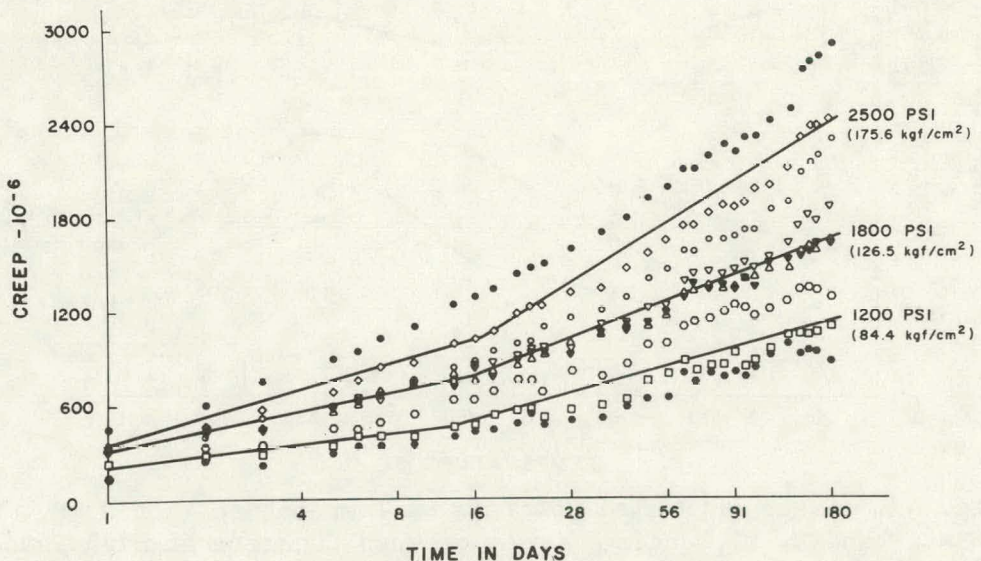


Fig. 45. Creep of Sealed Concrete Under Various Stress Levels at 177°C. Source: K. W. Nasser and R. P. Lohtia, "Creep of Mass Concrete at High Temperatures," *J. Am. Concr. Inst.* 68(4): 276 (April 1971).

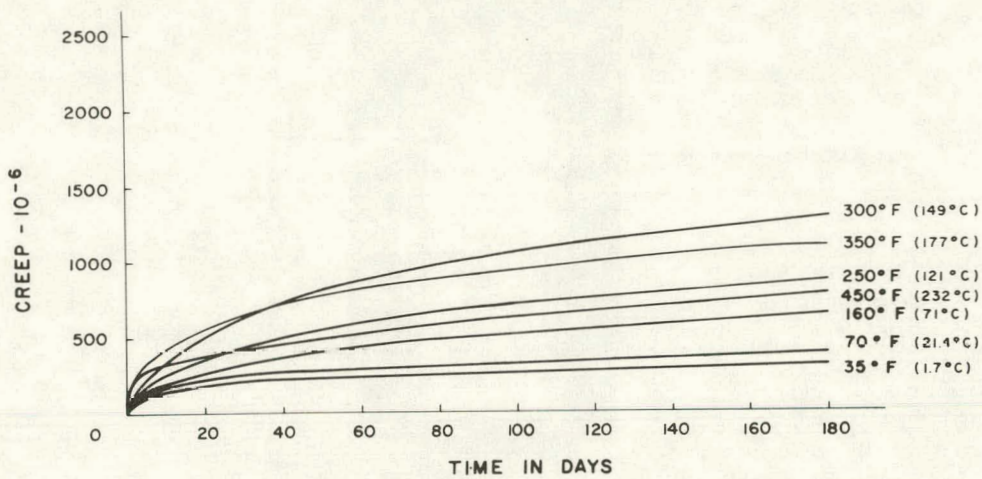


Fig. 46. Creep of Sealed Concrete at Various Temperatures. Source: K. W. Nasser and R. P. Lohtia, "Creep of Mass Concrete at High Temperatures," *J. Am. Concr. Inst.* 68(4): 276 (April 1971).

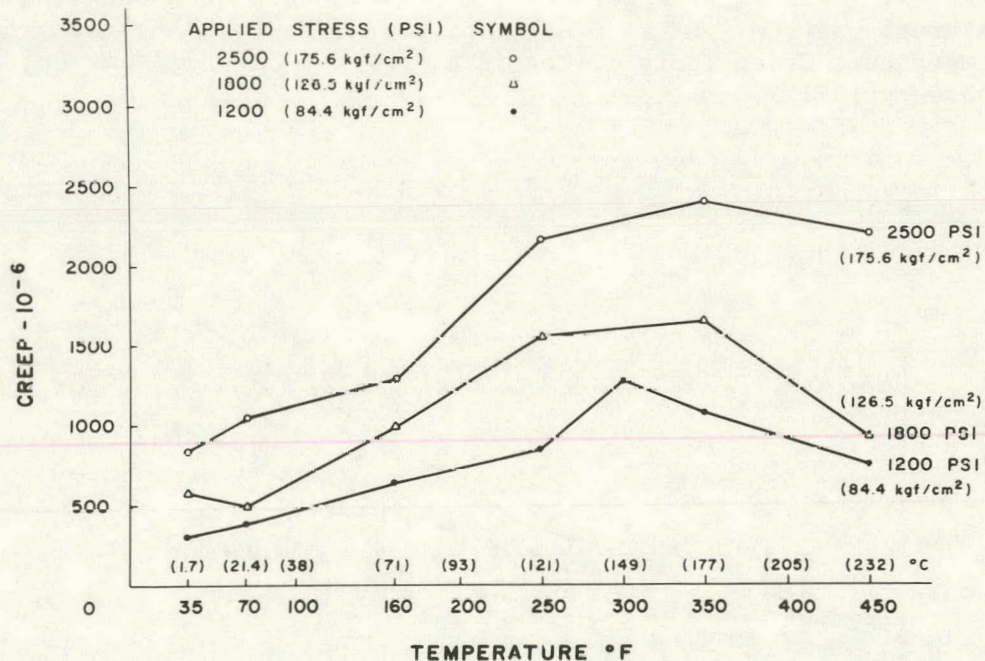


Fig. 47. Creep of Sealed Concrete vs Temperature, 180 days. Source: K. W. Nasser and R. P. Lohtia, "Creep of Mass Concrete at High Temperatures," *J. Am. Concr. Inst.* 68(4): 276 (April 1971).

amount of steam pressure present and the strength of the specimens as determined at the completion of the tests. It is not clear how they obtained their adjusted ratios. They showed no creep recovery data but stated that creep recovery was independent of temperature and dependent on stress. The maximum measured recovery strain was  $390 \times 10^{-6}$ . Nasser and Lohtia referred to the theory of absorbed moisture and the viscous nature of the creep mechanism.

With regard to the study in general, comments made previously concerning Nasser and Lohtia's study of strength and elasticity at high temperature<sup>33</sup> apply here. That is, their specimens were demolded at the age of one day and cured in a sealed condition at the test temperature. This procedure is not believed to be representative of the PCRV concrete, which would not be exposed to high temperatures until months after casting. In the PCRV, heat of hydration will cause most of the concrete to be exposed to early age elevated-temperature curing, but certainly not at temperatures of 100°C (212°F) and above. It would be interesting to compare data obtained in a similar manner, but using more mature concrete.

Experiments conducted by Kennedy<sup>47</sup> were designed to determine the long-term creep behavior of concrete at 20 and 65°C (68 and 149°F) in the sealed and unsealed conditions. He investigated the effects of curing time, curing history, and state of stress. The mixture consisted of fine and coarse limestone aggregate with type II cement and a water/cement ratio of 0.425. The tests involved 15.24-cm-diam, 40.64-cm-long (6 x 16 in.) cylinders tested under uniaxial, biaxial, and triaxial conditions. The multiaxial cases will be discussed later. A 34.47-MPa (5000-psi) hydraulic pressure loading system was utilized, and specimens were sealed with epoxy coatings and 0.020-cm-thick (0.008-in.) copper jackets. Vibrating wire strain gages were embedded in the specimens for strain measurements.

Measurements of shrinkage strains during a 90-day curing period at 20°C (68°F) showed almost negligible shrinkage in the sealed specimens, while the air-dried cylinders experienced continuous shrinkage to about 200 microstrain. During loading the sealed specimens showed no shrinkage at 20°C (68°F), but at 65°C (149°F), about 40 microstrain of expansion was recorded. For the creep tests at 20°C (68°F), curing history and curing time prior to loading were important. For a 16.54 MPa (2400-psi) uniaxial stress, shorter curing periods resulted in greater creep strains during loading. For the first 2 to 2.5 years the mass-cured specimens showed less creep strain than did the air-dried, but during the next 2.5 years the ratio of mass-cured to air-dried creep approached a value of 1. At 20°C (68°F) the ratios of five-year to one-year creep for 180- and 365-day mass-cured specimens were about 1.5 and 1.8, respectively, with the absolute values of specific creep being equal at about 27.6 microstrain/MPa (0.19 microstrain/psi). Interestingly, the five-year results at 20°C (68°F) for 180-day curing were essentially predicted by equations developed in an earlier study.<sup>48</sup> Those equations were based on tests of specimens loaded at 90 days and kept under load for one year. As an example, the axial creep strain for a mass-cured specimen loaded at 65°C (149°F) is given by

$$(\varepsilon_c)_a = 0.323 \left( 1 - e^{-0.118t} \right)^{0.374} (\sigma_a - 0.298\sigma_r) , \quad (3)$$

where

$$\begin{aligned}
 \sigma_a &\equiv \text{axial stress, psi,} \\
 r &\equiv \text{radial stress, psi,} \\
 t &\equiv \text{time after loading, days, and} \\
 (\varepsilon_c)_a &\equiv \text{creep strain in axial direction, microunits.}
 \end{aligned}$$

With regard to creep recovery, Chuang et al. found that a larger percentage of the creep strain, which occurred during one year under load, was recovered from the sealed concrete than from the air-dried concrete.<sup>49</sup> Thus the lack of dependence on temperature for creep recovery agrees with the observations of others.<sup>34, 45</sup>

A mathematical model for isothermal creep behavior was developed by Mukaddam<sup>50</sup> for sealed concrete specimens loaded at stress/strength ratios of 35 to 45% and temperatures up to about 100°C (212°F). The model was based on the linear, viscoelastic response of concrete and its behavior as a thermorheologically simple material. Based on the time-shift principle, then, Mukaddam demonstrated, using data from various investigators, that the total specific creep of concrete for any temperature is constant when considering ages at loading of 28 to 400 days and loading times up to 1000 days. He concluded that further work on the effects of temperature above 100°C (212°F), multiaxial stress states, and Poisson's ratio is needed, as well as additional analytical investigations. A summarized version of Mukaddam's work is given in ref. 51.

Creep tests on the concrete used in the Wylfa PCRV were reported by Browne.<sup>10</sup> Shrinkage was found to be very small in sealed concrete and indicated that heating could cause some expansion. A limit curve was constructed for shrinkage to a 30-year life based on expected conditions in the Wylfa vessel which showed that 400 microstrain was a conservative estimate. For temperature gradients and temperatures above those now in current use, more precise information would be required. In tests up to 95°C (203°F), Browne found that uniaxial creep did increase substantially with temperature, but much scatter was obtained using 15.24-cm-diam, 30.48-cm-long (6 x 12 in.) cylinders with 3.81-cm (1 1/2-in.) coarse aggregate. Generally, the creep deformation decreased with increasing age at loading and decreasing water/cement ratios. He expressed the creep behavior using an equation that considered the age at load application, the time after loading, and the temperature during loading. The equation includes factors that must be experimentally determined for the particular concrete being utilized in a design application. Browne reported that his limited data above 80°C (176°F) did not allow an observation as to whether the creep rate decreased at those temperatures as suggested by Nasser and Neville.<sup>34</sup>

Experiments conducted by Gross<sup>52</sup> on creep behavior showed, again, that creep increases very substantially at high temperatures. Tests at different stress levels showed, upon normalizing results to a stress level of 0.2, that thermal creep strains may be treated as linear, viscoelastic strains up to about 300°C (572°F) (within confidence limits of  $\pm 10\%$ ). Gross did not state whether specimens were sealed or unsealed, although the age at loading was given as 6 to 12 months; so it is presumed that they were not sealed against moisture loss. In addition, the time under load was only 7 to 15 days. The author provides various justifications

for this, mainly that about 75% of full creep response may be registered in that time period. No results in his paper were found to provide adequate justification for that kind of conclusion. In fact, with regard to high-temperature creep of sealed specimens, his statement is judged to be premature.

Tests by Wang<sup>53</sup> resulted in conclusions that (1) elevated-temperature [up to 425°C (797°F)] creep-time curves of concrete have the same shape as those at room temperature, (2) creep rate is higher at high temperatures and high stress/strength ratios, (3) low water/cement ratios result in less creep, (4) a nonlinear relationship generally exists between creep and stress/strength ratio, and (5) ultimate compressive strength at elevated temperatures is much higher than that predicted by others. The tests were not performed using sealed specimens. The conclusion regarding the nonlinear relationship between creep and stress/strength ratio was based on two ratios (40 and 60%) and extrapolated to zero. Some of the relationships did result in linearity, while some did not. The high ultimate strengths at high temperatures were probably observed because the specimens were heated while under load. The author felt that the heating while under load was more practical for actual structures. His high values of creep are considered to be a result of the unsealed nature of the specimens. The results of Seki and Kawasumi<sup>54</sup> substantiate that observation.

The investigations of behavior at elevated temperatures produce the common observation that increasing temperature results in substantially higher creep strains. In general, the specific creep of sealed specimens is shown to be less than that for specimens subjected to some degree of drying. Also, it is apparent that creep will be substantially greater for young concrete in both sealed and unsealed conditions. The phenomenon of a "creep maximum" has been observed by many investigators. The term is somewhat of a misnomer, because the observation is that the specific creep rate reaches a maximum with increasing temperature and is not necessarily accompanied by a corresponding maximum in actual creep strain. The observed maximum has been reported variously from 50 to 100°C (122 to 212°F) and for one case of a 20% stress/strength ratio, up to 150°C (302°F). In fact, not all studies have reported the maximum creep rate effect. Also, in general, most studies have reported that the shape of the curves for creep vs time at high temperatures is similar to those at room temperature. Creep recovery has been observed to be less than the associated creep strain. The degree of creep recovery appears to be independent of temperature but dependent on stress. In addition, shrinkage strains of concrete are reported to be very low for sealed specimens, and, in fact, high-temperature exposure has been shown to result in expansion. With regard to stress/strength ratio, increasing ratios increase creep substantially. Considering the reports on deterioration of compressive strength at temperatures over 100°C (212°F) for sealed specimens, the stress at which creep becomes structurally significant is substantially decreased. For temperatures below 100°C (212°F), the procedures of limit design appear to be adequate for prediction of structural behavior. For sustained temperatures above 100°C (212°F), the variations in experimental techniques, concrete mixtures, curing, and loading histories prohibit the development of a reliable general conclusion of long-term behavior.

### 3.3.5 Thermal Properties

The thermal properties of concrete affect its performance over a long period of time under varying conditions. The dissipation of heat from radiation absorption and from the reactor coolant is important in the PCRV for the development of thermal gradients and resultant thermal stresses. The ability of the concrete to dissipate heat is determined by the coefficient of thermal conductivity,  $k$ , the normal thermal diffusivity,  $\alpha$ , and the specific heat,  $c$ . The three parameters are related by the term  $\alpha = k/c\rho$ , where  $\rho$  is the density of the material. Specific heat is a measure of heat required to raise the temperature of a unit mass by 1°, while the normal thermal diffusivity relates to the ease with which the material will submit to a temperature change. The thermal conductivity is affected similarly by the other two parameters. That is,  $k$  will increase with increases in either diffusivity or specific heat. A high thermal conductivity will result in a rapid dissipation of heat flux into the material. That is desirable in order to minimize thermal gradients through the thickness. As shown in Table 3, Browne<sup>10</sup> states that the cooling requirement can be minimized with high thermal conductivity.

The coefficient of thermal expansion represents the change in volume of material subjected to a temperature differential. It is usually expressed as a change in length per degree of temperature change for test specimens. The thermal expansion is of importance to reduce structural movement and thermal stresses (Table 3). Thermal expansion is a complicated phenomenon in concrete because of the differential expansion of its components and the resulting development of internal stresses. These changes are dependent primarily on the properties of the cement paste and aggregate. The properties of the aggregate appear to control the thermal expansion characteristics of the concrete.<sup>55</sup> Furthermore, the main factor influencing the thermal expansion of rock and, therefore, of concrete is the proportion of quartz. Low coefficients of expansion are obtained with rocks having little or no quartz. In addition, the coefficient increases nonlinearly with temperature, and, thus, a particular coefficient can only be given over a limited temperature range. Moreover, the thermal coefficient of expansion in concrete is affected by the mix proportions, moisture content, age of concrete, and the coefficients of various constituents.

Harada et al.<sup>40</sup> measured the coefficients of thermal expansion for various concretes in the unsealed condition. Their results are shown in Fig. 48. The water/cement ratios varied from 60 to 70%, depending on the aggregate used. The coefficients for silica aggregate concrete coincide with those of the original stones. The limestone concrete was similar and was closest to the value of the reinforcing steel.

Tests by Marechal<sup>56</sup> indicated that microcracking affected the expansion measurements at temperatures as low as 300°C (572°F), but, for most concretes, 500°C (932°F) was more common. By submitting specimens to ten thermal cycles between 20 and 500°C (68 and 932°F), they showed that, when cooled to 20°C (68°F), the concrete retained shortening compared with its original state. In addition, it expanded a little less at the end of ten cycles than during the first cycle. Thus, at elevated temperatures below a critical temperature for microcracking, the concrete tends to evolve toward a more consistent thermal expansion behavior.

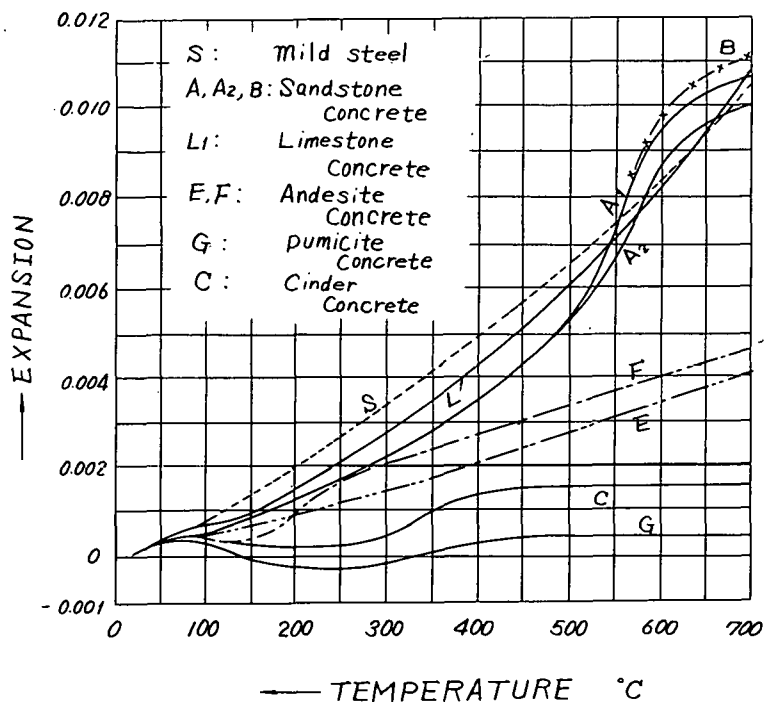


Fig. 48. Thermal Expansion of Various Concretes at Elevated Temperatures. Source: T. Harada et al., "Strength, Elasticity, and the Thermal Properties of Concrete Subjected to Elevated Temperatures," ACI SP-34, *Concrete for Nuclear Reactors*, pp. 377-406 (1972).

Campbell-Allen and Desai<sup>20</sup> reported coefficient values for aggregates, mortars, and concrete mixtures used in their program. From 20 to 300°C (68 to 572°F), the limestone concrete showed an increase in thermal expansion coefficient from 6.7 to 10.8 microstrain/°C (3.72 to 6.0 microstrain/°F), a change of 60%. The change for fireclay brick was slightly greater, while that of expanded shale concrete was slightly less.

Philleo<sup>36</sup> also measured expansion on unsealed specimens. The coefficient increased with water/cement ratio as expected. The values above 427°C (801°F) were, in most cases, two to three times higher than those below 260°C (500°F). He relates the results to dehydration of cement paste and attributed the differences above and below 427°C (801°F) to the fact that drying shrinkage of the paste keeps the coefficient low.

England and Ross<sup>57</sup> sealed specimens with a relatively impervious membrane of polyester resin and fiberglass reinforcement. The concrete had a water/cement ratio of 0.45 and was 14 days old at testing. After heating to 140°C (284°F), they reported coefficients of  $10.5 \times 10^{-6}/^{\circ}\text{C}$  ( $5.83 \times 10^{-6}/^{\circ}\text{F}$ ) for the sealed specimens and  $12.1 \times 10^{-6}/^{\circ}\text{C}$  ( $6.72 \times 10^{-6}/^{\circ}\text{F}$ ) for unsealed specimens. As drying progressed in the unsealed case, the coefficient value decreased.

Browne<sup>10</sup> emphasized that the coefficient of thermal expansion, even within a particular rock group, can vary considerably. He gleaned data from various sources and showed, as suggested by Griffiths (ref. 45 of ref. 10), that increasing silica content in the aggregate resulted in an

increased coefficient. For example, a limestone aggregate with negligible silica may have a coefficient 50% less than an aggregate of high silica content. Browne presented three graphs, reproduced in Figs. 49, 50, and 51, which relate the thermal strain and/or coefficient to temperature, humidity, and age respectively. The figures show that limestone concrete experienced a permanent expansion set, due to a thermal cycle, which Browne relates to differences in expansion coefficients of aggregate and cement paste. The effects of age and relative humidity on mass concrete may be related because of a slow decrease in relative humidity within the massive section as hydration proceeds. Browne's test results for sealed Wylfa concrete are shown in Fig. 52 for various concrete ages and temperatures. The changes with age vary only from 8.7 microstrain/°C (4.83 microstrain/°F) at 60 days to 7.9 microstrain/°C (4.39 microstrain/°F) at two years (not shown on the graph). Also, the coefficient given is representative for the entire range of 20 to 95°C (68 to 203°F). A water-stored specimen had a coefficient about 20% less than did the sealed specimen of the same age. Browne states that selection of an aggregate with a low thermal expansion could significantly reduce thermal stresses in the concrete. He does not address any affects it might have on the reinforcing and prestressing, such as some loss of prestress, of the structure because of large differences in expansion characteristics between concrete and steel.

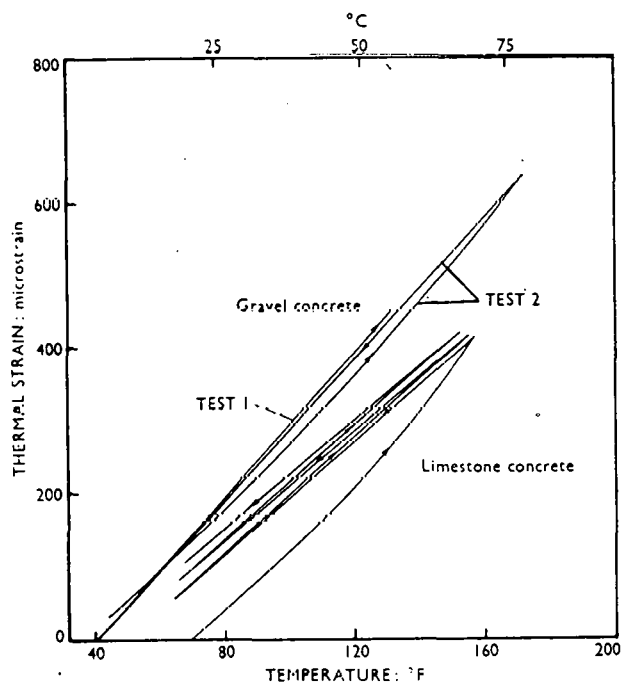


Fig. 49. Thermal Movement with Temperature Cycling of Concrete.  
 Source: R. D. Browne, "Properties of Concrete in Reactor Vessels," Group C, Paper 13, Conference on Prestressed Concrete Pressure Vessels, Westminster, S.W.I., March 1967.

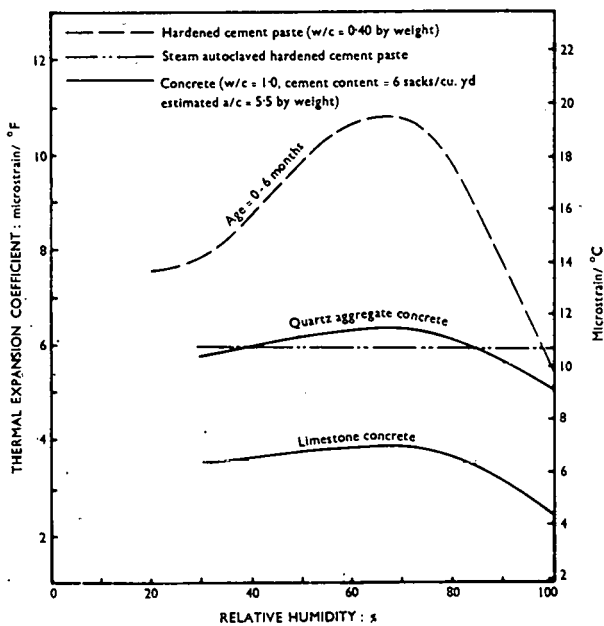


Fig. 50. Effect of Relative Humidity on Thermal Expansion of Concrete.  
 Source: R. D. Browne, "Properties of Concrete in Reactor Vessels," Group C, Paper 13, Conference on Prestressed Concrete Pressure Vessels, Westminster, S.W.I., March 1967.

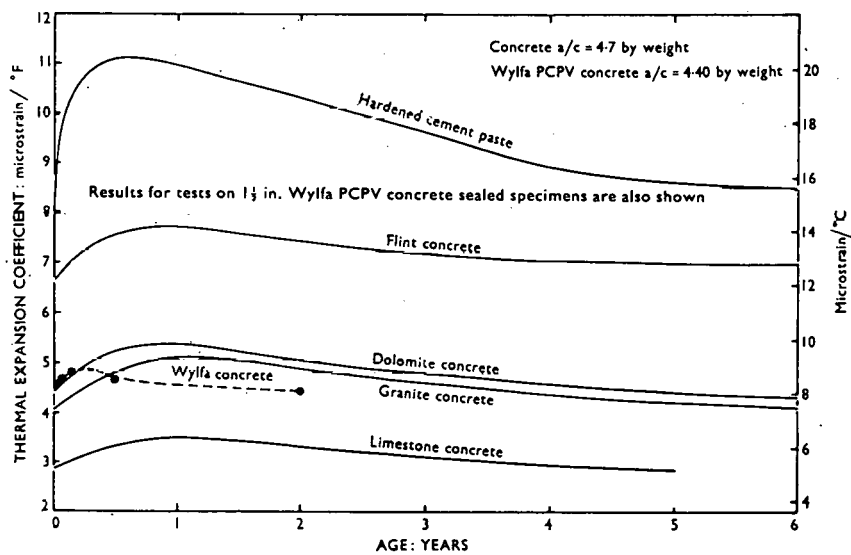


Fig. 51. Thermal Expansion Coefficient vs Age of Concrete, Sealed.  
 Source: R. D. Browne, "Properties of Concrete in Reactor Vessels," Group C, Paper 13, Conference on Prestressed Concrete Pressure Vessels, Westminster, S.W.I., March 1967.

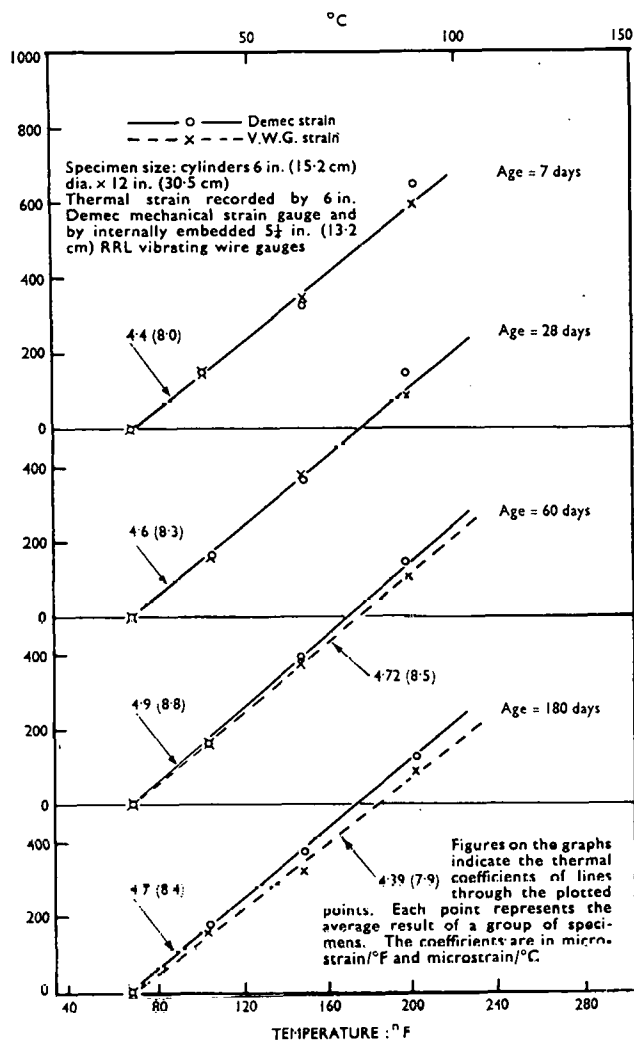


Fig. 52. Thermal Expansion of Wylfa Concrete. Source: R. D. Browne, "Properties of Concrete in Reactor Vessels," Group C, Paper 13, Conference on Prestressed Concrete Pressure Vessels, Westminster, S.W.I., March 1967.

Bertero and Polivka's<sup>31</sup> tests of sealed concrete shown in Fig. 53 revealed the same permanent expansive set phenomenon after one thermal cycle [to 149°C (300°F)] that Browne observed. In addition, they reported that the permanent expansion increased with number of cycles, but at a decreasing rate. The expansion strain at 149°C (300°F) for one cycle was 1200 microstrain, whereas for 14 cycles it was about 1600 microstrain. The permanent expansion after cooling was about 350 and 700 microstrain after 1 and 14 thermal cycles respectively. For a sealed specimen exposed to 149°C (300°F), the thermal strain increased from 1100 to 1520 microstrain when held at temperature for 14 days, analogous to the creep phenomenon. The authors reported a slight increase in coefficient of thermal expansion at high temperature. It is barely discernible from Fig. 53, but from 20 to 90°C (68 to 194°F) the average coefficient was reported as

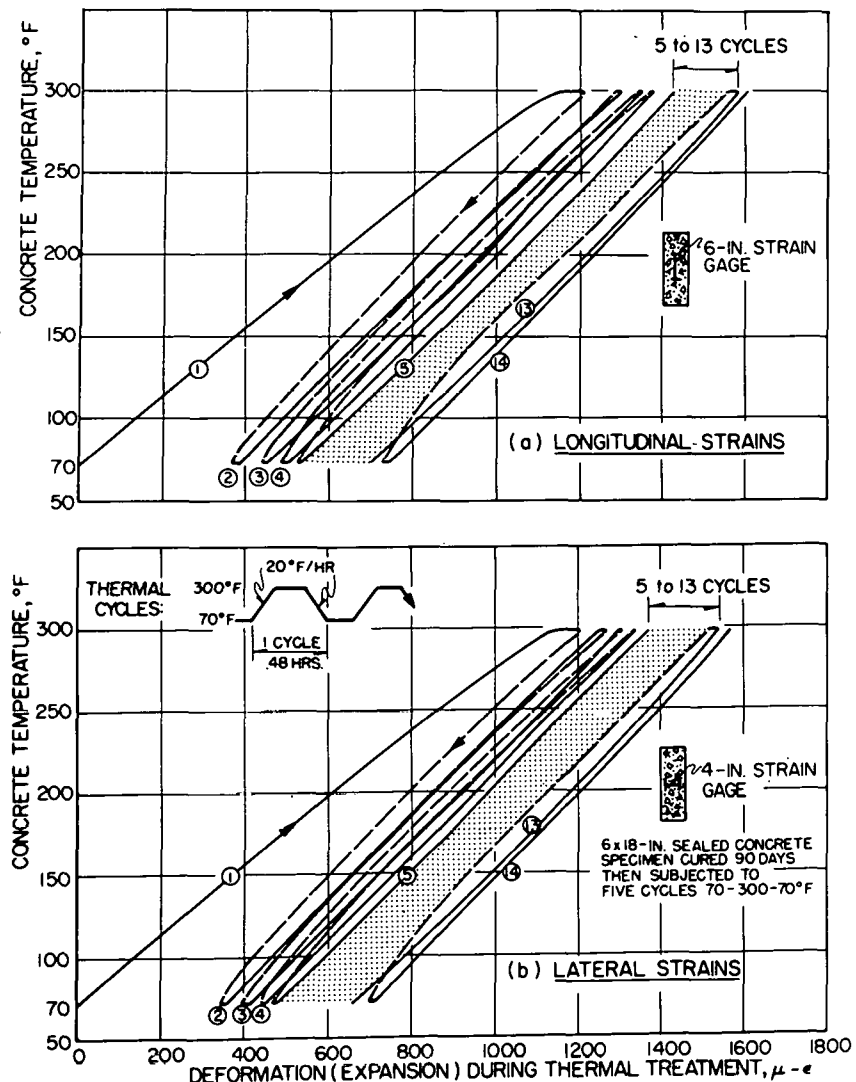


Fig. 53. Strain-Temperature History of Sealed Concrete. Source: V. V. Bertero and M. Polivka, "Influence of Thermal Exposure on Mechanical Characteristics of Concrete," ACI SP-34, *Concrete for Nuclear Reactors*, pp. 505-31 (1972).

7.74 microstrain/°C (4.3 microstrain/°F), and from 20 to 149°C (68 to 300°F) as 8.46 microstrain/°C (4.70 microstrain/°F). The difference is less than 10%, and the coefficient is considered constant up to 149°C (300°F). On the other hand, a heating rate of 5.5°C/hr (9.9°F/hr) resulted in a 16% increase over the coefficient obtained with a rate of 11°C/hr (19.8°F/hr). In addition, the coefficient decreased with number of thermal cycles. During the first cycle the value was about 8.60 microstrain/°C (4.78 microstrain/°F); during the 14th cycle it was only 6.73 microstrain/°C (3.74 microstrain/°F), a decrease of 22%. Even though the specimens were sealed, water escaped on heating and collected in the gap between specimen and jacket. Thus, some drying shrinkage must have occurred which caused the

measured value of thermal expansion to be less than that due simply to heating. The authors claim that the measurement of 730 microstrain permanent expansion after 14 thermal cycles must have been due to a considerable amount of microcracking. Specimens allowed to dry after initial heating showed much less expansion during subsequent thermal cycling. Because of this, they conclude that the presence of free moisture increases the amount of microcracking. Also, the coefficient was about 10% lower for the dried specimens.

As with many of the other properties discussed, the thermal expansion characteristics are dependent on many factors. In one case the unsealed condition resulted in a higher coefficient, and in another, a lower coefficient. In fact, even with the tremendous variation in mixtures, test techniques, and concrete conditioning, the coefficient of thermal expansion does not vary a great deal. It is a universal observation that the coefficient increases only slightly with temperatures to 250 or 300°C (482 or 52°F). Other factors such as moisture content, thermal cycles, and heating rate can affect a given concrete to a greater degree than the aforementioned temperature range.

Typical values of thermal conductivity for normal concretes are in the range of 1.0 to 5.2  $\text{W m}^{-1} \text{K}^{-1}$  (0.9 to 4.5  $\text{kcal hr}^{-1} \text{m}^{-1} \text{°C}^{-1}$ , 2.0 to 9.8  $\text{Btu hr}^{-1} \text{ft}^{-1} \text{°F}^{-1}$ ). Tests by Harada et al.<sup>40</sup> on unsealed silica concrete showed that the conductivity decreased with increased temperature. The magnitude of the decrease can be seen in Fig. 54. Curves F and G both show a decrease of about 8% from 20 to 200°C (68 to 392°F). Out to 750°C (1382°F) the decreases are over 50%. The thermal diffusivity measurements showed the same behavior.

Marechal's<sup>55</sup> measurements on unsealed quartzite concretes showed a decrease with higher temperature, but the conductivity,  $k$ , leveled off after 200°C (392°F). In fact, from 20 to 50°C (68 to 122°F) the  $k$  value increased about 7%. Then from 50 to 200°C (122 to 392°F) the  $k$  value decreased over 44% for the concrete with a high coarse/fine aggregate ratio, and about 30% for the concrete with a low coarse/fine ratio. Harada's tests resulted in only a 10% decrease up to 200°C (392°F), and the  $k$  value continued to decrease even above 700°C (1292°F). The respective reports do not provide many details of curing history, age, etc., to allow rigorous comparison for analysis. However, Browne<sup>10</sup> states that loss of water can change  $k$  considerably, as can development of microcracking. Also, the quartzitic concretes give the highest values of  $k$ , and the higher the saturated conductivity, the greater the decrease in  $k$  upon desorption. For the Wylfa concrete the maximum design value was chosen from conductivity measurements on oven-dried samples to represent the situation that may occur in the hot zones of the vessel after prolonged heating (i.e., adjacent to liner and penetrations).

The information on thermal conductivity at various temperatures in the sealed and unsealed conditions shows that the  $k$  value does decrease as temperature increases and as moisture is lost. The absolute value of the conductivity and the magnitude of change with temperature can vary substantially and are dependent on the aggregate and the relative constituent content of the mixture. For design of a PCRV, relative to thermal conductivity, the prudent procedure appears to prescribe measurements in the dry state at the maximum design temperature. This will provide for a minimum value applicable to that portion of the vessel receiving the initial heat flux.

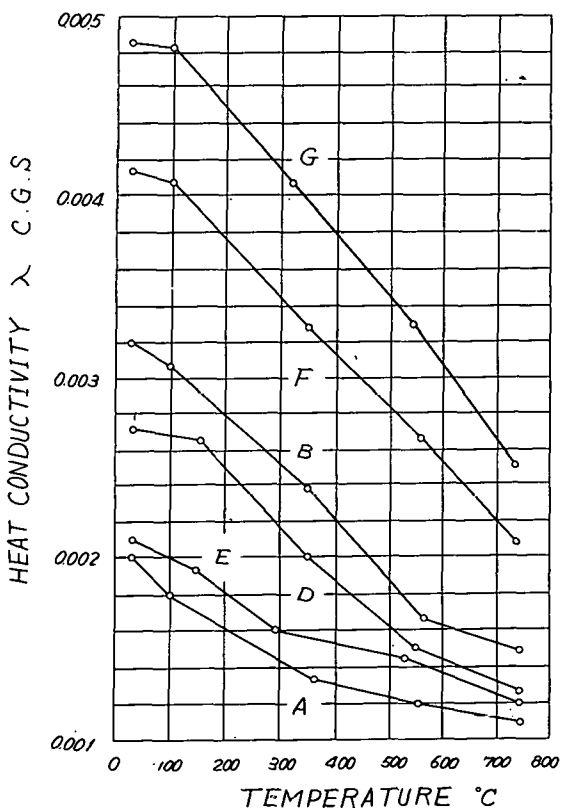


Fig. 54. Heat Conductivities of Mortars and Concretes at Elevated Temperatures. Concrete: F, w/c = 0.60; G, w/c = 0.70. Mortar: A, B, D, E. Source: T. Harada et al., "Strength, Elasticity, and the Thermal Properties of Concrete Subjected to Elevated Temperatures," ACI SP-34, *Concrete for Nuclear Reactors*, pp. 377-406 (1972).

### 3.3.6 Properties Under Multiaxial Stress States

A review of the behavior of concrete under combined states of stress could involve discussion of phenomenological and physical theories of failure, as well as the analytical methods used to predict behavior under various loading conditions. Such a review is beyond the scope of this report. Rather, we intend to review a few representative studies of concrete properties under multiaxial stress conditions only, to provide perspective for the previous section which dealt with concrete under uniaxial stress. Thus, it is desirable to review studies which have investigated the effects of high temperatures on strength, creep, etc., of mass concrete. Although there are many studies of concrete behavior under biaxial and compressive triaxial stress conditions, the more specific cases of multiaxial compression and tension, with infinitely varying ratios of stress, are not plentiful. When considering the additional effects of moisture and temperature, the available data are even more scarce.

Simply speaking, after all prestressing is applied, the bulk concrete of a PCRV will always be in a multiaxial state of stress. Most of the multiaxial strength studies on concrete have been performed on cylinders where radial pressure results in two of the principal stresses being equal, while the third stress is varied in the axial direction. In addition, very few tests have been conducted with a combination of compressive and tensile stresses. One of the major thrusts of current multiaxial research is directed at the method of load application. In most studies of compressive properties, steel platens are used in contact with the specimen, while it is loaded to failure. It is well recognized that the application of a uniform stress or strain depends on the stiffness of the platens and that end restraints, that is, friction or restraint at the platen-concrete interface, can significantly affect the results of the compression test. The end restraints can be responsible for substantial overestimations of the real strength of a specimen. On the other hand, it is also well established that the ultimate strength of concrete increases when multiaxial conditions are imposed. The questions requiring answers relate to the true strength of concrete under any stress state and the most realistic method of measuring it. Questions concerning moisture and temperature can possibly be answered, since the effects of those parameters are measured in a relative manner. It is the true strength value that is required for more precise and realistic structural design.

Richart, Brandtzaeg, and Brown<sup>58</sup> reported, in 1928, that the magnitude of the maximum principal stress was roughly equal to the uniaxial strength plus 4.1 times the lateral pressure. Their triaxial tests were on 10.16-cm-diam (4-in.), 20.32-cm-long (8-in.) cylinders that were tested one day after removal from a moist room and were somewhat wet when tested. Axial deformations up to 7% maximum load were recorded, much of which they attributed to an inelastic compaction (simply a reduction in volume under the high three-dimensional stresses).

Chinn and Zimmerman,<sup>59</sup> in 1965, reviewed the work on triaxial testing of concrete by many authors. Tests in which the lateral pressure was supplied by fluid pressure produced curvilinear relations between principal stresses,  $\sigma_1$  and  $\sigma_3$ . However, tests in which lateral pressure was produced with spiral wrapping or by a metallic jacket showed linear relationships between  $\sigma_1$  and  $\sigma_3$ . Generally speaking, the expression  $\sigma_1 = f_c' + 4\sigma_3$  fit the results fairly well, as mentioned for Richart, Brandtzaeg, and Brown ( $f_c'$  is uniaxial compressive strength). Chinn and Zimmerman performed tests on a large triaxial machine, using cylindrical specimens with type I cement, gravel aggregate, and various constituent ratios. All specimens were oven-dried at 100°C (212°F) and air-dried for one to ten days. Type I loading involved application of a hydrostatic stress condition and then increasing the axial stress to failure. Type IV loading consisted in maintaining the lateral stress at a constant fraction of the axial stress and increasing both to failure. Types I and IV results were almost identical, indicating no effect of the path of loading. The authors combined the results and fit equations to the data as follows:

$$0 < \sigma_3 < 35 \text{ ksi} ,$$

$$\sigma_1 = f_c' + 4.690\sigma_3^{0.8830} , \quad (4)$$

$$35 < \sigma_3 \leq 75 \text{ ksi} ,$$

$$\sigma_1 = f_c' + 10.570\sigma_3^{0.6329} , \quad (5)$$

where the maximum discrepancies were calculated for  $\sigma_1 - f_c'$  rather than for  $\sigma_1$  and were about 13% for both cases. Because of the great amount of bulging in the specimens, the stress distribution was changed considerably, and the validity of calculating axial stress as axial load divided by original area is doubtful. They calculated the normal stress at midheight on the basis of the bulged section, and the stress at which bulging began was sort of a yield stress, which was nearly constant over a wide range of axial strain. Thus the equations given above are conservative. Type II loading involved the application of a hydrostatic stress followed by increases in the lateral stress until failure. Results indicated some effect of the intermediate principal stress. Tests showed that a cylinder can withstand  $2.105 f_c'$  when stress is applied as an all-around lateral stress. Chinn and Zimmerman's results did not allow a single Mohr envelope to be applied to all stress states, nor did the octahedral shear stress theory fit the data. Their studies were restricted to dried specimens at room temperature only.

Goode and Helmy<sup>60</sup> tested hollow cylinders 91.4 cm (36 in.) long to reduce the effect of end restraint and measured the strength in compression and tension at room temperature. They found that the tensile strength of the hollow cylinder in pure torsion was 60 to 70% of the split-cylinder strength, and that the tensile strength was not linearly related to the crushing strength. Their results were generally represented by Mohr's theory, with the adoption of Leon's parabolic envelope for direct compressive and shear stresses. The octahedral stress theory was found to be no more accurate.

Gardner<sup>61</sup> concluded that the failure strength, ductility, and value of the instantaneous Poisson's ratio at failure all increase with increasing confining pressure. He presented an equation for predicting triaxial test results from unconfined cylinder tests, using the instantaneous Poisson's ratio. The expression is representative only at stresses below 80% of ultimate.

Hansson and Schimmelepfennig<sup>62</sup> reviewed multiaxial testing up to 1970 and stated that tests which guarantee that the assumed stress state exists in the failure region of the specimen are:

1. biaxial compression tests with slabs,
2. triaxial compression tests with solid cylinders,
3. biaxial and triaxial tests with cubes.

They say that the biaxial compression state is of most interest in PCRVs and that test techniques must minimize end restraints. They present a failure criterion for design use that is based on results of other investigators. The authors used the more conservative results obtained by researchers who minimized the end restraints during testing. They also state that limestone concrete shows higher multiaxial strength than does gravel concrete.

Launay and Gachon<sup>63</sup> measured triaxial strength of 6.98-cm (2 3/4-in.) cubes at 20, 40, and 60°C (68, 104, 140°F). Their machine is shown in Fig. 55. The loading platens rest on ball-and-socket joints, and an aluminum pad [four aluminum sheets 0.4 mm (0.016 in.) thick, with each face lubricated with talc] is inserted between platens and cube faces to minimize friction. Figure 56 shows the undimensional ultimate-strength surface, where  $\sigma_0$  represents the uniaxial ultimate strength. No mention was made of elevated-temperature tests.

Bremer<sup>64</sup> used cubes and tested multiaxial strength for both compressive and tensile stresses. He states that tensile forces are applied with a rigid steel plate cemented to the specimen and that the residual friction in compression was reduced to less than 1%. He does not give the method of load application, but indicates that Launay and Gachon<sup>63</sup> used his technology. Figure 57 shows Bremer's multiaxial strength relationships, with the results of Launay<sup>63</sup> for comparison. He concluded that concrete is subject to strain failures rather than stress failures and that the mean principal stress is important to strength. For design, Bremer recommended allowing tensile stresses and local cracks to occur but using slack reinforcement to take up a predetermined amount of tensile force to ensure structural elasticity.

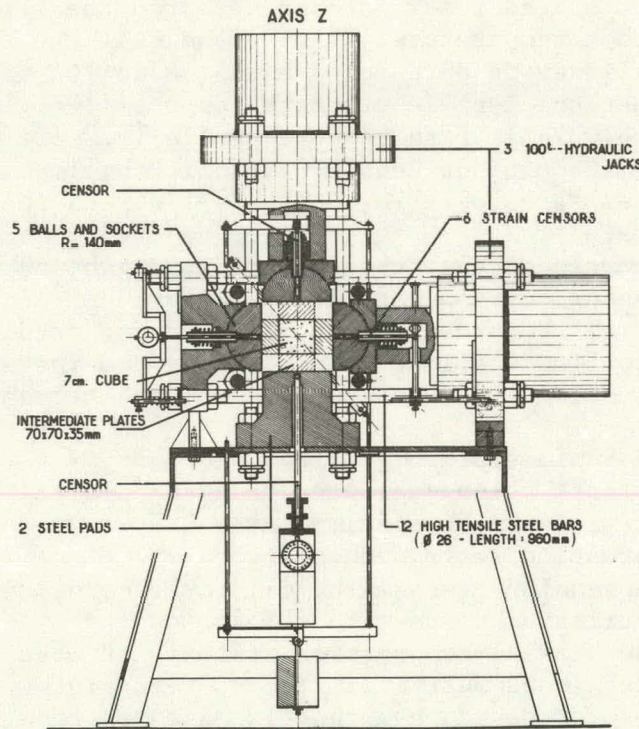


Fig. 55. Triaxial Testing Machine. Source: P. Launay and H. Gachon, "Strain and Ultimate Strength of Concrete Under Triaxial Stress," ACI SP-34, *Concrete for Nuclear Reactors*, pp. 269-82 (1972).

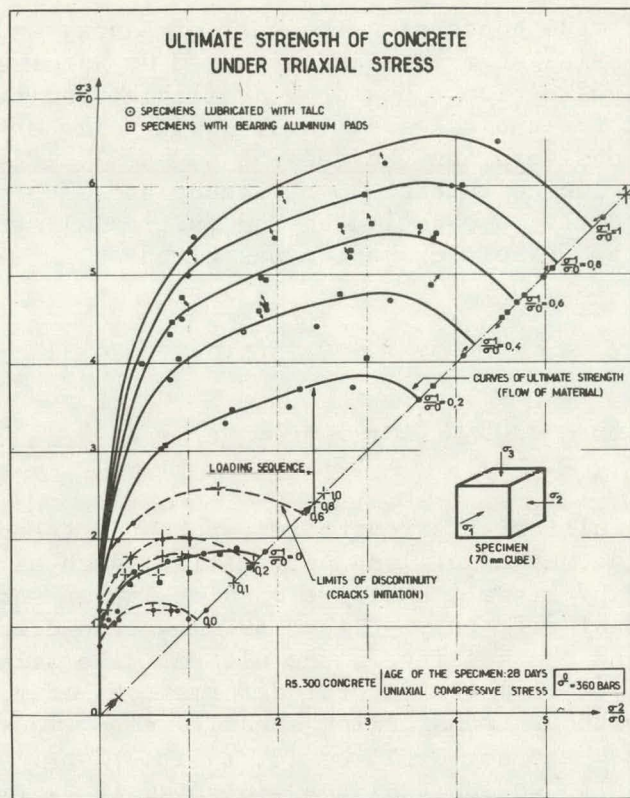


Fig. 56. Triaxial Strength Envelopes. Source: P. Launay and H. Gachon, "Strain and Ultimate Strength of Concrete Under Triaxial Stress," ACI SP-34, *Concrete for Nuclear Reactors*, pp. 269-82 (1972).

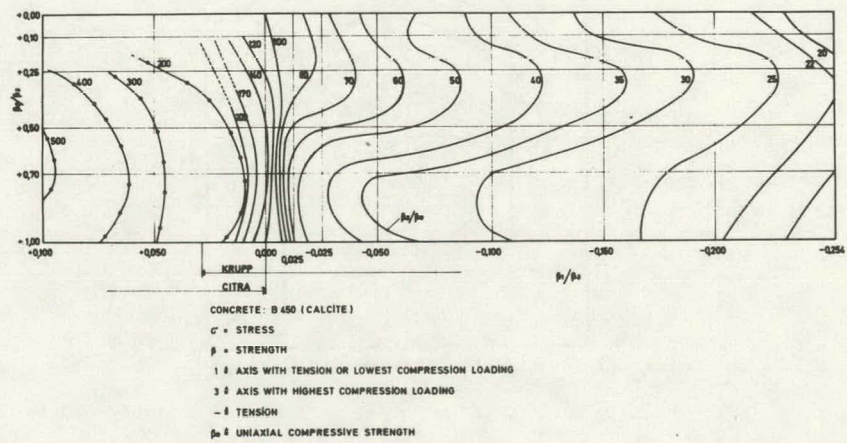


Fig. 57. Ultimate Strength of Concrete Under Multiaxial Loading. Source: F. Bremer, "On a Triaxial Strength Criterion for Concrete," ACI SP-34, *Concrete for Nuclear Reactors*, pp. 283-94 (1972).

In a comment made concerning the work of Launay and Gachon, Garas<sup>65</sup> stated that multiaxial strengths are affected by specimen size (for cubes) and load application. Based on available results, he constructed failure envelopes for cubical specimens, taking size effects and loading conditions into consideration (he doesn't say how). Figure 58 shows his curves, and comparison with Fig. 56 of Launay and Gachon<sup>63</sup> shows that their data, apparently, overestimated the multiaxial strength. The parabolic nature of the failure criterion was given as

$$\begin{aligned}
 & (\sigma_1^2 + \sigma_2^2 + \sigma_3^2) - 0.75(\sigma_1\sigma_2 + \sigma_2\sigma_3 + \sigma_3\sigma_1) \\
 & - 2.05 f_c (\sigma_1 + \sigma_2 + \sigma_3) + 2.45 f_c^2 = 0 . \quad (6)
 \end{aligned}$$

Much of the multiaxial strength research undertaken in recent years has centered on the method of load application, such as the brush-bearing platens described by Linse<sup>66</sup> and developed by Kupfer and Hilsdorf (see refs. 1, 2, and 3 of ref. 66). Figure 59 shows the dimensions of the steel filaments and the spacing on the platen. The filaments are so flexible that they follow the lateral deformations of the concrete surfaces almost without transferring shear forces. They are clamped rigidly at the base and are 9.525 cm (3 3/4 in.) long. Sufficient buckling resistance and small bending resistance are required. In a later report,<sup>67</sup> Linse describes the use of a massive prestressed concrete frame which houses the 10-cm (3.94-in.) cube specimen and separately controlled presses, which can exert compressive or tensile force in each of the

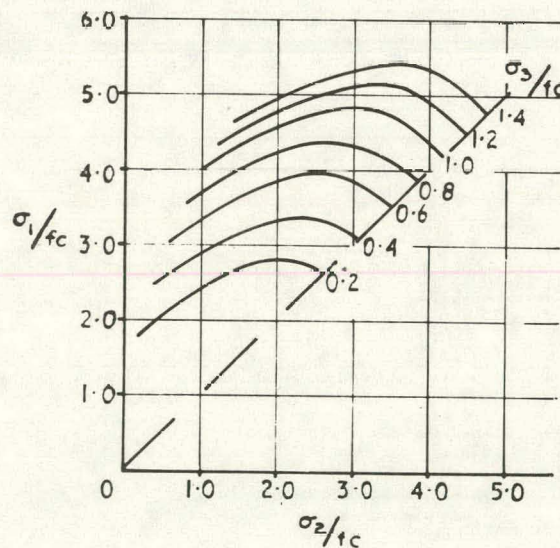


Fig. 58. Ultimate Strength of Concrete Under Triaxial Stress. Source: F. K. Garas, discussion attachment to: P. Launay and H. Gachon, "Strain and Ultimate Strength of Concrete Under Triaxial Stress," Proceedings of the First International Conference on Structural Mechanics in Reactor Technology, 1976, Vol. 74, part 4, pp. 35-38 (1972).

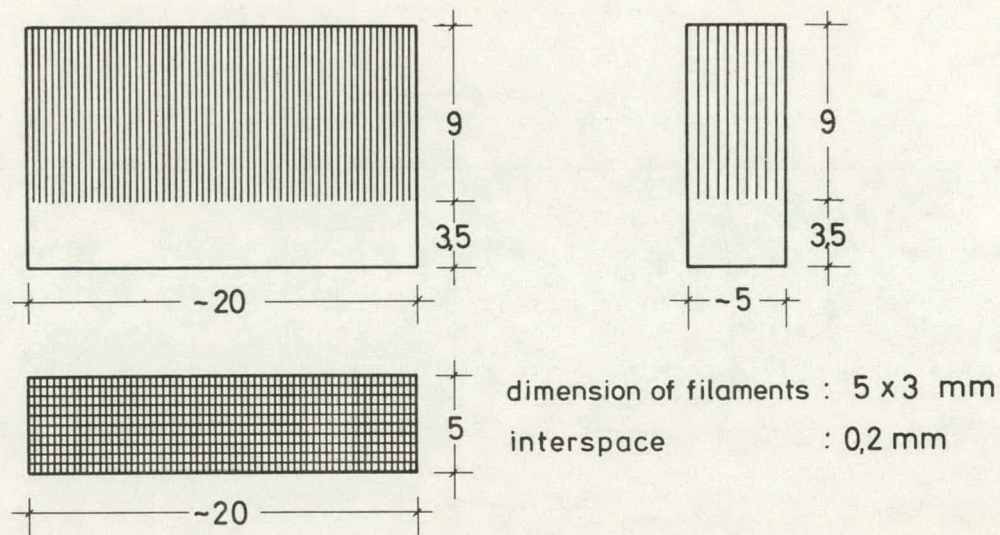


Fig. 59. Description of Brush-Bearing Platens. Source: D. Linse, "Strength of Concrete Under Biaxial Sustained Load," ACI SP-34, *Concrete for Nuclear Reactors*, pp. 327-34 (1972).

three directions for triaxial testing. The results of biaxial strength measurements are shown in Fig. 60. For short-time tests, the highest increase in strength (25%) was at a stress ratio of about 2:1. At a ratio of 1:1 the increase was 15%. For sustained loading, the ratio of 2:1 resulted in only a few percent increase in strength, while the 1:1 ratio gave a decrease in strength to about 95% of uniaxial. Triaxial testing with the brush platens showed that the increased strength was dependent on the stress ratio and is greater for more nearly equal stresses. Even at  $\sigma_1/\sigma_3 = 0.30$ , a load up to six times the uniaxial strength did not break the specimen.

In a review of multiaxial test apparatus, Schickert<sup>68</sup> emphasizes the need for a device to test cubic specimens with three independent loading directions. He discounts the steel platens, as discussed previously, as well as the use of lubricants, because of nonuniform stress distribution due to extrusion of lubricant at the specimen edges. He stated that multilayer insertions of laminated materials have limitations but have given reasonable results. They have to be proven at elevated temperatures, however. The brush platens do not guarantee uniform loading on bigger specimens, due to displacement differences between inner and outer teeth. His design would incorporate a deformable bearing platen in which the platen is divided into 64 pistons (loading stamps or rods) guided through a deformable platen and supported by a hydraulic cell. Thus the bearing platen can follow the deformation of the test specimen. Comparisons will be made with rigid platens having laminated aluminum and lubricants. Specimens will be 20-cm (7.87-in.) cubes. He has also experimented with various combinations of rod size and number in the platens.

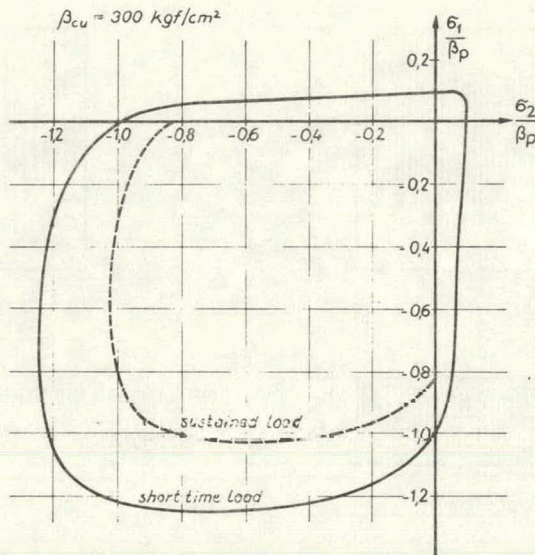


Fig. 60. Ultimate Strength of Biaxially Loaded Specimens. Source: D. Linse, "Strength of Concrete Under Biaxial Sustained Load," ACI SP-34, *Concrete for Nuclear Reactors*, pp. 327-34 (1972).

Atkinson and Ko<sup>69</sup> have developed a multiaxial test cell that employs fluid-pressurized cushions in loading cubical specimens. The frame was machined from a solid steel billet, using electrical discharge machining for final dimensions. A specially designed seal of leather and vinyl is sufficiently flexible to transmit full fluid pressure uniformly to the cube faces and is strong enough to close the gap between specimen and frame. Figures 61 and 62 from Andenes<sup>70</sup> show details of a recently designed frame and fluid cushion. Hydraulic oil fills the seal and transmits the load, while deformation measurements are made with proximitron probes. The probes use the inductive principle to determine the distance between a conductive target of aluminum foil on the specimen and a coil embedded in the tip of the measuring probe. In this way, physical connection to the specimen is not required by the transducer.<sup>69</sup> The frame is designed for about 137.9 MPa (20,000 psi) for the uniaxial loading and 68.95 MPa (10,000 psi) for the hydrostatic condition, although a stronger frame has more recently been constructed.<sup>71</sup> Photoelastic studies were conducted to measure the development of shear stresses during loading and to verify the uniformity of loading and minimization of end restraints. The leather pad seal produced a shear stress of about 3 to 4% of the load compared with 1 to 2% for plastic seals. With steel platens, stress concentration factors of 2 or greater were recorded, even with a teflon-grease-teflon friction reducing layer.

Andenes<sup>70</sup> tested mortar specimens in biaxial loading, using the fluid cushion device. The uniaxial tests showed an ultimate strength of 40.48 MPa (5875 psi) with the fluid cushion and 51.67 MPa (7500 psi) with steel platens, a difference of about 27%. The biaxial failure envelopes are shown in Fig. 63. The ratios are normalized to the strength of the mortar, using the fluid cushion platen. The steel platen shows

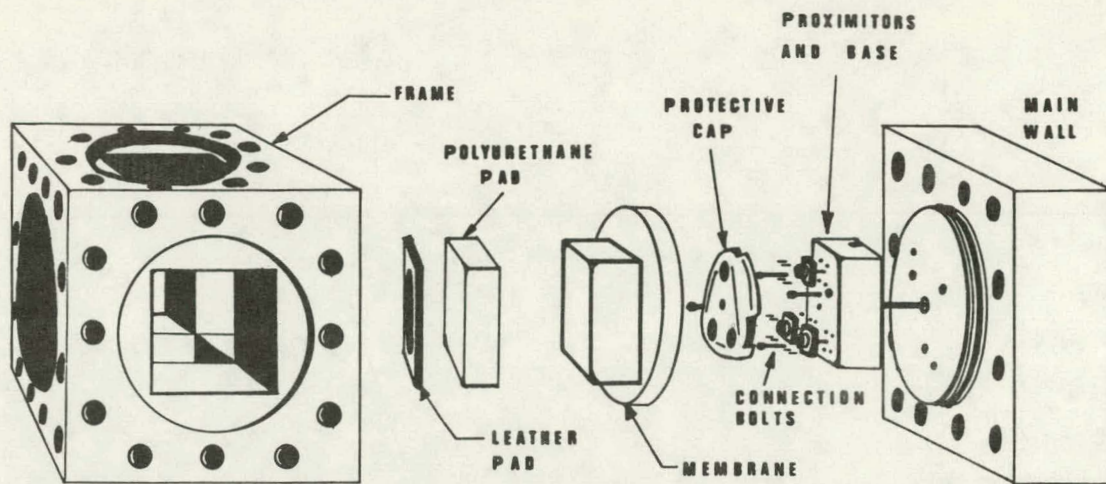


Fig. 61. Exploded View of the Fluid Cushion Test Cell. Source: E. Andenes, "Response of Mortar to Biaxial Compression," M.S. thesis, University of Colorado, 1974.

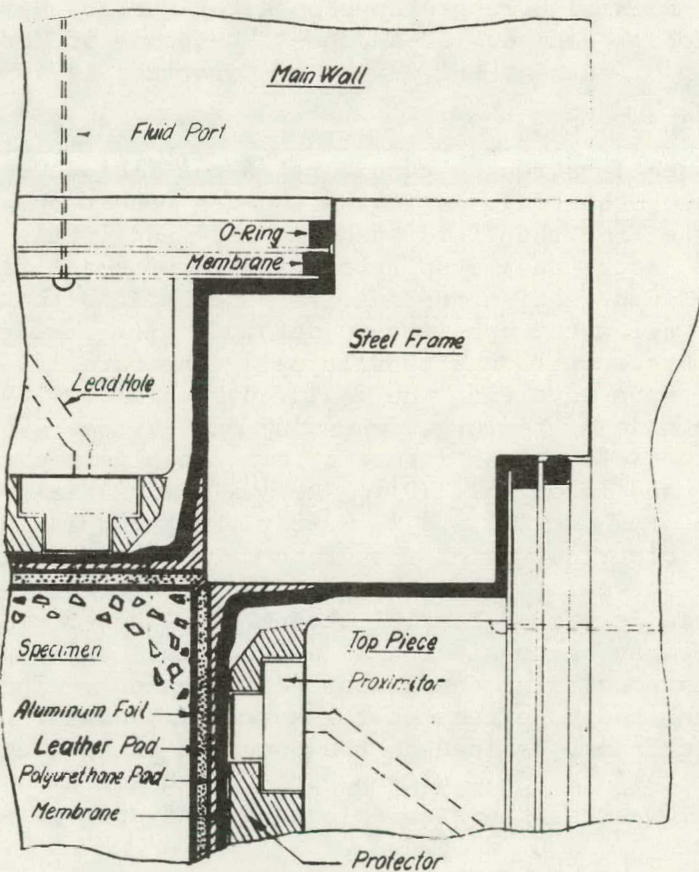


Fig. 62. Details of Assembled Fluid Cushion Test Cell With Oil Cushions. Source: E. Andenes, "Response of Mortar to Biaxial Compression," M.S. thesis, University of Colorado, 1974.

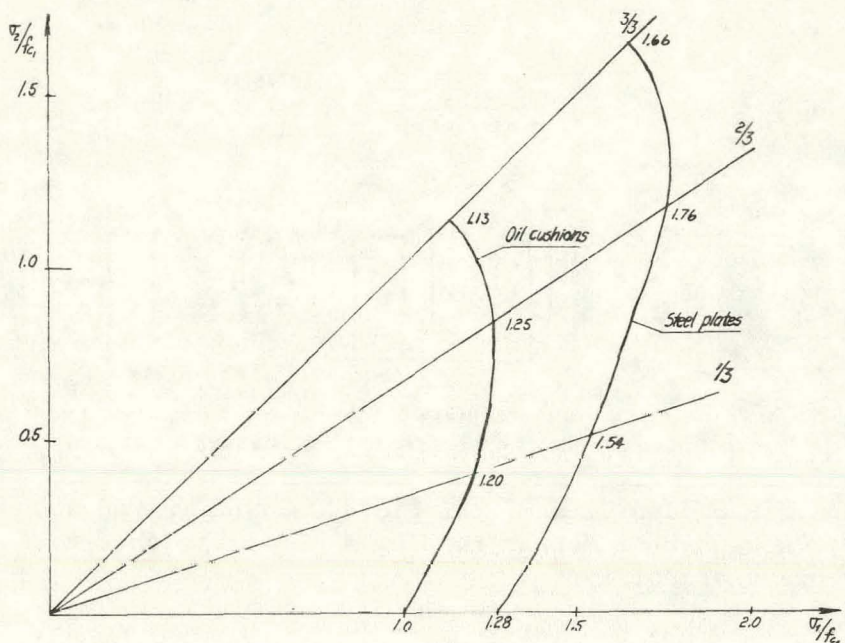


Fig. 63. Biaxial Strength Envelopes for Mortar, Using Fluid Cushion and Steel Platens. Source: E. Andenes, "Response of Mortar to Biaxial Compression," M.S. thesis, University of Colorado, 1974.

greater increases in strength than that of the fluid cushion because of end restraints. Other figures in the Andenes report show a considerable amount of scatter for the fluid cushion tests and little scatter for the steel platens. Both tensile splitting and corner-edge failure were observed with fluid cushion testing. Andenes states that brush-bearing platens do not allow the specimen to deform at the surface and, therefore, will always result in a tensile splitting parallel to the unloaded faces. He says that the fluid cushion allows the specimen to choose its own mode of failure, depending on local stress concentrations, etc. Comparisons of various investigators' results are shown in Fig. 64 (refs. 11, 14, and 15 of ref. 70). The maximum biaxial stress occurs at a stress ratio of about 2/3 and is 1.25 times the uniaxial fluid cushion strength. The other curves on the graph were obtained with brush-bearing platens. Also shown is the Von Mises failure envelope, which provides a conservative prediction of biaxial strength. Andenes concludes that concrete-mortar may be considered as a nonlinear continuum to failure when tested under nonconstraint conditions (oil cushion). The constraint due to steel platens had no effect on the material behavior until after it became a discontinuum, defined as the onset of extensive internal micro-cracking. The failures of fluid-cushion-tested specimens were brittle but indistinct, whereas the steel-platen-tested specimens failed in a ductile manner.

The fluid cushion device appears to offer potential for multiaxial testing but requires additional study relative to failure modes, measuring techniques, and scatter of results.

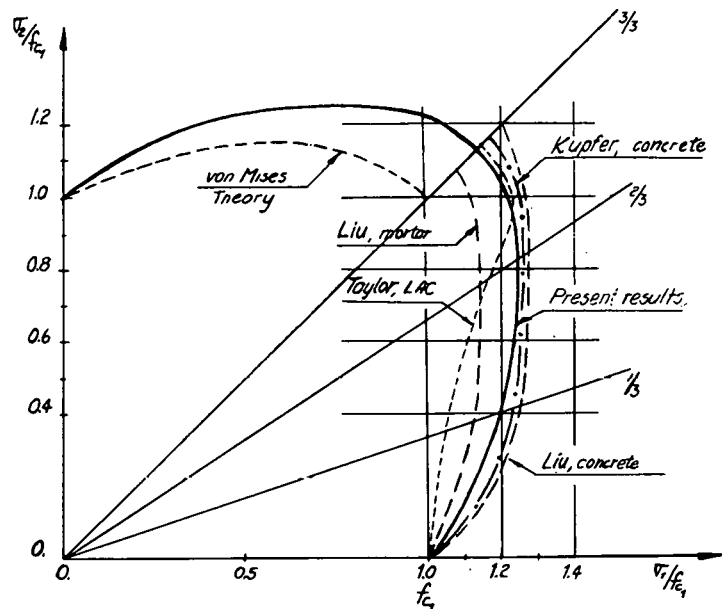


Fig. 64. Biaxial Failure Envelopes Obtained with Either Oil Cushions or Steel Brush-Bearing Platens. Source: E. Andenes, "Response of Mortar to Biaxial Compression," M.S. Thesis, University of Colorado, 1974.

Taylor and Patel<sup>72</sup> tested biaxial and uniaxial specimens, using four platen designs. The various platens and the uniaxial compressive strength that they produced on 4.76-cm (1 7/8-in.) dry cubes were:

1. solid steel plates, 23.49 MPa (3.41 ksi);
2. steel brushes made by inserting short lengths of 0.159-cm (1/16-in.) wire into holes in brass plates, 21.36 MPa (3.10 ksi);
3. steel plates with 0.079-cm (1/32-in.) ball bearings, 16.19 MPa (2.35 ksi);
4. steel plates with 0.159-cm (1/16-in.) ball bearings, 15.85 MPa (2.30 ksi).

The specimens loaded with solid steel plate failed on planes inclined 45° to the loading axis, or by general disintegration. Brush- and ball-loaded specimens generally split in planes parallel to the loading axis, indicating true uniaxial conditions. The ball bearings did produce indentations in the specimen surfaces about one-third the ball diameter. Because they did produce the lowest strength measurements, and due to alignment problems with the brushes (specimens also tended to slide out sideways under load, indicating possible shearing stresses), the ball-bearing platens were used for biaxial testing. For a gravel concrete [0.635 cm (0.25 in.) maximum aggregate] with a water/cement ratio of 0.67, the biaxial envelopes are shown in Fig. 65 along with those of other investigators. The saturated concrete resulted in greater relative increase in strength under proportional biaxial conditions. This was true for mixtures of other water/cement ratios also, although the wet specimens were weaker than the dry specimens. The envelopes were larger than expected for the ball-bearing loading, possibly because of friction induced by increased penetration into the concrete as a result of higher

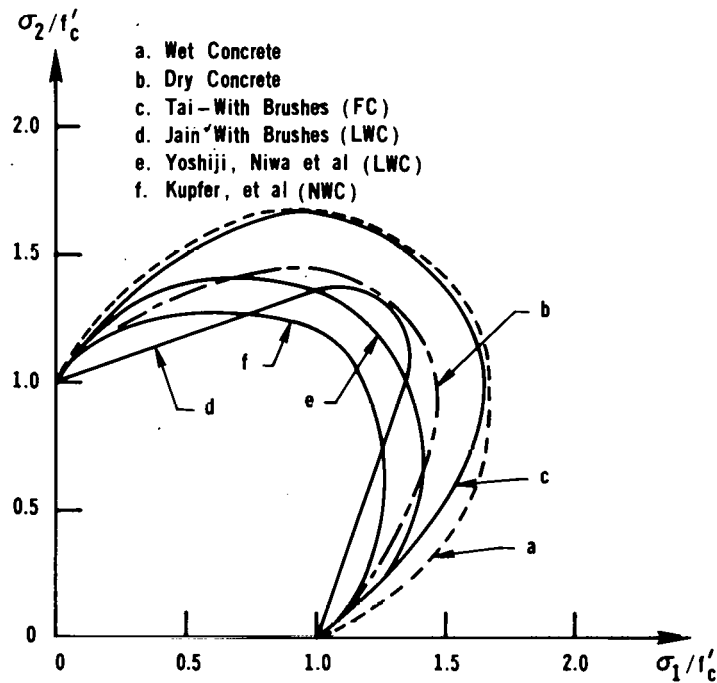


Fig. 65. Comparison of Biaxial Failure Envelopes of Various Investigations. Source: M. A. Taylor and B. K. Patel, "The Influence of Path Dependency and Moisture Conditions on the Biaxial Compression Envelope for Normal Weight Concrete," *J. Am. Concr. Inst.* 71(12): 627 (December 1974).

stress levels than in uniaxial loading. Since the mixture with the highest water/cement ratio showed the greatest difference between wet and dry specimens, the authors stated that the hydrostatic load-carrying capability of contained free water could be the reason for greater strength increases for wet concrete. However, they minimize that mechanism for various reasons, such as the improbability of completely isolated spaces existing in concrete, and say that biaxial stress relaxation tests might help to explain the observations. They also recommend further study concerning the ball-bearing platen concept. Further in-depth comparisons between results obtained with brush-bearing platens, deformable platens, fluid cushion, ball bearing, and rigid steel platens should provide answers to this complex experimental problem.

Kupfer<sup>73</sup> reported that the behavior of concrete under biaxial loading could be described accurately by simple mathematical expressions. Those for stress are approximated as follows:

compression-compression region,

$$\left( \frac{\sigma_1}{\beta_p} + \frac{\sigma_2}{\beta_p} \right)^2 + \frac{\sigma_1}{\beta_p} + 3.65 \frac{\sigma_2}{\beta_p} = 0 ; \quad (7)$$

compression-tension region,

$$\frac{\sigma_2}{\beta_z} = 1 + 0.8 \frac{\sigma_1}{\beta_p} ; \quad (8)$$

tension-tension region,

$$\sigma_2 = \beta_z = 0.64 \sqrt[3]{\beta_p^2} = \text{constant} ; \quad (9)$$

where

$$\begin{aligned} \sigma_1, \sigma_2 &= \text{principal stresses,} \\ \beta_p &= \text{uniaxial compressive strength,} \\ \beta_z &= \text{uniaxial tensile strength.} \end{aligned}$$

The behavioral equations were obtained by breaking down the stress and strain states into hydrostatic and deviator components. Using these equations in conjunction with finite-element methods and construction of a so-called rigidity matrix (interrelates force and deformation) provides the means for performing nonlinear analyses of conventional structures.

With further reference to effects of moisture, Akroyd<sup>74</sup> found that saturated concrete failed at a much lower load than did dry concrete, and the shear strength reached a maximum of about five times the uncombined compressive strength. He observed that sufficiently high lateral pressure in test cylinders caused the saturated specimens to behave more like saturated plastic material, such as clay. However, the failures were sudden and rapid and clearly like those of a brittle material. Generally, conical-shaped fractures were produced using rigid steel platens.

Isenberg<sup>75</sup> tested hollow cylinders in the saturated, air-dried, and oven-dried conditions by subjecting them to combined torsion and compression. For a ratio of compressive to tensile stress of 1 or greater, the saturated specimens were weaker than dried specimens. At a ratio of 3, the oven-dried specimens were twice as strong as the saturated ones. Thus, his observations agree with those of Taylor and Patel.<sup>72</sup>

With regard to temperature, Hannant<sup>15</sup> tested solid and hollow cylinders in the sealed and unsealed conditions after exposure to temperatures up to 150°C (302°F). He imposed a triaxial stress distribution by applying a hydrostatic pressure of 3.31 MPa (480 psi) during axial loading (the unheated compressive strength was not given). The moisture loss varied directly with the strength after heat exposure. The sealed specimen compressive strengths were reduced to about 70 and 60% of the reference strength at 100 and 150°C (212 and 302°F) respectively.

Browne<sup>10</sup> references work by Newman (ref. 14 of ref. 10) on biaxial loading in which he claimed that, before the ultimate strength of concrete is reached under short-term loading, a critical stress level exists at which severe permanent damage takes place within the specimen. This stress may be as low as 50% of the ultimate and varies with many factors. Under sustained loading, a critical stress also exists above which eventual

failure can occur, about 70% of the short-term ultimate strength. Figure 66 shows the biaxial envelopes of Newman. Browne points out that vessel design should consider the critical stress under short- and long-term loading rather than the uniaxial ultimate strength.

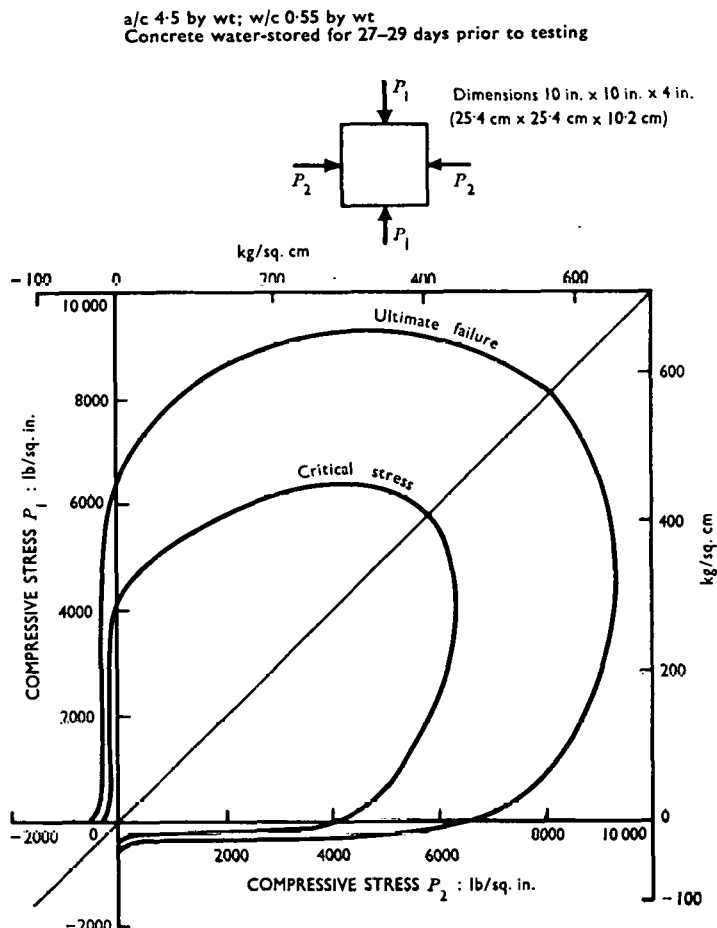


Fig. 66. Strength of Concrete Under Biaxial Stress. Source: R. D. Browne, "Properties of Concrete in Reactor Vessels," Group C, Paper 13, Conference on Prestressed Concrete Pressure Vessels, Westminster, S.W.1., March 1967.

### 3.3.7 Mechanisms Causing Observed Temperature Effects

It is the intent of this section to provide a brief summary of the approach of various authors to the mechanisms which caused variation in concrete behavior with increasing temperature. Because the concretes tested varied widely in many ways and because experimental methods and treatment procedures also varied, hypotheses have been formulated to explain the observed behavior.

A universal observation, of course, is that the results can be related to the amount of free moisture in the concrete during exposure and testing. Campbell-Allen and Desai<sup>20</sup> noted the often-stated hypothesis that the incompatibility of the linear expansion coefficients of various concrete constituents is the primary cause of property deterioration at high temperatures. They performed tests to determine the coefficients of the mortar mixes, aggregates, and concretes used in their study. The results are given in Table 7 and are interesting because they show, for instance, that the coefficient of thermal expansion for limestone becomes compatible with the mortar mix above 150°C (302°F), while it was less than one-half the mortar mix value at 20°C (68°F). However, the limestone concrete showed the most deterioration in properties at temperatures of 150°C (302°F) and above. The fireclay brick aggregate showed the least compatibility of expansion coefficients with mortar above 150°C (302°F), yet it showed the least deterioration in mechanical properties. The authors showed photos of broken concrete depicting the dislodged limestone aggregate and firmly held fireclay brick aggregate. They attributed the excellent bond to the influence of surface texture and shape of aggregate, plus a possible chemical reaction between cement and fireclay brick. Expanded shale-clay aggregate was as stable as fireclay brick but had a smooth texture and rounded shape which caused dislodging of the rocks at high temperature. Tests on the limestone aggregate revealed that limestone may not be entirely stable at 300°C (572°F). The excellent bond at room temperature, caused by a surface chemical reaction, was virtually destroyed by chemical changes in minor constituents and, particularly, iron oxides of the limestone. Their concrete specimens were unsealed, and, thus, free moisture was not a consideration.

Table 7. Coefficients of Thermal Expansions from 20 to 300°C

Material	Mean coefficient of thermal expansion (microstrain/°C)	
	Below 150°C	Above 150°C
Cement mortar mix 1 + limestone aggregate	6.7 ± 0.6	10.8 ± 0.7
Cement mortar mix 1	10.5 ± 0.6	12.1 ± 0.4
Cement mortar mix 2 + fireclay brick	7.9 ± 0.6	13.6 ± 0.5
Cement mortar mix 2	10.7 ± 1.0	12.0 ± 0.6
Cement mortar mix 3 + expanded shale	6.6 ± 0.6	10.0 ± 0.5
Cement mortar mix 3	10.7 ± 1.0	12.1 ± 0.3
Limestone rock core perpendicular to bedding plane	4.5 ± 1.0	10.0 ± 0.6
Fireclay brick	4.0 ± 1.0	5.7 ± 0.6

Source: D. Campbell-Allen and P. M. Desai, "The Influence of Aggregate on the Behavior of Concrete at Elevated Temperatures," *Nucl. Eng. Des.* 6(1): 20 (August 1967).

Lankard et al.<sup>30</sup> attribute the effects of heat exposure on unsealed specimens to the absence of free moisture. The desorption of cement paste results in a collapse of the gel structure and closure of gaps between primary gel particles. Reference is made to work by Mills (ref. 16 of ref. 30) and by Philleo (ref. 18 of ref. 30), who showed that molding pastes under pressure force gel particles closer together, resulting in creation of additional bonds and increased strength. Sealed concrete contains superheated water and/or water vapor when heated. That hot-tested specimens were only slightly weaker than the cold-tested specimens led them to conclude that the effect of high-pressure steam in the flaws was minor. They conclude that reaction in the matrix between hydrated calcium silicates and  $\text{Ca(OH)}_2$  produces lime-rich crystalline hydrates, resulting in a decrease in the coherency of the matrix. A beneficial effect can also occur, they say, from reaction of the silica with  $\text{Ca(OH)}_2$  or with the products of the first reaction. Their observation of greater property deterioration for low-silica-content limestone relative to the highly siliceous gravel supports that conclusion. Because the mineralogical phase changes are increasing functions of temperature and time, deterioration in properties should decrease with both parameters, which was their observation. Thus, Lankard et al. recommend that siliceous aggregates be used whenever free moisture is retained in the concrete during heating.

Bertero and Polivka<sup>31</sup> also concluded that retention of moisture and duration of exposure to high temperature resulted in severe deterioration of properties, but they offered no mechanistic explanation for their observations.

Nasser and Lohtia<sup>33</sup> did not study the physical, chemical, and mineralogical changes in concrete during their testing program. They did, however, utilize information from other researchers to analyze their results. They reference the observations of Lankard et al.<sup>30</sup> regarding the hydrothermal reactions that transform the tobermorite gel. They say, however, that their results, and those of others on cement pastes (refs. 5 and 7 of ref. 33), show that those changes start around  $120^\circ\text{C}$  ( $248^\circ\text{F}$ ), though at a relatively sluggish rate. They emphasize that the relative amount of the new weak compounds and the extent of crystallization should increase with temperature and age of curing, resulting in aggravation of property deterioration as shown in their studies.

With regard to increasing creep deformation with increasing temperature, Nasser and Neville<sup>34</sup> discussed the work of Ali and Kesler (ref. 2 of ref. 34), in which they considered true creep to be a process of molecular diffusion and shear flow of the gel, and of adsorbed water under load. High temperature increases mobility of those processes. At a certain temperature the adsorbed water begins to evaporate, so that the rate of creep decreases. They postulate a temperature of about  $80^\circ\text{C}$  ( $176^\circ\text{F}$ ) for that process and state that higher temperatures would cause the gel to change to a microcrystalline form and further resist creep deformation. Using creep recovery observations along with the creep results, they hypothesize that the creep mechanism at high temperature is essentially the same as at room temperature. The character of the creep equation is primarily viscous and not elastic.

Gross,<sup>52</sup> however, concluded that the superposition principle in creep analyses, analyzed by normalizing his creep data to a 0.2 stress/cold-strength ratio, does apply and justifies the treatment of thermal creep strains as linear thermoviscoelastic strains up to about 300°C (572°F). The author discusses in detail the development of an equation for determining the stress, temperature, and time-dependent strains occurring in virgin concrete. The expression is used in conjunction with thermal relaxation weighting factors and experimentally determined temperature-dependent parameters. Because of the many variables affecting creep compliance, relevance of the results is claimed only for the particular mixture used. A full discussion of Gross's methodology for creep analysis is not within the scope of this report, but it deserves detailed attention, albeit developed with unsealed specimen data, for more general application to thermal creep analyses.

Geymayer,<sup>42</sup> in his review, stated that most test results seem to lend support to the seepage theory and cast further doubt on other concepts such as the capillary condensation theory, plastic theories, and differential shrinkage.

Seki and Kawasumi<sup>54</sup> postulated that the decrease of the viscosity of leaching water due to temperature, and the formation of crystals due to hydration, lead to the creep increase at elevated temperature [up to 70°C (158°F)].

### 3.4 Effects of Radiation

As mentioned previously, the PCRV serves not only as the primary pressure-retaining structure but, in the case of a nuclear reactor, is subjected to nuclear radiation emanating from the core and must serve as a biological shield. The primary concern is the attenuation of gamma rays and neutrons. Neutrinos are of no concern because they do not cause damage to tissue and materials. Charged particles are highly interacting, and relatively small amounts of material can provide a sufficient shield (they may be important, however, with regard to thermal effects). Concrete has been traditionally used as a shielding material because of its ability to attenuate gamma rays and neutrons with reasonable thickness requirements, has sufficient mechanical strength, can be constructed at reasonable cost, and requires little maintenance. An important factor is that concrete is hydrogenous. The slowing down of fast neutrons to thermal neutrons is best accomplished with hydrogen. Oxygen is also light enough to possess high efficiency in the slowing-down process. Thus the water present in concrete provides an excellent thermalizing medium that most other materials do not have. Once the neutrons are thermalized, they can be absorbed or captured by many of the constituents in the concrete. Thus it is apparent that the success of concrete as a shielding material depends heavily on its water content, and migration of moisture in concrete can be important from a shielding standpoint. Many shielding concretes are so-called heavy concretes, because they are made with heavy elements as aggregates, such as iron ore or barite.

Operation of a reactor for 30 to 40 years will result in exposure of the concrete to fast and thermal neutron fluxes for the entire time. The concern, then, is the effect that this exposure will have on the concrete properties. Nuclear heating caused by interaction of gamma rays and neutrons must be investigated, as well as any radiation damage that occurs and the level of exposure at which significant damage occurs. Exposure is usually expressed in terms of fluence, which is the integrated neutron dose (the neutron flux, neutrons  $\text{cm}^{-2} \text{ sec}^{-1}$ , multiplied by time of exposure results in neutrons/ $\text{cm}^2$ , called  $nvt$ ). The gamma-ray exposure is expressed in rads. This report is concerned primarily with ordinary portland cement concretes as used for current PCRV designs. Discussion of the physics of gamma-ray and neutron attenuation involves consideration of factors such as secondary radiation, produced by neutron absorption, and energy of the incident radiation; these items will not be discussed except as they might relate to damage to the material (direct radiation damage or indirect damage due to such things as thermal effects). The collision of a neutron with the nucleus of an atom can, depending on incident energy, etc., destroy the crystal lattice equilibrium, and long-term exposure can lead to changes in the material's physical and chemical properties. It is well known that properties of various materials are affected to varying degrees and at different levels of exposure.

Information on properties of irradiated concrete is scanty. Most of the available data have been measured on specimens removed from concrete shields and other structures. As a result, the concrete was subjected to elevated temperatures as well as radiation. Any changes in properties due to radiation alone are difficult to ascertain, because there is generally no material available for testing which has been subjected to the radiation without accompanying the elevated temperature. As mentioned earlier, the temperature can be elevated in the concrete from nuclear heating alone.

Clark,<sup>76</sup> in 1958, reported that there were no data that uniquely measured radiation damage for exposure to integrated neutron fluxes up to  $2 \times 10^{19} nvt$  and where temperatures did not exceed 120°C (248°F). He concluded that induced heating appeared to be more of a problem than direct radiation damage up to that exposure level. However, he referenced work at Harwell by Price et al. (ref. 31 of ref. 76). Their data showed that a thermal neutron fluence up to  $7 \times 10^{19}$  resulted in a decrease of about 30% in the rupture stress of a portland cement concrete. They concluded, however, that radiation damage for reactors built to that data was not as severe as overstressing due to nuclear heating.

The ORNL Graphite Reactor shield was studied and the findings were reported in 1958.<sup>77</sup> A cross-sectional view of the shield is shown in Fig. 67. The shield consists of a 1.52-m-thick (5-ft) section of barytes-hydrite concrete sandwiched between two 0.305-m (1-ft) sections of ordinary portland cement concrete. Cylinders 11.75 cm (4 5/8 in.) in diameter were cored out of the shield, using an air-cooled, diamond-edged drill. During full-power operation at 3.5 MW, the temperature gradient through the shield varied from 40°C (104°F) at the inner face to 19°C (66°F) at the outer face. Measurements were made of the dose rates for gamma rays and fast neutrons, as well as the thermal neutron flux, as a function of shield thickness. Also, activity measurements were made from concrete dust removed during each coring.

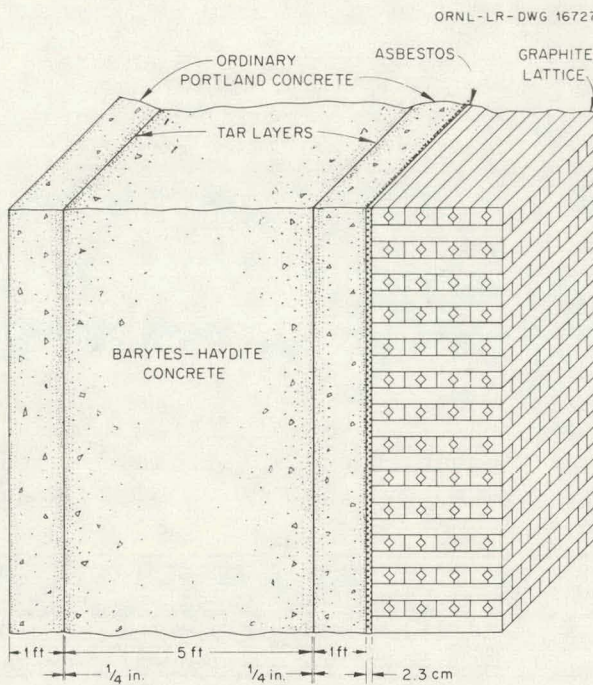


Fig. 67. Cross Section of ORNL Graphite Reactor Shield. Source: T. V. Blosser et al., *A Study of the Nuclear and Physical Properties of the ORNL Graphite Reactor Shield*, ORNL-2195 (August 1958).

Results of water content, density, and compressive strength are given in Table 8. The data are not compared with original data before exposure, but, rather, they are compared with data obtained in a similar study in 1948 (ref. 1 of ref. 77). The study in 1948, however, was of limited usefulness, since water was used to cool and clean the drill bit, although the effect of the water could not be determined.<sup>77</sup> The report observed that the chemical properties and density of the concrete had not been substantially changed since the 1948 study. However, the compressive strength was generally lower. Table 8 shows that the compressive strength was reduced 50% at the 0.15- and 0.30-m (1/2- and 1-ft) marks and about 30% as far into the shield as 0.762 m (2 1/2 ft). The unusually high strength for drilling 5 could not be explained by the authors. Figure 68 shows the fast-neutron and gamma-ray dose rates as well as the thermal neutron flux through the shield thickness. The reactor had been in operation for 12 years at the time of the study, but the fluences were not provided. It cannot be assumed that the reactor operated at full power continuously during the 12 years, and thus the total fluence is not known. The compressive strength, however, did decrease at locations closer to the reactor core. However, Table 8 shows that the strength decreased 20% at a depth of 0.914 m (3 ft) into the shield. Figure 68 shows a thermal flux of about  $2 \times 10^4$  neutrons  $\text{cm}^{-2} \text{ sec}^{-1}$  at that location.

Table 8. Water Content, Density, and Compressive Strength of Samples of Concrete from the ORNL Graphite Reactor Shield

Drilling No. <sup>a</sup>	Shield Thickness (ft)	Water Content (wt%), This Study	Density (g/cc)		Compressive Strength (psi)	
			This Study	1948 <sup>b</sup>	This Study	1948 <sup>b</sup>
1	6 - 7	6.73	2.22	2.20	1605	1650
2	5 - 6	9.96	2.26	2.27	2410	2460
3	4 - 5	11.9	2.35	2.28	2550	2775
4	3 - 4	12.0	2.34	2.26	2320	2891
5	2.5 - 3	10.2	2.36	2.17	3970	2980
6	2 - 2.5	13.2	2.34	2.17	2140	2953
7	1.5 - 2	15.0	2.35	2.16	2050	2765
8	1 - 1.5	13.5	2.15	1.96	1585	2170
9	0.6 - 1	9.24	2.36	2.21	1610	2676
10	0 - 0.6	6.93	2.54	2.11	1470	2150

a. Drillings 1, 9, and 10 were in Portland concrete; other drillings were in barytes-haydite concrete.

b. Average values from Ref. 1.

Source: T. V. Blosser et al., *A Study of the Nuclear and Physical Properties of the ORNL Graphite Reactor Shield*, ORNL-2195 (August 1958).

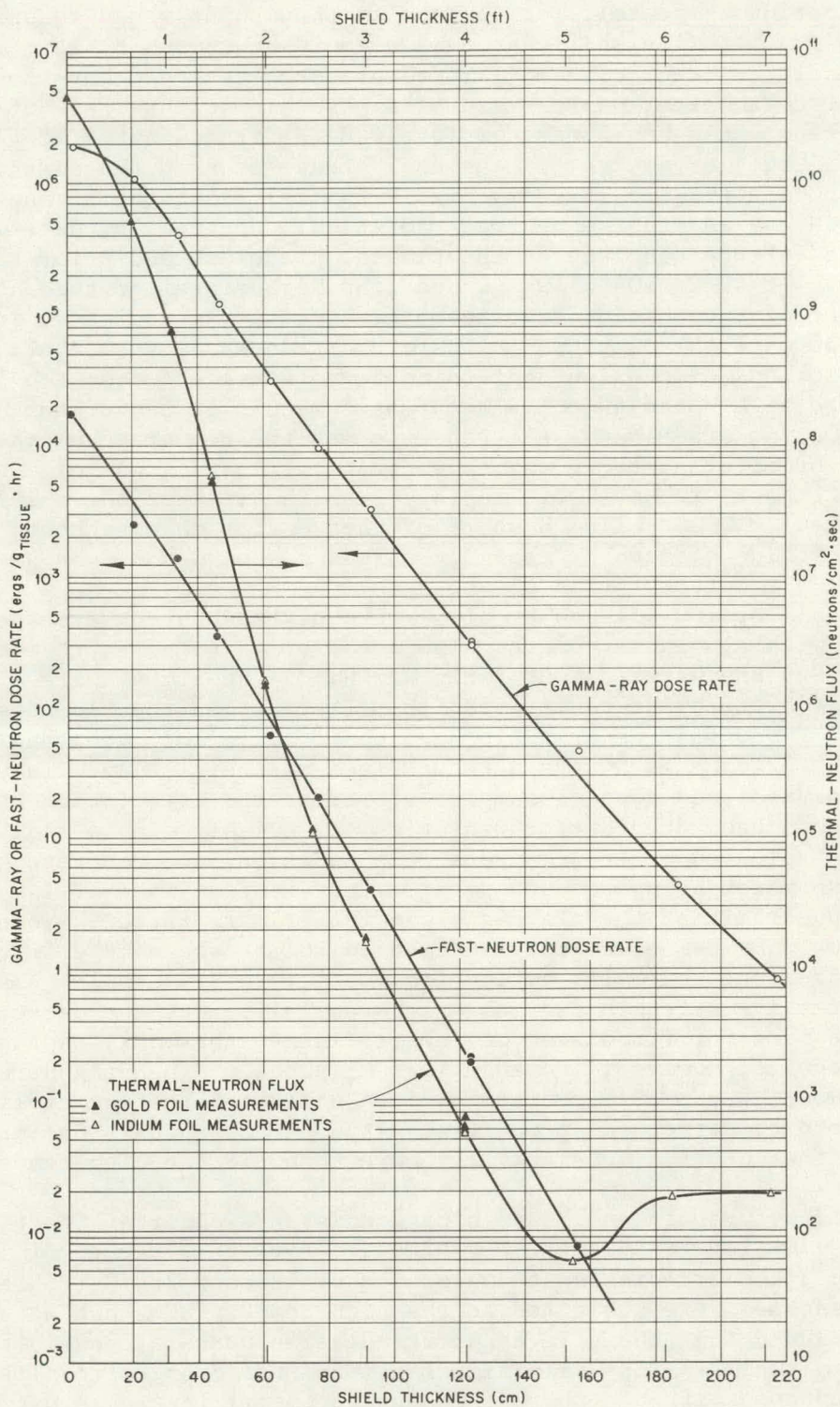
UNCLASSIFIED  
2-01-058-0-383

Fig. 68. Gamma-Ray Dose Rate, Fast-Neutron Dose Rate, and Thermal Neutron Flux vs Shield Thickness of the ORNL Graphite Reactor Shield.  
 Source: T. V. Blosser et al., *A Study of the Nuclear and Physical Properties of the ORNL Graphite Reactor Shield*, ORNL-2195 (August 1958).

Even if one assumes the maximum possible exposure (i.e., full power for 12 continuous years), the fluence at that point would be only  $7.5 \times 10^{12} \text{ nvt}$ . If significant damage could be caused by that low level of fluence, the inner 0.15 m (1/2 ft) of concrete would have lost 20% of its strength after only 12 min of exposure. At that rate of damage, the concrete would have been completely deteriorated after 12 years of operation, but, of course, it was not. Thus, even in the absence of radiation damage data, it seems highly unlikely that the strength loss was due in any way to the neutron radiation. Apparently, data were not available for the concrete at the time of placement and prior to any exposure. If  $40^\circ\text{C}$  ( $104^\circ\text{F}$ ) was indeed the highest temperature at the inner face of the shield, and the water content was decreased in the first 0.30 m (1 ft) as shown in Table 8, it does not seem that, in light of the previous discussion concerning temperature effects, the loss of 40% compressive strength could occur as a result of temperature exposure alone. On the other hand, the report gives the temperature gradients at 5 and 10 hr after shutdown and shows that the inside foot of concrete changes temperature much more rapidly than the rest of the shield (this is expected). The cycling history of the reactor is not known, but the thermal cycling effects of changing stresses, etc., could be an important factor in the deterioration of strength.

Experiments by Elleuch et al.<sup>78</sup> were carried out on a serpentine concrete with aluminous cement. The irradiation temperature was  $200^\circ\text{C}$  ( $392^\circ\text{F}$ ), and the water/cement ratio was 0.38. Specimens were also dried at  $250^\circ\text{C}$  ( $482^\circ\text{F}$ ) prior to irradiation. Thermal neutron fluences up to  $6.5 \times 10^{20} \text{ nvt}$ , fast neutron fluences up to  $1.1 \times 10^{20} \text{ nvt}$ , and gamma exposures to  $1.3 \times 10^{12} \text{ rads}$  were utilized in their study. They also tested unirradiated control samples stored at the irradiation temperature. Much gas was generated during radiation, presumably due to radiolysis of the water released by the concrete. In addition, the concrete samples showed expansion of up to  $7000 \mu\text{m}$  at a fast neutron dose of  $1 \times 10^{20} \text{ nvt}$ , and it appeared that the aggregate was the primary factor. Young's modulus (as measured by pulse velocity) decreased 20% at the same dose over an unirradiated but thermally cycled [to  $200^\circ\text{C}$  ( $392^\circ\text{F}$ )] sample. The bending and compressive strength decreased substantially, but the decrease was about the same for irradiated and unirradiated, thermally exposed samples. The serpentine, however, showed a loss of about 65% bending strength under a dose of  $9 \times 10^{19} \text{ nvt}$  and no loss under temperature cycling. Thus, with regard to structural properties, it does not appear that irradiation affected the concrete substantially more than did the high-temperature exposure.

Tests by Granata and Montagnini<sup>79</sup> on standard mortar (portland cement and fine limestone sand) were performed at neutron fluences of  $10^{18}$  to  $10^{20} \text{ nvt}$  and irradiation temperatures of 130 and  $280^\circ\text{C}$  (266 and  $536^\circ\text{F}$ ). Control samples were subjected to the high temperatures but not the radiation. They concluded that the effects of irradiation up to around  $10^{19} \text{ nvt}$  are relatively small, and no significant dimensional changes resulted. The thermal conductivity and thermal expansion coefficient were not affected. However, the mortar samples were affected at the higher exposure of  $10^{20} \text{ nvt}$ . They reported that specimens irradiated to that fluence level at  $280^\circ\text{C}$  ( $536^\circ\text{F}$ ) were so severely cracked and damaged that it was not possible to

✓

carry out measurements on them. There are some points in this report that require discussion. The authors did report that the thermal history samples were all in good condition (not cracked, etc.). The samples in the 130°C (266°F) test rig irradiated to  $10^{19}$  were partially cracked and damaged. These samples showed about a 10% lower flexural strength. However, the compressive strength was not measured. Therefore, it seems that the authors' conclusion regarding relatively small effects of  $10^{19}$  *nvt* is somewhat contradictory. If the irradiated specimens were visibly cracked and damaged, it seems that a significant effect occurred. Obviously, damage at  $10^{20}$  *nvt* was quite severe, since the samples could not even be tested.

Browne<sup>10</sup> states that the maximum integrated neutron irradiation dose in PCRVs is kept below  $3 \times 10^{19}$  *nvt* and higher irradiation levels are thought to affect concrete properties. He also stated that the data regarding critical doses and the magnitude of their effects are inadequate.

Table 9 gives the radiation exposure levels allowable under Section III, Division 2, of the ASME Boiler and Pressure Vessel Code<sup>12</sup> (Table CB3430-2). It should be noted that the allowable neutron exposure for concrete is  $10 \times 10^{20}$  or  $1.0 \times 10^{21}$  *nvt*. The criteria upon which that number is based are not known. It may well be that exposure limits to other portions of the vessel, such as the liner, cooling tubes, or reinforcement, may naturally limit the exposure of the concrete to a fluence far below the established limit. It is also recognized that the data regarding radiation effects on concretes, especially normal concretes as used in PCRVs, are scarce. However, in view of some of the results presented,<sup>77,79</sup> a fluence of  $1.0 \times 10^{21}$  seems to be quite high and should be examined for justification.

Table 9. Radiation Exposure Limits

Material	Exposure
Liner and attachments	As specified in Design Specification
Concrete	$10 \times 10^{20}$ <i>nvt</i>
Reinforcing steel	$1 \times 10^{18}$ <i>nvt</i> > 1 MeV
Prestressing steel	$1 \times 10^{17}$ <i>nvt</i> > 1 MeV
Permanent coatings	$10^6$ rads <sup>1</sup>

NOTE:

(1) Higher exposure may be permitted as long as the effect on permanent coatings is shown to be acceptable.

Source: "Concrete Reactor Vessels and Containments," AMSE Boiler and Pressure Vessel Code, Section III, Division 2 (1975).

As far as is known, present-day PCRV designs do not allow exposures over  $3 \times 10^{19}$  nvt. Changes in design to decrease the size of the PCRV and allow greater irradiation exposure cannot be supported with reliable information nor by experience. The effects of radiation on concrete properties are not well known or understood, especially at fluences above  $10^{19}$  nvt.

### 3.5 Moisture Migration

In most of the discussions of concrete properties for PCRVs, reference has been made to testing of sealed and unsealed specimens. The concept of sealing is, of course, to provide moisture conditions in the small laboratory test specimens that simulate those in mass concrete. Presumably, the testing of sealed and unsealed specimens provides limits for material behavior, with the actual PCRV concrete somewhere between those limits. The variation of concrete properties at elevated temperatures has been seen to have a strong dependence on the free-moisture content during the high-temperature exposure. In addition, the shielding properties of normal PCRV concrete are dependent on the water content, because hydrogen is relied on to slow down fast neutrons to thermal energies. Also, the thermal conductivity will decrease with moisture loss, with a resultant temperature increase and inducement of thermal stresses. The presence and movement of moisture are also thought to be associated with the cracking of concrete. With regard to creep, moisture movement has been proposed and supported by many investigators as a mechanism of creep deformation.

Yuan, Hilsdorf, and Kesler<sup>80</sup> studied the drying of mortar specimens [5.08-cm-diam  $\times$  10.16-cm-long (2  $\times$  4 in.) cylinders] with water/cement ratios of 0.40, 0.45, 0.55, and 0.70 at temperatures from 4 to 60°C (39 to 140°F). They concluded that moisture loss is a function of the water/cement ratio, temperature, and relative humidity. The rate of moisture loss decreases with increase in time. For temperatures of 40, 52, and 60°C (104, 126, and 140°F), the equilibrium moisture content is dependent on water/cement ratio under all relative vapor pressures. They also concluded that diffusion coefficients could adequately describe the drying process of mortars under the tested conditions. The diffusion coefficients, K, increased with water/cement ratio, given similar moisture conditions, and increased with increasing temperature. The variation of K with temperature appeared to be a parabolic function.

England and Ross<sup>81</sup> performed experiments on thick sections of concrete to measure long-term shrinkage, pore pressures, and moisture distribution. Hot-face temperatures up to 150°C (302°F) and a cold-face temperature of 20°C (68°F) were utilized, with moisture paths up to 3.05 m (10 ft) in length. Drying occurred simultaneously at both the hot and cold faces. At temperatures less than 100°C (212°F), drying is not likely to be an important factor in thick sections, such as for PCRVs, because drying, even after many years, is unlikely to penetrate more than half a meter from either face.<sup>81</sup> Figure 69 shows the moisture distribution for various lengths of moisture path and a hot-face temperature of 125°C (257°F) after 887 days for a 3.05-m (10-ft) section. The depth of drying was

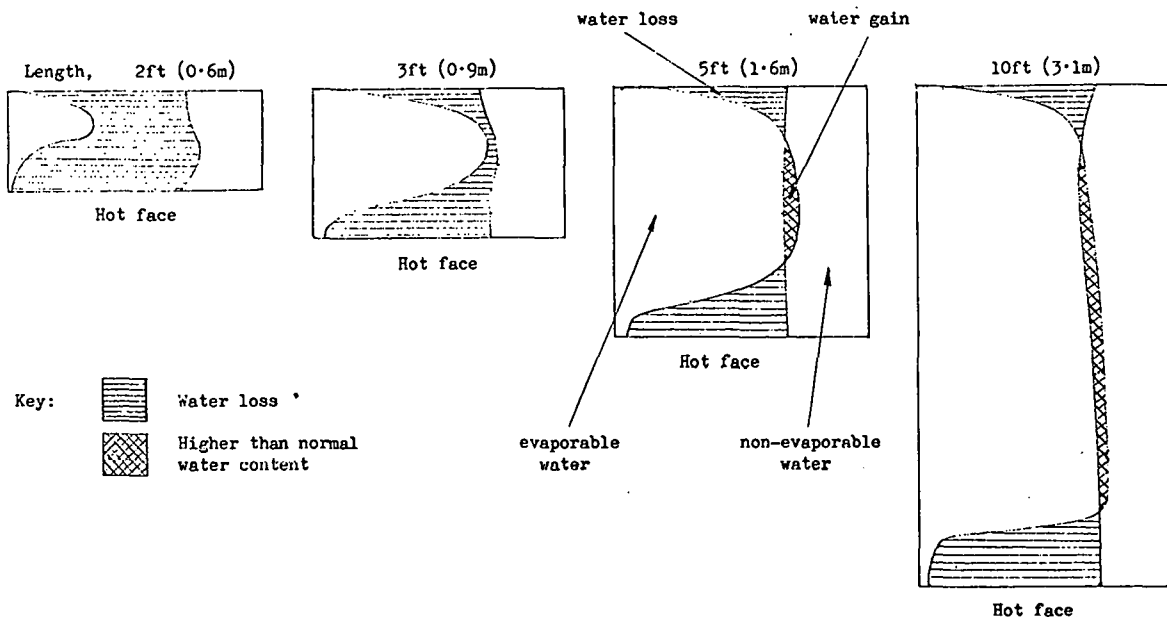


Fig. 69. Phase Diagrams for Water in Concrete Specimens of Various Lengths After 887 Days and a Hot-Face Temperature of 125°C (257°F).  
Source: G. L. England and A. D. Ross, "Shrinkage, Moisture, and Pore Pressures in Hardened Concrete," ACI SP-34, *Concrete for Nuclear Reactors*, pp. 883-908 (1972).

about 0.49 m (1.6 ft). This compares with depths of about 0.305 and 0.914 m (1 and 3 ft) for hot-face temperatures of 100 and 150°C (212 and 302°F) respectively. In addition, for the longer specimens, more water migrated into the intermediate regions than from those producing zones of higher than normal water content. The authors also concluded that pore pressures are unlikely to be important in the bulk of the PCRV concrete, but could be important to vessel liner instability. England and Ross did not describe how moisture measurements were obtained, but it is assumed that a gravimetric technique was utilized.

Browne<sup>10</sup> discussed the moisture migration for the Wylfa vessel and concluded that no significant moisture migration should occur over 30 years, except near the outer face. The maximum temperature for the Wylfa vessel, however, is 35°C (95°F). He references work by Lowe (ref. 9 of ref. 10), which showed Fick's law of diffusion to apply to moisture migration in concrete, particularly at elevated temperatures. Those results also show, in agreement with Yuan, Hilsdorf, and Kesler,<sup>80</sup> that the diffusion coefficient is small, decreases with moisture content, and increases parabolically with temperature.

The concept of a thermal moisture conductivity,  $S_t$  [ $\text{kg m}^{-3} (\text{°C})^{-1}$ ], is discussed by Pihlajavaara and Tiusanen.<sup>82</sup> The value of  $S_t$  decreases with moisture content and is zero for saturated cement stone. In addition, it varies proportionally with the inverse of temperature. The authors state that definitive conclusions regarding thermal moisture transfer in concrete cannot be made with existing knowledge, but that further research regarding the thermal moisture conductivity concept is warranted.

In an effort to more accurately simulate the dimensional effects on moisture migration in cylindrical PCRVs, McDonald<sup>83</sup> utilized a pie-shaped specimen. The specimen was 2.74 m (9 ft) long with cross-sectional dimensions of 0.61 by 0.61 m (2 by 2 ft) on one end and 0.61 by 0.81 m (2 by 2.67 ft) on the other end. The small end (representing the inner face of a PCRV) and the lateral surfaces were sealed with copper sheet and epoxy. The large end (representing the outer face of a PCRV) was exposed to ambient air. Relative humidity and neutron scattering methods, as well as a capacitance-type embedded moisture gage known as the open-wire-line (OWL) probe, were used to measure moisture contents along the specimen. The OWL probe measures the dielectric constant. In addition, a Monfore gage was used for relative-humidity measurements. Strain and temperature readings were provided by Carlson strain meters and thermocouples. The peak temperature of hydration was 75°C (167°F) reached at 98 hr after coating. Temperatures stabilized at room temperature 60 days after casting. When 510 days old, the inner face was exposed to a temperature of 65°C (149°F) with a series of heat lamps. A steady-state temperature distribution was reached after about three weeks. At the end of one year, the moisture content near the ends of the specimen was about 15% less than the bulk value, and the authors provided Fig. 70 to show the effect. One must be careful in attributing significant moisture migration to the imposed temperature gradient. Figure 71 shows the change in moisture content along the specimen as a result of the one-year period of heating. The greatest change recorded was about 0.5 pcft, using the

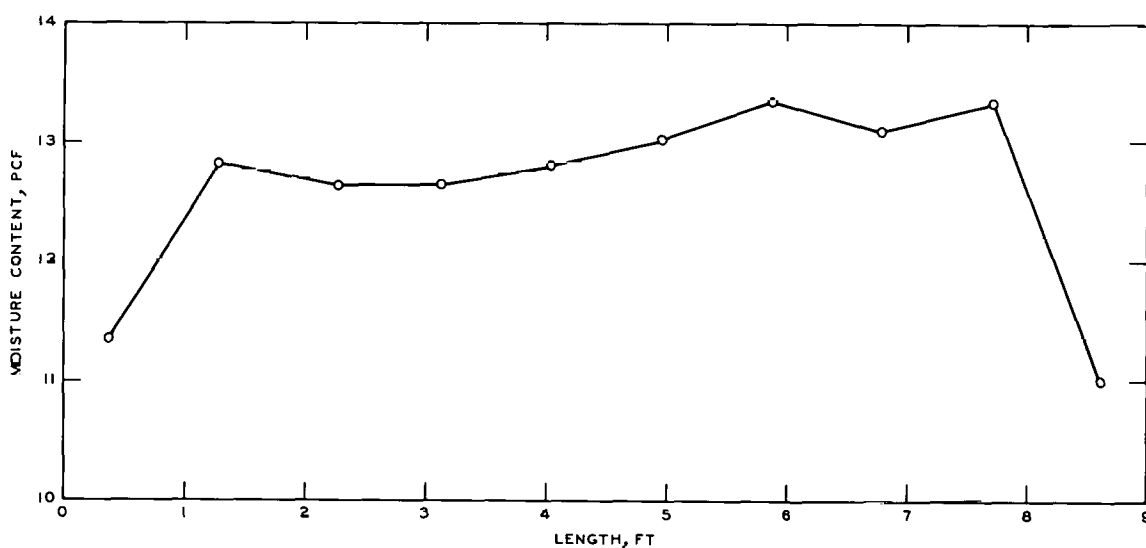


Fig. 70. Specimen Moisture Content Profile at the end of Test Period. Source: J. E. McDonald, *Moisture Migration in Concrete*, ORNL-TM-5051 (May 1975).

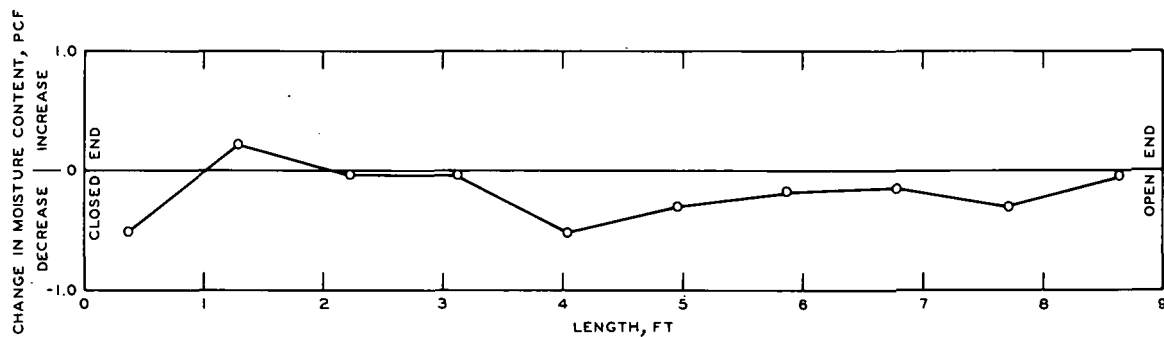


Fig. 71. Changes in Moisture Content at Various Measuring Stations in the Specimen After Heating. Source: J. E. McDonald, *Moisture Migration in Concrete*, ORNL-TM-5051 (May 1975).

least-squares-fit equations for each data point. That represents a change of less than 5%. An examination of the data for the position nearest the sealed end shows that the individual readings varied by as much as  $\pm 6\%$  from the best-fit line. Thus, almost all of the moisture exchange recorded occurred prior to heating, and one year of heating at  $65^\circ\text{C}$  ( $149^\circ\text{F}$ ) [with a temperature gradient of about  $16.4^\circ\text{C}/\text{m}$  ( $9^\circ\text{F}/\text{ft}$ )] produced no significant change in the moisture condition of the 2.74-m-thick (9-ft) specimen.

Although the data are scarce regarding moisture migration in mass concrete structures, a qualitative statement appears to be justified concerning the probable moisture condition of PCRV concrete. It is apparent that moisture migration in thick concrete sections is a very slow process at the temperatures expected in current PCRV designs [ $<100^\circ\text{C}$  ( $212^\circ\text{F}$ )]. Results indicate that the zones of moisture loss, in a 3.05-m-thick (10-ft) section, would include only about 0.305 m (1 ft) of concrete nearest the inner and outer surfaces. The moisture will migrate in the direction of decreasing temperature. As temperatures increase, the rate and amount of migration will increase, so that the affected zones will penetrate deeper into the structure. Indications are that the moisture movement under a given set of conditions could be predicted with diffusion theory, provided that certain boundary conditions and the diffusion coefficient are known. For current PCRV operating conditions [ $\leq 100^\circ\text{C}$  ( $212^\circ\text{F}$ )], it does not appear that a massive research effort to provide precise quantitative data regarding moisture migration is necessary for assessment of vessel reliability. For understanding of long-term behavior and efficiency in concrete vessel design, moisture migration studies are warranted. However, for extensions of present design thermal conditions [ $\geq 100^\circ\text{C}$  ( $212^\circ\text{F}$ )], indications are that moisture movement could be quite significant, and the ability to design for that effect would rely on parameters such as the thermal moisture conductivity. For efficient and reliable nondestructive moisture measurements, instrumentation and measuring techniques should receive emphasis.

### 3.6 Hot Spots and Models

Most of the previous discussions of concrete properties have resulted from investigations with laboratory specimens of small dimensions relative to the PCRV structure. The problems of size effects are often brought to focus in attempting to analyze structural behavior from small-sample test results. For example, the analysis of thermal stresses in a very thick section on the order of 3 m (~10 ft) is difficult, if not unrealistic, when based on test results obtained from specimens only a few inches thick. An obvious alternative is through the use of model testing. In this way, analyses of vessel deformation under conditions more representative of actual PCRV operating conditions can be made in the context of proper geometry, stress distribution, and thermal gradients. The determination of the effects due to localized temperature increases (hot spots) are particularly suited to model testing. The effect of hot spots on structural integrity is of great interest to designers and operators. A localized failure of the vessel cooling system, for example, could result in a localized portion of the concrete being subjected to over-design temperatures. Table 4 showed that the ASME Boiler and Pressure Vessel Code has established a temperature limit of 121°C (250°F) at local hot spots during normal operation of the reactor. During abnormal and severe environmental conditions, the local hot spot allowable is 190°C (374°F). In the event that a portion of the concrete is subjected to very high temperatures for limited periods of time (days, weeks), an assessment must be made concerning the structural integrity of the vessel.

A model study was conducted by Dubois et al.<sup>84</sup> on a one-tenth-scale PCRV model of the French EDF3. They subjected the model to eight thermal cycles from 20 to 200°C (68 to 392°F) for varying lengths of time, using different temperature gradients. The total time involved was two years and three months. They reported that the first cracks appeared during the initial heating between 175 and 200°C (347 and 392°F) and extended to within about 12.7 cm (5 in.) of the outer surface of the 40.6-cm-thick (16-in.) vessel. The outer surface, however, retained its integrity. The authors stated that, even though a thermal gradient of 200°C [499°C/m (274°F/ft)] induced cracking in the cylinder, equilibrium was maintained with cracking at a depth of 10.16 cm (4 in.) and very acceptable thermal compressive stresses in the uncracked region. The authors attach most importance to their observation of the detachment of the outside layer of the cylinder as a result of cracking. The authors concluded that the behavior of the vessel was satisfactory when held for nine months at 200°C (392°F), even though considerable concrete cracking was observed. They supported the present concrete temperature limit of 80°C (176°F) as being justifiably safe and suggested that an inner wall concrete temperature of 150°C (302°F) is possible for normal operation. The use of wire fabric reinforcement at the outer face was suggested as a method for controlling the cracking of the vessel.

A one-fourth-scale model of the Fort St. Vrain PCRV was tested by Northrup and Ople<sup>85</sup> to investigate elevated-temperature effects on long-term behavior. The maximum temperature used was 60°C (140°F). Small specimens were tested under the same conditions to characterize the

material and provide reference data. Moisture measurements showed that a considerable length of time would be required for the dry condition to be reached and that it may not be attained at all if equilibrium with surrounding air is considered. A significant result was that the creep rate (including shrinkage) during the combined condition of prestress loading and elevated temperature was lower than or equal to the creep rate (including shrinkage) under prestress and ambient temperature. They attributed this to opposing effects of thermal stresses and thermal expansion strains as well as to increased strength due to age and additional hydration due to heating. Also, all the creep rates in the model were less than the creep rates of reference specimens. Because the effects of temperature were much greater with the specimens than with the model, calculated creep rates overestimated the measured values on the model, when elevated temperatures were used, by as much as ten times. The authors emphasize the inadequacy of using directly measured uniaxial creep data from small test specimens in simple design techniques. However, they also point to the finite-element method as a procedure which can utilize the uniaxial data. Thus the major observation was that the effect of elevated temperature [60°C (140°F)] on creep of concrete in a PCRV model was less severe than observed on small, plain concrete test specimens. The main reason for that observation, according to Northrup and Ople, was the difference in restraint conditions. That is, the configuration and size of the model and the presence of bonded steel elements provide restraints (such as multiaxial stress conditions) against creep and shrinkage. Their testing did not include sustained temperatures above 60°C (140°F) or hot spots.

Tests by Irving, Carmichael, and Hornby<sup>86</sup> were undertaken to assess the damage, if any, resulting from measured hot-spot temperatures, up to 180°C (356°F), during the commissioning trials of the Oldbury PCRV. They constructed a full-scale model of the penetration region, where the highest temperatures were observed. Since hot spots can induce high thermal stresses in the concrete, a theoretical study was performed, and it showed that there was no cause for concern about the safety margin against failure of the vessel. The study did show, however, that it was possible that cracking could occur in the concrete close to the liner. The model test was designed to assess the extent of cracking and the effect in the liner retention system. The 1.524-m (5-ft) model was heated to 180°C (356°F) for 98 days. They used dye penetrants, core samples, and ultrasonic testing to detect and measure cracking, as well as embedded strain instrumentation. The hot spot was confined to a small area of the model. Gages indicated that some cracking occurred during reactor start-up when the penetration liner was only 24°C (75°F) hotter than the adjacent concrete. This was attributed to thermal diffusivity differences between steel and concrete, resulting in strain differentials. No cracking of the concrete was observed at heated locations away from steel parts. Cracking was limited to a central region of about 0.46 m (1 1/2 ft) where the concrete temperature was 100°C (212°F). No damage was observed outside that region. A second degree of cracking occurred during shutdown, after a period of sustained operation, caused by stress reversals due to residual creep strains. Uncracked regions of the heated concrete showed no loss of strength over control samples stored

separately. In addition, measurements of vapor pressures behind the liner showed less severe pressures than those corresponding to the concrete temperatures imposed. Thus, no pressure buildup would occur at the hot spot, probably because of pressure relief along the liner-concrete interface. The authors conclude that the sustained high hot-spot temperature in the Oldbury vessel did not cause serious damage to the liner or to the concrete.

Fluge, Gausel, and Lenschow<sup>87</sup> reported the results of an experimental and analytical study that utilized four cylindrical models of 1:12 size relative to an 800-MW(e) prototype reactor. Two of the models were constructed without bonded reinforcement. Models of this type underwent explosive rupture, while the models with the reinforcement failed with uniform crack distribution and gradual, progressive failure. The authors obtained good agreement between experimental results and analytical predictions for the static failure state, using finite-element methods. However, for deformation in the plastic range, simple failure considerations resulted in better correlations. This study did not include the investigation of sustained high temperatures or hot spots.

A PCRV thermal cylinder model about one-sixth scale of the central barrel section of a cylindrical PCRV was tested at Oak Ridge National Laboratory. A description of the model and test procedures are detailed in refs. 88 and 89, while the initial results are described in ref. 90. The model was 1.22 m (4 ft) high, 0.46 m (1.5 ft) thick, and 2.06 m (6.75 ft) in outer diameter. It was constructed with an inner concrete core allowing for a pressure annulus of about 3.81 cm (1 1/2 in.) and was prestressed with both axial and circumferential tendons. A mild-steel liner provided the inner seal, while the outer surface of the model was sealed against moisture loss with sheet metal. The top surfaces of the cylinder and core were coated with layers of epoxy and copper foil. The model was subjected to internal pressure and elevated temperatures. A temperature of 65°C (150°F) was sustained for about 14 months. During a subsequent period, a narrow circumferential band on the inner surface of the test section was heated to 232°C (450°F) for 84 days to investigate the effect of a hot-spot condition. Sectioning of the model after testing revealed "no significant defects"<sup>90</sup> in the cut surfaces, although the concrete immediately surrounding the heating elements was darkened. A sclerometer (impact hammer) was utilized to approximate the compressive strength of the concrete at the hot-spot location. Neglecting excessively high readings associated with the aggregate particles, the results showed that a substantial decrease in strength (lower reading on sclerometer) occurred close to the heater. The amount of reduction decreased with increasing distance from the heater location. At a distance of 10.16 cm (4 in.) from the heater, the strength was that of the unaffected concrete. The strength at the heater location was only about 61% of that of the unaffected concrete (actually measured on the matrix). Thus, there appeared to be a decrease in strength of the concrete subjected to the 232°C (450°F) temperature, but no observable cracking or other loss of structural integrity.

The purpose of the foregoing was not to discuss or even present the state of the art of model testing relative to PCRVs. Rather, the intent was to present a few representative examples of research investigations

which have attempted to examine the behavior of concrete under loading and environmental conditions more closely resembling those existing in a real PCRV. The few results presented are difficult to compare, but the two studies that investigated the effects of hot spots were in agreement: local hot spots up to 200-250°C (392-482°F) for extended lengths of time (a few months) did not result in damage (except, possibly, loss of strength) to the concrete itself.<sup>86,90</sup> Cracking was observed in the vicinity of steel components because of differences in expansion characteristics.<sup>86</sup> Some models without bonded reinforcement experienced explosive, catastrophic rupture, whereas reinforced structures failed in a progressive, controlled manner.<sup>87</sup> Because it is felt by many investigators that cracking is inevitable in a PCRV type of structure, it has been suggested that the structural designer take advantage of that situation and utilize it to construct a vessel of segmented design.<sup>91,92</sup> In simple terms, a segmented vessel would be one in which large cracks (joints) essentially exist at the locations desired by the designer, in order to reduce stress and thermal gradients through the entire vessel. There is, of course, disagreement as to the feasibility or even usefulness of such a concept.

It seems apparent that the limitations of laboratory specimens are sufficient enough to motivate further testing of model structures and analyses of their behavior with regard to prediction of actual PCRV structures. Much information can be gained from such testing; further improvements in embedded instrumentation and analytical methods will provide results even more representative of actual vessel behavior than now available.

#### 4. SUMMARY, CONCLUSIONS, AND RECOMMENDATIONS

##### 4.1 Summary

The introduction to this report made mention that many investigations have been conducted through the years to develop data for various concrete properties of specific interest to designers of prestressed concrete reactor vessels (PCRVs). It was also mentioned in Sect. 3, and emphasized throughout the discussions, that concrete is a very general term for a class of materials that vary widely in properties and applications. Even with regard to PCRVs, it was stated that concrete mixtures vary substantially, as reported by many investigators. The unusual amount of detail provided herein for many of the reports reviewed was intended to show that that is, in fact, the case. For most of the properties considered, only representative studies were discussed. In addition, the purpose of this review was to direct attention to plain concrete, sans reinforcement or prestressing components. Most studies of concrete properties for PCRV applications have been concerned with plain concrete.

It is apparent from the results presented that a plethora of data has been reported regarding temperature effects on concrete properties. Most of the reports taken singularly appear to provide reasonable results with credible justification for the observations and conclusions. However, the results taken together provide a confusing display of information

that appears to preclude reasonable predictions of concrete behavior in a given situation. On the other hand, those two outlooks represent extremes of the situation untempered by a reasonable and prudent examination of the data within the perspective of application. As mentioned in Sect. 3.3.1, the data shown in Fig. 22 provide a representative cross section of results from the literature regarding concrete compressive strength at high temperatures. Any attempts to present those data as average behavior with expected deviations would be ridiculous because of the tremendous variation in types of concrete, experimental treatment, and testing procedures, and, indeed, that is not the intent of this report. Rather, one intent is to show that a person cannot simply make an entry into the technical literature, extract data from one or two reports that provide results on high-temperature testing of concrete, and generally apply the data to structural design situations. The studies of compressive strength and modulus of elasticity are, perhaps, most indicative that the observed effects are functions of many variables. Some of these variables are mixture constituents, curing procedures, curing time, age at loading, time of exposure, temperature of testing (i.e., hot- or cold-tested), moisture condition, number of exposures (i.e., thermal cycling), and test methods. A normalized comparison of all data reviewed, Figs. 22 and 31, showed that the compressive strength and modulus of elasticity both decreased with increases in temperature, time of exposure, free-moisture content, and thermal cycles. Beyond that, precise statements cannot be made without consideration of more specific variables, such as those mentioned below. The data cannot realistically be represented by a line of average behavior. The most conservative use of the data would show losses of 70 and 60% in compressive strength and elastic modulus at 150°C (302°F). The most liberal use would show improvement in both properties at 150°C (302°F). Thus an answer as to the effect of temperature on concrete is not easily obtained from the available literature. With regard to high temperatures, many researchers observed that limestone aggregates generally resulted in greater losses of strength and elastic properties than did other aggregates, such as siliceous gravels. In fact, in a few reports, recommendations were made that limestone definitely not be utilized for applications where the concrete could be subjected to sustained temperatures above 100°C (212°F). Previously, it had been thought that compatibility differences between the aggregate and the matrix were the cause of strength deterioration. Reports reviewed here have shown, for example, that the thermal expansion characteristics of limestone aggregate are more compatible with the mortar at elevated temperatures than at room temperature. Many studies have pointed to silica content of the aggregate as having affected various properties substantially. Higher silica contents resulted in greater thermal expansion but less deterioration of properties at high temperatures. It was suggested that a chemical reaction between silica and  $\text{Ca}(\text{OH})_2$ , or between silica and the products of the  $\text{Ca}(\text{OH})_2$  and hydrated calcium silicates reaction, could be responsible for improving properties. It has also been stated often that high-pressure steam develops in the flaws and pores, creating internal stresses, which lead to cracking and loss of strength. Specimens

that are cold tested, in fact, generally appear to give lower (or equal) strength than those tested at the exposure temperature, indicating that the vapor pressure effect is minor.

It is obvious from the results that the specimens sealed against moisture loss showed much greater deterioration in strength properties than did dry specimens. Even though a quantitative description of average behavior is not reasonable, it is felt that an analysis of the results of sealed specimens does indicate severe deterioration of some concretes, particularly limestone, at sustained temperatures above 100°C (212°F). There is no evidence to suggest that exposure temperatures below 100°C (212°F) would result in significant damage to PCRV concretes. With regard to tensile strength, that property appears to be affected by temperature in about the same manner as that of the compressive strength.

The creep of concrete varies with the parameters mentioned previously and is also affected by increases in temperature. At current PCRV design temperatures, indications are that creep will not result in excessive deformation; that is, it can be incorporated in the design. At elevated temperatures, substantially higher creep strains were observed. The specific creep of sealed concretes appears to be less than that for dried specimens. As stated throughout the literature, the creep will be substantially greater for young concrete regardless of moisture condition. Also, the "creep maximum" observation, in which the creep rate supposedly begins to decrease at some temperature around 80°C (176°F), cannot be labeled as representative of general concrete behavior. It is important that further investigations of high-temperature creep be undertaken to confirm that type of behavior. The very limited amount of data concerning creep of sealed and unsealed concrete over 100°C (212°F) makes comparison difficult because of great variations in testing procedures and concretes. High-temperature creep of concrete should be a primary task of research for any program seeking to evaluate concrete properties for high-temperature applications. It is important to note that one cannot separate creep and strength when evaluating performance under load. As the stress/strength ratio increases, the specific creep will increase. Thus, if the compressive strength of the concrete deteriorates at some particular temperature, the stress/strength ratio (assuming a constant loading stress) will increase, and the deformation may increase, whether the material's creep resistance is affected or not.

With regard to thermal properties, there is not a large amount of data, especially for the effects of free moisture. Available results indicate that the coefficient of thermal expansion will be less as drying increases. Practically speaking, the coefficient of thermal expansion, relative to the degree of change observed for other properties, does not vary a great deal and increases only slightly with temperatures to 250 or 300°C (482 or 572°F). The coefficient can be affected more by other factors such as moisture, thermal cycles, and heating rate. Again, with regard to aggregate, limestone gave the lowest coefficient, and increasing silica resulted in greater coefficients of expansion.

The thermal conductivity decreases as temperature increases and as moisture is lost. The conservative procedure is to obtain conductivity

measurements on dry concrete at the maximum design temperature. This would provide a minimum value applicable to that portion of the vessel receiving the initial heat flux.

As stated often herein, experimental investigations have largely considered the properties shown under uniaxial loading. The concrete in a vessel will be in a multiaxial state of stress, biaxial or triaxial compression. It appears that the biaxial case would be of most concern, because immediately after reactor shutdown, the vessel will be hot and subjected to the full prestressing load. It is generally accepted that the ultimate strength of concrete increases when sustaining multiaxial stresses are imposed. The method of load application is a primary topic of research, and recent results with steel-brush platens, ball-bearing platens, fluid-cushion platens, and deformable platens have shown promise of reducing end restraints to tolerable levels so that the true ultimate strength can be measured. The most reliable data indicate a maximum biaxial compressive strength of 1.25 times the uniaxial strength measured with the same apparatus. Triaxial tests indicate strengths up to four to six times uniaxial strength. Tests at elevated temperatures and with sealed specimens are very limited. Results indicate that the sealed specimens are weaker than dry concrete, but that wet concrete gives a greater relative increase in strength under multiaxial stress conditions. An important observation concerns that of a supposed critical stress level under biaxial loading, a stress that may occur as low as 50% of the ultimate and at which severe permanent damage takes place within the specimen. Since uniaxial strength is generally used as a material property for design, one may suppose that the actual vessel conditions involving biaxial stresses will make that data conservative by 25%. However, tests conducted with steel platens, the common method, indicate a strength measurement that is 25% too high, meaning that there may be, essentially, no additional margin for strength data obtained with steel platens. The additional observation of a critical stress below ultimate for short- and long-term loading, may be more realistic for design purposes. Much work needs to be done to develop an understanding of multiaxial behavior as well as methods of providing accurate strength and creep data, especially with regard to sealed concrete and elevated temperatures.

Concerning the mechanisms responsible for observed effects of elevated temperature on concrete properties, the presence of free moisture is generally seen as the major contributing factor to the deterioration. Evidence indicates that the commonly accepted theory of differences between the aggregate and cement paste thermal expansion characteristics may not be the primary cause of strength loss at high temperature. The strength of dry concrete, according to some, results from the desorption of cement paste, leading to a collapse of the gel structure and closure of gaps between primary gel particles. In addition, it does not appear that high-pressure steam in the flaws has much effect on strength. Rather, chemical reactions may occur that weaken the matrix coherency. The recommendation by some authors that limestone aggregate (low silica) not be used for sustained high-temperature application [above 100°C (212°F)] correlates well with other recommendations that siliceous aggregates be utilized because of favorable chemical reactions involving the silica.

The seepage theory has gained support as an explanation of creep behavior, but controversy still abounds and the character of the creep equation is not well defined.

The effects of radiation on concrete are not well documented. The loss of moisture has an effect on neutron attenuation because hydrogen is the primary element responsible for slowing down fast neutrons. Most data on radiation damage have resulted from tests on core samples removed from reactor shields, and any property deterioration due to irradiation is difficult to separate from that due to thermal conditions. Available studies indicate that damage may occur at neutron fluences between  $10^{19}$  and  $10^{20}$  nvt. One author recommends that  $3 \times 10^{19}$  nvt be the maximum allowable exposure until definitive data become available, while the ASME Boiler and Pressure Vessel Code allows  $1 \times 10^{21}$  nvt exposure for concrete.

The question of moisture migration in mass concrete structures is a central one and is the primary motivation for testing of sealed specimens. It is generally believed that moisture movement in thick sections such as PCRVs is slow, but quantitative data with regard to the depth of drying, the time involved, and effects of temperature are scarce and inconclusive. For inner-face temperatures less than  $100^{\circ}\text{C}$  ( $212^{\circ}\text{F}$ ), results indicate that drying, even after many years, is unlikely to penetrate more than half a meter from either the inner or outer face of a PCRV. Increasing temperature will cause greater migration toward the inner portion of the vessel (i.e., moisture migration proceeds in the direction of decreasing temperature). There is no question that the loss of moisture at the inner face would result in loss of attenuation capability in the affected area. However, the thickness of concrete needed for adequate biological shielding is only on the order of a few feet, and the effect of, say, the first 2 ft being fully dried would not affect the shielding capacity of present-day PCRVs, which are much thicker than required for shielding. For sustained exposure at temperatures of  $150^{\circ}\text{C}$  ( $302^{\circ}\text{F}$ ) and above, however, the situation could be considerably different. The results of creep testing showed that sealed specimens experienced less specific creep than did dry specimens. Since the bulk of the vessel will more closely represent the sealed case, it seems that the drying effect would not have much impact on long-term deformation, unless the creep rates are very different, so as to induce significant strain differentials. That is not apparent from results to date. With regard to strength, the effect of drying would be to increase strength and increase resistance to elevated temperatures. Up to  $150^{\circ}\text{C}$  ( $302^{\circ}\text{F}$ ) the largest loss of strength observed in the reports reviewed for unsealed specimens was 30% in uniaxial compression. The effect of the high temperature will be less for the bulk concrete with less moisture, because the temperature will be lower toward the outer portion of the vessel.

Because of these observations and the great importance of thermal stresses when operating at elevated temperatures, it seems that model testing is the best method available for investigating vessel behavior under a set of conditions. Thermal gradients are more realistic, as are stress conditions, and the movement of moisture can be more nearly represented. In addition, the important effects of reinforcement can

be evaluated with models. As shown in one report, models without bonded reinforcement can undergo explosive rupture, while those with the reinforcement fail with uniform crack distribution in a controlled, progressive manner. Also, the effects of local hot spots can be evaluated with models. The hot-spot tests reviewed were in agreement that hot-spot temperatures of 200 to 250°C (392 to 482°F), for up to three months exposure, did not cause visible damage to the concrete except in local areas of concrete-reinforcement interfaces.

It seems, from the foregoing, that current operating conditions for PCRVs will not produce any loading situation that cannot be reasonably incorporated into the structural design. Also, currently known limits for temperature and radiation should not result in any loss of character to the concrete that could lead to a significant decrease in structural integrity. The lack of knowledge regarding moisture movement in mass concrete, and the strong effects of temperatures above 100°C (212°F) on concrete with retained free moisture, do not allow a statement advocating PCRV operation much above current limits.

Short- and long-term multiaxial testing of sealed and unsealed concrete is necessary to gain a good understanding of plain concrete behavior at high temperatures. When combined with reliable testing methods to provide "real" strength data, it may be shown that the relative effects of such conditions as high temperature can be conducted with uniaxial testing. These kinds of data will help to provide understanding of plain concrete. But it must be emphasized that vessel design should incorporate bonded reinforcement, and that some type of reinforced specimen, such as a model structure, can more nearly represent the actual vessel.

Test specimens in the laboratory are usually plain concrete and do not exceed about 15 cm (~6 in.) in diameter or thickness. The models are usually reinforced and/or prestressed structures of a few feet in diameter and range in thickness from 0.305 to 1.524 m (1 to 5 ft) or more. Thermal gradients are applied to models but not generally to laboratory specimens. It is most difficult, therefore, to base a prediction of PCRV structural behavior on the results of small, plain concrete specimens. In certain cases, results on plain concrete may indicate loss of structural integrity that would not occur in the actual structure. That is not to say that laboratory testing is not useful. On the contrary, it is the most efficient way to obtain large quantities of data for specific, but limited, conditions. It seems that the most efficient and productive program to determine data for PCRV design would be to engage in experiments with models and laboratory specimens of the same concrete mixture. Once the behavior of the reinforced and prestressed structure is understood and characterized as to the importance of various material properties, laboratory testing on a specific concrete will be sufficient to enable a prediction of vessel performance.

There are other programs being undertaken in PCRV research studies that have not been discussed. The concept of a segmented vessel was mentioned, and it is felt that serious consideration is warranted. Since the concrete cooling system is an expensive undertaking, any steps that might allow its elimination or, at least, reduction are attractive from an economical standpoint. Elimination of the cooling system is attractive with regard to safety also, because breakdown of a cooling system can lead to abnormal conditions and shutdown of the reactor. The principle of the

hot-liner (hot-wall) concept is to place a layer of special concrete behind the liner that will be subjected to the full temperature gradient. This is also sometimes referred to as the sacrificial concrete concept, in which the initial layer of special concrete is allowed to deteriorate as long as it can still transfer structural load to the main vessel concrete. There are many studies under way in West Germany, Italy, and Austria on short- and long-term multiaxial concrete behavior, along with the effects of temperature and radiation.<sup>93</sup> In addition, intensive effort is being expended to develop test methods and equipment for multiaxial studies in this country as well as in Europe.

#### 4.2 Conclusions

1. The available data regarding most concrete properties are voluminous and must be extracted from the literature very discriminately to avoid making generalizations of data not representative of a particular situation.
2. Most properties of concrete are degraded at elevated temperatures. The degree of degradation at a particular temperature is dependent on many factors such as mixture constituents, curing history, age at loading, moisture conditions, number of thermal exposures, and test methods employed.
3. Strength and modulus of elasticity generally decrease with increasing temperature, time of exposure, free-moisture content, and number of thermal cycles. The effects are marked above 100°C (212°F) for sealed concrete. Chemical reactions, rather than stresses due to pore pressure, are thought to be responsible for severe degradation.
4. The most conservative evaluation of available data indicates losses from unheated test values of 70 and 60% in compressive strength and elastic modulus, respectively, at 150°C (302°F).
5. There is no evidence to suggest that sustained exposure of typical portland cement concretes to current PCRV normal operating conditions will result in any significant loss of properties.
6. Properties of mass concrete cannot be obtained by testing of unsealed laboratory specimens because of the effects of retained free moisture.
7. There are strong indications that sealed concrete suffers much deterioration at sustained temperatures over 100°C (212°F), with limestone aggregate concrete being most susceptible. Increased silica content in the aggregates results in less deterioration.
8. Creep is enhanced at elevated temperatures, but there is some evidence that a maximum may occur in the curve of specific creep rate vs time at some temperature from 50 to 150°C (122 to 302°F).
9. The specific creep of sealed specimens, at least at temperatures less than 100°C (212°F), is less than for unsealed specimens. Shrinkage of sealed concrete is very low, and expansion can occur at high temperatures.
10. Young concrete is much more susceptible to creep deformation than mature concrete, regardless of moisture condition.
11. As temperature increases and drying proceeds, the coefficient of thermal expansion ( $\alpha$ ) and thermal conductivity ( $k$ ) both increase. But  $\alpha$  changes very slightly up to 250°C (482°F).

12. The biaxial state of stress is of most interest for the large prestressed vessels, and the most reliable data indicate a maximum biaxial compressive strength of 1.25 times uniaxial strength at normal temperatures.

13. Development of reliable equipment and testing techniques to eliminate end restraints in uniaxial and multiaxial compression testing is imperative to the understanding of concrete behavior, as well as for the generation of reliable design data.

14. The significance of a critical stress, much lower than ultimate strength, in sustained biaxial loading deserves serious consideration in any strength investigations for its ramifications to structural integrity.

15. Reliable evidence is lacking for radiation effects on normal concretes, but it appears that damage may occur at a total neutron fluence of  $10^{19}$  to  $10^{20}$  nvt. The fluence limit of  $1.0 \times 10^{21}$  nvt for concrete allowed by the ASME Boiler and Pressure Vessel Code should be reevaluated.

16. At current PCRV temperatures, moisture migration is not seen to be a limiting parameter for design. Sustained temperatures over  $100^{\circ}\text{C}$  ( $212^{\circ}\text{F}$ ) cause faster and deeper drying and would therefore require serious evaluation.

17. The limited data available indicated that hot-spot temperatures of  $200$  to  $250^{\circ}\text{C}$  ( $392$  to  $482^{\circ}\text{F}$ ), for up to three months exposure, will not cause serious damage to the concrete at locations away from steel reinforcement. However, cracking at concrete reinforcement junctions may occur.

18. Model testing should be used to evaluate PCRV reliability under a given set of conditions. Until analytical description is developed that can define the contribution of the plain concrete properties to the overall behavior of the reinforced vessel, laboratory specimens cannot be used to predict vessel integrity.

19. Specimen testing should be accomplished by simulating the PCRV concrete as closely as possible. This includes such things as the use of an early age hydration heat cycle and retention of free moisture (sealed specimens).

20. The lack of knowledge concerning moisture migration in mass concrete, and the strong effects of temperatures above  $100^{\circ}\text{C}$  ( $212^{\circ}\text{F}$ ) on plain concrete with retained free moisture, do not allow a statement advocating PCRV operation much above current limits.

21. For reliability and economy, the investigations of hot-liner concepts, segmented vessel designs, and new concrete material development should be pursued. The minimization or elimination of the vessel cooling system is desirable.

#### 4.3 Recommendations for Further Study

The following recommendations are made within the scope of this report and may not reflect the needs for study in areas not considered herein. Although the report was primarily concerned with concrete properties in a nuclear environment for the HTGR, it is necessary to point out that prestressed concrete primary containment structures are being proposed and seriously considered for many other applications. Thus the impact on reliability and economy is more wide-ranging than if based solely on HTGR applications.

The three areas of study listed may have common and/or overlapping requirements, especially with regard to temperature.

1. A major program is needed to perfect the design, testing, and evaluation of PCRV model structures. Some of the important aspects involved in this program are:

- a. Development of reliable instrumentation.
- b. Determination of the effects of thermal gradients (may entail models of various thicknesses).
- c. Testing of models with and without bonded reinforcement.
- d. Flexibility of design to allow application of sustained elevated temperatures and local hot spots.
- e. Detailed chemical and microstructural examinations.
- f. Testing of laboratory specimens that simulate, as closely as possible, the concrete conditions of the model and the PCRV. This would include the use of an early age hydration heat cycle, and it may also be necessary to simulate the high (PCRV) heat of hydration on the model.
- g. Continued development of three-dimensional analytical techniques to describe PCRV behavior.

The ultimate goal of the program should be the development of an analytical procedure that describes the model behavior and identifies the contributions of various plain concrete properties so that reasonable predictions of PCRV behavior could be made on the basis of laboratory test results.

2. Other studies are recommended that are applicable to improvement and/or understanding of current PCRV designs.

- a. Continued development of multiaxial testing techniques and equipment (short and long term). Equipment should be designed to test cubical specimens, which allow infinite variation of the three principal stresses. Testing of sealed specimens up to 100°C (212°F) is required. The minimization of end restraints is a primary problem and is applicable to uniaxial compressive testing as well.
- b. Further development of the creep equation and relationship of plain concrete to that of a reinforced structure. Investigation of the relationship between creep and stress/strength ratio should also be performed.
- c. Investigation of the supposed critical stress observed in biaxial loading.
- d. Refinement of already developed techniques for testing of sealed specimens to be used for testing of strength and elastic properties at temperatures up to 100°C (212°F). Testing is required for each particular concrete mixture used.
- e. Because limestone is a commonly used aggregate for concrete construction in the U.S., the investigation of techniques to improve resistance of limestone concrete to property deterioration at high temperatures, especially over 100°C (212°F), is desirable. The addition of silica, for example, might provide one method for improvement.
- f. More detailed chemical and microstructural studies of sealed concrete exposed to elevated temperatures.
- g. A feasibility study of the establishment of more precise standardization for concrete mixtures to be used for nuclear applications.

3. For extensions of current PCRV design criteria, the following items of research are strongly recommended:

- a. Development of techniques to measure physical properties of sealed concrete under multiaxial loading conditions at temperatures well above 100°C (212°F). This would include short- and long-term (creep) testing.
- b. An evaluation of the extent of moisture migration in thick concrete at temperatures of 100°C (212°F) and above.
- c. Additional testing to verify the occurrence and/or validity of a maximum in the curves of specific creep rate or total creep vs temperature for sealed concrete. This would involve long-term tests to investigate the possibility of an inflection in the creep-time behavior.
- d. Concrete material development to maximize resistance to temperature. A concrete with very low water content might be desirable. The effects on radiation shielding must be considered, especially if improvements in design and properties allow for a considerable reduction in vessel thickness.
- e. Determination of the effects of radiation on properties of normal plain concrete and the dose at which deterioration occurs. The radiation effects must be separated from any effects of temperature.
- f. A detailed feasibility study of other vessel concepts such as the hot-wall and segmented designs.

#### ACKNOWLEDGMENTS

The author wishes to extend his gratitude to W. N. Butcher for typing the draft manuscript and to D. A. Canonico, J. P. Callahan, and W. R. Martin for their reviews. I would also like to express my appreciation to M. R. Hill for supervising the preparation of the final document, R. B. Parker for editing, and J. L. Bishop for preparing the manuscript. I want to give a special note of gratitude to J. P. Callahan for his technical assistance and guidance during the preparation of this report.

#### REFERENCES

1. J. L. Plaehn, "A Practical Approach to the Design Philosophy of Prestressed Concrete Reactor Vessels: The Importance of Concrete Properties to PCRV Design," ACI SP-34, *Concrete for Nuclear Reactors*, p. 103 (1972).
2. M. P. Schelp, *Development Plan for the GCFR Prestressed Concrete Reactor Vessel*, GA-A13269, General Atomic Company (February 1975).
3. *Planning Guide for HTGR Safety and Safety-Related Research and Development*, ORNL-4968 (May 1974).

4. W. Fürste, G. Hohnerlein, and H. G. Schafstall, "Prestressed Concrete Reactor Vessels for Nuclear Power Plants Compared to Thick-Walled and Multilayer Steel Vessels," Second. Int. Conf. on Pressure Vessel Technology, Part 1, San Antonio, October 1973.
5. J. L. Plaehn, op. cit., pp. 103-34.
6. C. P. Tan, *Prestressed Concrete in Nuclear Pressure Vessels. A Critical Review of Current Literature*, ORNL-4227 (May 1968).
7. D. Costes, R. Riquois, and R. Lacroix, "Recent Development in Nuclear Prestressed Concrete Pressure Vessels in France," Second Int. Conf. on Pressure Vessel Technology, Part 1, San Antonio, October 1973.
8. W. Rockenhauser, "Structural Design Criteria for Primary Containment Structures," lecture V of lecture notes from the program, *Prestressed Concrete Nuclear Reactor Structures*, March 1968.
9. ACI Committee 116, ACI SP-19, *Cement and Concrete Terminology* (1967).
10. R. D. Browne, "Properties of Concrete in Reactor Vessels," Group C, Paper 13, Conference on Prestressed Concrete Pressure Vessels, Westminster, S.W.I., March 1967.
11. E. G. Endebrock, *Prestressed Concrete Reactor Vessels: Review of Design and Failure Criteria*, LA-5902-MS, Los Alamos Scientific Laboratory (May 1975).
12. "Concrete Reactor Vessels and Containments," ASME Boiler and Pressure Vessel Code, Section III, Division 2 (1975).
13. *ACI Manual of Concrete Practice*, Part 1 - 1974, American Concrete Institute (1974).
14. J. W. Dougill, "Structural Properties of Concrete: A Review," Lecture X of lecture notes from the program, *Prestressed Concrete Nuclear Reactor Structures*, March 1968.
15. D. J. Hannant, "Effects of Heat on Concrete Strength," *Engineering* 197: 302 (Feb. 21, 1964).
16. J. C. Saemann and G. W. Washa, "Variation of Mortar and Concrete Properties with Temperature," *J. Am. Concr. Inst.* 29(5): 385-95 (November 1957).
17. H. S. Davis, "Effects of High Temperature Exposure on Concrete," RL-SA-20, presented at ANS Meeting, Gatlinburg, June 1965.
18. M. O. Withey, "Fifty-Year Compression Test of Concrete," *J. Am. Concr. Inst.* 58: 695 (December 1961).

19. D. Campbell-Allen, E.W.E. Low, and H. Roper, "An Investigation on the Effect of Elevated Temperatures on Concrete for Reactor Vessels," *Nucl. Struct. Eng.* 6: 382-88 (1965).
20. D. Campbell-Allen and P. M. Desai, "The Influence of Aggregate on the Behavior of Concrete at Elevated Temperatures," *Nucl. Eng. Des.* 6(1): 20 (August 1967).
21. Y. Kawahara and A. Haraguchi, "Dynamic Properties of Concrete Exposed to High Temperature," *Concrete* 7(3): 12-19 (March 1969).
22. M. S. Abrams, "Compressive Strength of Concrete at Temperatures to 1600°F," ACI SP-25, *Temperature and Concrete* (1970).
23. H. L. Malhotra, "The Effect of Temperature on the Compressive Strength of Concrete," *Mag. Concr. Res.* 8(22): 85-94 (August 1956).
24. K. W. Nasser, "Creep of Concrete at Low Stress-Strength Ratios and Elevated Temperatures," ACI SP-25, *Temperature and Concrete* (1970).
25. D. Ravina and R. Shalon, "Effect of Elevated Temperature on Strength of Portland Cements," ACI SP-25, *Temperature and Concrete* (1970).
26. R. D. Browne and R. Blundell, "Relevance of Concrete Property Research to Pressure Vessel Design," ACI SP-34, *Concrete for Nuclear Reactors*, pp. 69-102 (1972).
27. D. J. Hannant, "Effects on the Strength of Various Concretes of Sustained Temperatures Near 100°C," *Civ. Eng. Public Works Rev.* 62: 665 (June 1967).
28. J. D. Parkinson, "The Variation with Time of Water Content and Shrinkage in Concrete Subjected to a Thermal Gradient," Ph.D. thesis, University of London, May 1966.
29. R. A. Lapinas, "Strength Development of High Cement Content Concrete Construction in Large Sections," ACI Fall Meeting, Toronto, 1963.
30. D. R. Lankard et al., "Effects of Moisture Content on the Structural Properties of Portland Cement Concrete Exposed to Temperatures up to 500°F," ACI SP-25, *Temperature and Concrete* (1970).
31. V. V. Bertero and M. Polivka, "Influence of Thermal Exposure on Mechanical Characteristics of Concrete," ACI SP-34, *Concrete for Nuclear Reactors*, pp. 505-31 (1972).
32. V. V. Bertero, B. Bresler, and M. Polivka, "Instrumentation and Techniques for Study of Concrete Properties at Elevated Temperatures," ACI SP-34, *Concrete for Nuclear Reactors*, pp. 1377-1420 (1972).

33. K. W. Nasser and R. P. Lohtia, "Mass Concrete Properties at High Temperatures," *J. Am. Concr. Inst.* 68: 180-86 (March 1971).
34. K. W. Nasser and A. M. Neville, "Creep of Concrete at Elevated Temperatures," *J. Am. Concr. Inst.* 62: 1567-79 (December 1965).
35. A. M. Neville, *Properties of Concrete*, 2nd ed., Halsted, New York, 1973.
36. R. Philleo, "Some Physical Properties of Concrete at High Temperatures," *J. Am. Concr. Inst.* 29(10): 857-64 (April 1958).
37. C. R. Cruz, "Elastic Properties of Concrete at High Temperatures," *Portland Cem. Assoc., Res. Dev. Lab., Dev. Dep. Bull. D* 8: 37-47 (January 1966).
38. P. J. Sullivan and M. P. Poucher, "Influence of Temperature on the Physical Properties of Concrete and Mortar in the Range 20 to 400°C," ACI SP-25, *Temperature and Concrete* (1970).
39. J. C. Marechal, "Variations in the Modulus of Elasticity and Poisson's Ratio with Temperature," ACI SP-34, *Concrete for Nuclear Reactors*, pp. 495-504 (1972).
40. T. Harada et al., "Strength, Elasticity, and the Thermal Properties of Concrete Subjected to Elevated Temperatures," ACI SP-34, *Concrete for Nuclear Reactors*, pp. 377-406 (1972).
41. M. F. Kaplan and F.J.P. Roux, "Effects of Elevated Temperatures on the Properties of Concrete for the Containment and Shielding of Nuclear Reactors," ACI SP-34, *Concrete for Nuclear Reactors*, pp. 437-42 (1972).
42. H. G. Geymayer, "Effect of Temperature on Creep of Concrete: A Literature Review," ACI SP-34, *Concrete for Nuclear Reactors*, pp. 565-90 (1972).
43. A. F. DaSilviera and C. A. Florentino, "Influence of Temperature on the Creep of Mass Concrete," ACI SP-25, *Temperature and Concrete* (1970).
44. D. McHenry, "A New Aspect of Creep in Concrete and Its Application to Design," *Proc. ASTM* 43: 1069-84 (1943).
45. K. W. Nasser and R. P. Lohtia, "Creep of Mass Concrete at High Temperatures," *J. Am. Concr. Inst.* 68(4): 276 (April 1971).
46. R. P. Lohtia and K. W. Nasser, "Apparatus for High Temperature Creep Tests of Concrete," *J. Am. Concr. Inst.* 68(2): 114 (February 1971).

47. T. W. Kennedy, *Long-Term Creep Behavior of Concrete*, ORNL/Sub-3899, Report No. 1 (January 1975).
48. J. W. Chuang, T. W. Kennedy, and E. S. Perry, "An Approach to Estimating Long-Term Multiaxial Creep Behavior from Short-Term Uniaxial Creep Results," Research Report 2864-3, Department of Civil Engineering, University of Texas-Austin (June 1970).
49. G. P. York, T. W. Kennedy, and E. S. Perry, "Experimental Investigation of Creep in Concrete Subjected to Multiaxial Compressive Stresses and Elevated Temperatures," Research Report 2864-2, Department of Civil Engineering, University of Texas-Austin (June 1970).
50. M. A. Mukaddam, *Behavior of Concrete Under Variable Temperature and Loading*, Interim Technical Report to Oak Ridge National Laboratory, University of California-Berkeley (August 1969).
51. M. A. Mukaddam and B. Bresler, "Behavior of Concrete Under Variable Temperature and Loading," ACI SP-34, *Concrete for Nuclear Reactors*, pp. 771-98 (1972).
52. H. Gross, "High-Temperature Creep of Concrete," *Nucl. Eng. Des.* 32(1): 129 (1975).
53. C. H. Wang, "Creep of Concrete at Elevated Temperature," ACI SP-27, *Designing for Effects of Creep, Shrinkage, Temperature, in Concrete Structures*, pp. 387-400.
54. S. Seki and M. Kawasumi, "Creep of Concrete at Elevated Temperature," ACI SP-34, *Concrete for Nuclear Reactors*, pp. 591-638 (1972).
55. N. G. Zoldner, "Thermal Properties of Concrete Under Sustained Elevated Temperatures," ACI SP-25, *Temperature and Concrete* (1970).
56. J. C. Marechal, "Thermal Conductivity and Thermal Expansion Coefficients of Concrete as a Function of Temperature and Humidity," ACI SP-34, *Concrete for Nuclear Reactors*, pp. 1047-58 (1972).
57. G. L. England and A. D. Ross, "Reinforced Concrete Under Thermal Gradients," *Mag. Concr. Res.* 14(40): 5-12 (March 1962).
58. F. E. Richart, A. Brandtzaeg, and R. L. Brown, "A Study of the Failure of Concrete Under Combined Compressive Stresses," Bulletin No. 185, Engineering Experiment Station, University of Illinois-Urbana (Nov. 20, 1928).
59. J. Chinn and R. M. Zimmerman, "Behavior of Plain Concrete Under Various High Triaxial Compression Loading Conditions," WL TR 64-163, Air Force Weapons Laboratory (August 1965).

60. C. D. Goode and M. A. Helmy, "The Strength of Concrete Under Combined Shear and Direct Stress," *Mag. Concr. Res.* 19(59): 105 (June 1967).
61. N. J. Gardner, "Triaxial Behavior of Concrete," *J. Am. Concr. Inst.* 66(2): 136 (February 1969).
62. V. Hansson and K. Schimmelpfennig, "Concrete Strength in Multiaxial Stress States," ACI SP-34, *Concrete for Nuclear Reactors*, pp. 295-312 (1972).
63. P. Launay and H. Gachon, "Strain and Ultimate Strength of Concrete Under Triaxial Stress," ACI SP-34, *Concrete for Nuclear Reactors*, pp. 269-82 (1972).
64. F. Bremer, "On a Triaxial Strength Criterion for Concrete," ACI SP-34, *Concrete for Nuclear Reactors*, pp. 283-94 (1972).
65. F. K. Garas, discussion attachment to: P. Launay and H. Gachon, "Strain and Ultimate Strength of Concrete Under Triaxial Stress," *Proceedings of the First International Conference on Structural Mechanics in Reactor Technology*, 1976, vol. 4, part H, pp. 35-38 (1972).
66. D. Linse, "Strength of Concrete Under Biaxial Sustained Load," ACI SP-34, *Concrete for Nuclear Reactors*, pp. 327-34 (1972).
67. D. Linse, "Experimental Apparatus for Determining the Triaxial Strength of Concrete: First Results of Experiments," *Cem. Concr. Res.* 3: 445-57 (1973), ORNL-tr-2878.
68. G. Schickert, "Design of an Apparatus for Short-Time Testing of Concrete Under Triaxial Load," ACI SP-34, *Concrete for Nuclear Reactors*, pp. 1355-76 (1972).
69. R. H. Atkinson and H. Y. Ko, "A Fluid Cushion, Multiaxial Cell for Testing Cubical Rock Specimens," *Int. J. Rock Mech. Min. Sci.* 10: 351-61 (1973).
70. E. Andrenes, "Response of Mortar to Biaxial Compression," M.S. thesis, University of Colorado, 1974.
71. R. H. Atkinson, H. Y. Ko, and K. Gerstle, private communication, March 1975.
72. M. A. Taylor and B. K. Patel, "The Influence of Path Dependency and Moisture Conditions on the Biaxial Compression Envelope for Normal Weight Concrete," *J. Am. Concr. Inst.* 71(12): 627 (December 1974).
73. H. B. Kupfer, "Nonlinear Behavior of Concrete in Biaxial Stress," *Beton-Stahlbetonbau* 11: 269-74 (1973), ORNL-tr-2909.

74. T.N.W. Akroyd, "Concrete Under Triaxial Stress," *Mag. Concr. Res.* 13(39): 111-18 (November 1961).
75. J. Isenberg, "Strength of Concrete Under Combined Stress," *Civ. Eng. Public Works Rev.* (October 1965).
76. R. G. Clark, *Radiation Damage to Concrete*, HW-56195, Hanford Atomic Products Operation (Mar. 31, 1958).
77. T. V. Blosser et al., *A Study of the Nuclear and Physical Properties of the ORNL Graphite Reactor Shield*, ORNL-2195 (August 1958).
78. M. F. Elleuch, F. Dubois, and J. Rappeneau, "Effects of Neutron Radiation on Special Concretes and Their Components," *ACI SP-34, Concrete for Nuclear Reactors*, pp. 1071-1108 (1972).
79. S. Granata and A. Montagnini, "Studies on Behavior of Concrete Under Irradiation," *ACI SP-34, Concrete for Nuclear Reactors*, pp. 1163-74 (1972).
80. R. L. Yuan, H. K. Hilsdorf, and C. E. Kesler, *Effect of Temperature on the Drying of Concrete*, T. & A. M. Report No. 316, University of Illinois-Urbana (September 1968).
81. G. L. England and A. D. Ross, "Shrinkage, Moisture, and Pore Pressures in Hardened Concrete," *ACI SP-34, Concrete for Nuclear Reactors*, pp. 883-908 (1972).
82. S. E. Pihlajavaara and K. Tiusanen, "A Preliminary Study of Thermal Moisture Transfer in Concrete," *ACI SP-34, Concrete for Nuclear Reactors*, pp. 883-908 (1972).
83. J. E. McDonald, *Moisture Migration in Concrete*, ORNL-TM-5051 (May 1975).
84. F. Dubois et al., "Study of a Reduced Scale Model of a Prestressed Concrete Vessel Subjected to a Large Thermal Gradient," *Ann. Inst. Tech. Batim. Trav. Publics*, No. 214 (October 1965), ORNL-tr-1350.
85. T. E. Northrup and F. S. Ople, Jr., "Effects of Temperature on a Prestressed Concrete Reactor Vessel Model," *ACI SP-25, Temperature and Concrete* (1970).
86. J. Irving, G.D.T. Carmichael, and I. W. Hornby, "A Full-Scale Model Test of Hot Spots in the Prestressed Concrete Pressure Vessels of Oldbury Nuclear Power Station," *ICE Journal, Proceedings*, Part 2, pp. 331-50 (1974).
87. F. Fluge, E. Gausel, and R. Lenschow, "Experimental and Analytical Capacity Study of a Prestressed Concrete Structure Under Hard Stress," SNB, No. 5, 1973, ORNL-tr-2916.

88. G. D. Whitman, J. P. Callahan, and J. M. Corum, "An Investigation of the Time-Dependent Behavior of Prestressed Concrete Pressure Vessels," ACI SP-34, *Concrete for Nuclear Reactors*, pp. 823-45 (1972).
89. J. P. Callahan, R. L. Valachovic, and G. C. Robinson, "PCRV Thermal Cylinder Test," *GCR Programs Annu. Prog. Rep. 1972*, ORNL-4911, pp. 181-209.
90. J. P. Callahan and G. C. Robinson, "PCRV Thermal Cylinder Test," *GCR Programs Annu. Prog. Rep. 1973*, ORNL-4975 (to be published).
91. M. Dumas, discussion attachment to ref. 84.
92. F. L. Scotto, "Concrete Behavior Under Combined Stresses up to Failure: Test Results on Small Dimension Prestressed Concrete Pressure Vessel Models," ACI SP-34, *Concrete for Nuclear Reactors*, pp. 1471-1512 (1972).
93. J. P. Callahan, *Report of Foreign Travel to Germany, France, and England (May 24-June 11, 1975)*, ORNL-FTR-2 (July 15, 1975).

ORNL/TM-5497  
 Distribution  
 Category UC-77

## INTERNAL DISTRIBUTION

1-3.	Central Research Library	49.	P. R. Kasten
4.	Document Reference Section	50.	W. J. Lackey
5-12.	Laboratory Records Department	51.	A. L. Lotts
13.	Laboratory Records, ORNL RC	52.	R. E. MacPherson
14.	ORNL Patent Office	53.	A. P. Malinauskas
15.	G. M. Adamson	54.	W. R. Martin
16.	J. L. Anderson	55.	H. E. McCoy
17.	S. J. Ball	56.	C. J. McHargue
18.	A. L. Boch	57-63.	R. K. Nanstad
19.	C. R. Brinkman	64.	D. J. Naus
20-23.	J. P. Callahan	65.	K. J. Notz
24.	D. A. Canonico	66.	L. C. Oakes
25.	J. A. Conlin	67.	C. B. Oland
26.	J. H. Coobs	68.	P. Patriarca
27.	D. A. Costanzo	69.	H. Postma
28.	F. L. Culler	70.	M. N. Raftenburg
29.	F. C. Davis	71.	C. C. Robinson
30.	J. H. DeVan	72.	J. P. Sanders
31.	J. R. DiStefano	73.	Dunlap Scott
32.	W. G. Dodge	74.	J. L. Scott
33.	R. G. Donnelly	75.	J. H. Shaffer
34.	B. C. Duggins	76.	G. M. Slaughter
35.	W. P. Eatherly	77.	J. E. Smith
36.	D. N. Fanning	78.	R. S. Stone
37.	G. G. Fee	79.	V. J. Tennery
38.	Uri Gat	80.	M. L. Tobias
39.	R. W. Glass	81.	D. B. Trauger
40.	J. C. Griess	82.	J. R. Weir, Jr.
41.	P. A. Haas	83.	G. D. Whitman
42.	R. F. Hibbs	84.	P. M. Brister (consultant)
43.	J. W. Hill	85.	John Moteff (consultant)
44-46.	M. R. Hill	86.	Hayne Palmour III (consultant)
47.	R. M. Hill, Jr.	87.	J. W. Prados (consultant)
48.	F. J. Homan	88.	N. E. Promisel (consultant)
		89.	D. F. Stein (consultant)

## Other Consultants and Subcontractors:

90. Civil Engineering Department, University of Tennessee, Knoxville,  
 TN 37916

D. W. Goodpasture

91. J. L. Lott, 128 Kingswood, Naperville, IL 60540

92-93. Civil Engineering Department, University of Illinois, Urbana, IL 61801  
W. C. Schnobrich  
M. A. Sozen

94. Civil Engineering Department, Northwestern University, Evanston, IL 60201  
Z. P. Bazant

## EXTERNAL DISTRIBUTION

95-96. ERDA DIVISION OF NUCLEAR FUEL CYCLE AND PRODUCTION, Washington, DC 20545  
Director

97-98. ERDA DIVISION OF NUCLEAR RESEARCH AND APPLICATION, Washington, DC 20545  
Director

99-100. ERDA OAK RIDGE OPERATIONS OFFICE, P.O. Box E, Oak Ridge, TN 37830  
Director, Reactor Division  
Direct, Research and Technical Support Division

101-267. ERDA TECHNICAL INFORMATION CENTER, Office of Information Services, P.O. Box 62, Oak Ridge, TN 37830  
For distribution as shown in TID-4500 Distribution Category, UC-77 (Gas-Cooled Reactor Technology)